AD-775 744

PREDICTION OF AIRCRAFT GROUND PERFORMANCE BY EVALUATION OF GROUND VEHICLE RUT DEPTHS

G. W. Turnage, et al

Army Engineer Waterways Experiment Station
Vicksburg, Mississippi

February 1974

UNCLASSIFIED

Security Classification

DOCUMENT CONTROL DATA - R & D AD 775 744

(Security classification of title, body of abstract and indexing annotation must be entered when the overall report is classified)

1. ORIGINATING ACTIVITY *(Corporate author)* USA Engineer Waterways Experiment Station Vicksburg, Mississippi 39180	2a. REPORT SECURITY CLASSIFICATION UNCLASSIFIED 2b. GROUP

3. REPORT TITLE

PREDICTION OF AIRCRAFT GROUND PERFORMANCE BY EVALUATION OF GROUND VEHICLE RUT DEPTHS

4. DESCRIPTIVE NOTES *(Type of report and inclusive dates)*

January 1973 through July 1973

5. AUTHOR(S) *(First name, middle initial, last name)*

G. W. Turnage
D. N. Brown

6. REPORT DATE	7a. TOTAL NO. OF PAGES	7b. NO. OF REFS
February 1974	~~116~~ 127	14

8a. CONTRACT OR GRANT NO.	9a. ORIGINATOR'S REPORT NUMBER(S) AFWL-TR-73-213
b. PROJECT NO. 683M c. TASK 4M10 d.	9b. OTHER REPORT NO(S) *(Any other numbers that may be assigned this report)*

10. DISTRIBUTION STATEMENT

Approved for public release; distribution unlimited.

11. SUPPLEMENTARY NOTES	12. SPONSORING MILITARY ACTIVITY AFWL (DEZ) Kirtland AFB, NM 87117

13. ABSTRACT

(Distribution Limitation Statement A)

Two single aircraft tires (20-20, 22-PR and 49-17, 26-PR) and three standard military trucks (M715, 1-1/4-ton; M35A2, 2-1/2-ton; and M51, 5-ton) were tested under towed (nonpowered, nonbraked) and self-powered conditions, respectively, in buckshot clay test beds whose strengths ranged from about 110 to 600 cone index. Tests included multiple passes over the prepared test beds (usually 100 passes for the aircraft tires, 10 for the trucks) at low speeds. Only single-wheel configurations were examined (i.e., outer second- and third-axle wheels of the M35A2 and M51 were removed). Curves were developed to allow soil strength (airfield index) to be estimated directly from the rut produced by single or multiple passes of any of the three trucks. These curves were developed through use of a dimensionless prediction term (tire-clay numeric N_c) that allows pneumatic tire performance to be scaled over a wide range of soil strengths, wheel loads, and tire size, shape, and deflection conditions. The same numeric was shown to be capable of describing multipass rut depth and towed coefficients for the aircraft tires, as well as multipass rut depth for the trucks. Examples illustrate how airfield index (AI) estimated from truck rut depth can easily be used with curves that describe the N_c versus rut depth and towed force coefficient relations for aircraft tires to predict multipass aircraft tire performance. Appendix A shows that values of AI estimated from truck rut depth can be converted to California Bearing Ratio values and used as input for a nomograph description of aircraft operation on unsurfaced soils.

DD FORM 1 NOV 65 1473

UNCLASSIFIED

Security Classification

14 KEY WORDS	LINK A		LINK B		LINK C	
	ROLE	WT	ROLE	WT	ROLE	WT
rut depths						
aircraft ground performance prediction						
soil runways						

AFWL-TR-73-213

PREDICTION OF AIRCRAFT GROUND PERFORMANCE BY EVALUATION OF GROUND VEHICLE RUT DEPTHS

G. W. Turnage

D. N. Brown

US Army Engineers Waterways Experiment Station
Vicksburg, Mississippi 39180

Final Report for Period January 1973 through July 1973

Approved for public release; distribution unlimited.

FOREWORD

This report was prepared by the U.S. Army Engineer Waterways Experiment Station, Vicksburg, Mississippi, under Project Order AFWL 73-191. The research was performed under Program Element 63723F, Project 683M, Task 4M10. The research was sponsored by the Air Force Weapons Laboratory.

Inclusive dates of research were January 1973 through July 1973. The report was submitted 5 December 1973 by the Air Force Weapons Laboratory Project Engineer, Mr. L. M. Womack (DEZ). The former Project Officer was Mr. Harry Marien.

The investigation was conducted under the general supervision of Messrs. J. P. Sale and R. G. Ahlvin, Chief and Assistant Chief, respectively, Soil and Pavements Laboratory (SPL), and Mr. W. G. Shockley, Chief, Mobility and Environmental Systems Laboratory (MESL). The program was supervised directly by Mr. D. N. Brown (SPL) and Messrs. C. J. Nuttall and G. W. Turnage (MESL). The laboratory tests were conducted by personnel of the Mobility Investigations Branch, MESL; resulting data were processed by the Data Handling Branch, MESL. The main text of this report was prepared by Mr. Turnage, and the appendix by Mr. Brown.

This technical report has been reviewed and is approved.

L. M. Womack

L. M. WOMACK
Project Engineer

Oren G. Strom

OREN G. STROM
Lt Colonel, USAF
Chief, Aerospace Facilities Branch

William B. Liddicoet

WILLIAM B. LIDDICOET
Colonel, USAF
Chief, Civil Engineering Research Division

CONTENTS

Preceding page blank

ILLUSTRATIONS

ILLUSTRATIONS (Continued)

TABLES

ABBREVIATIONS AND SYMBOLS

AI	Airfield index
CBR	California Bearing Ratio
CI	Cone index
D	Wheel drag
ESWL	Equivalent single-wheel load
M	Torque
N_c	Tire-clay numeric
P	Pull
P_T	Towed force
W	Load
b	Tire section width
c	Soil cohesion
d	Tire carcass diameter
h	Tire carcass section height
n	Pass number
r	Tire rut depth
s	Nontracking distance
z	Tire sinkage
δ	Maximum hard-surface tire deflection

SECTION I

INTRODUCTION

1. BACKGROUND

Military aircraft are subject to a variety of field situations that require their operation from remote soil-surfaced sites. For example, the current concept of aircraft operation in a theater of operations is that heavy cargo aircraft must be capable of providing close-in support to ground combat troops (reference 1). In this role, Air Force aircraft often must land and take off from unsurfaced runways.

Among the many problems associated with operation of military aircraft from bare soil surfaces are increase in drag resistance due to wheel sinkage into the soil; dynamic structural loads caused by soil surface roughness and wheel sinkage; and injuries to the aircraft, or worst of all, to aircraft personnel that can be traced ultimately to the interaction of the soil and the aircraft running gear. A major cause of these problems is that the pilot often must evaluate his aircraft's ability to operate from an earthen airstrip solely on the basis of his experience or from very limited, often purely qualitative, information supplied to him by personnel on the ground.

In recent past, various methods have been investigated to aid the pilot in determining aircraft operational capability on earthen airstrips. The methods evaluated included: aerial and airfield penetrometer measurements; remote sensing; and correlation between military ground vehicle sinkage and light aircraft operational capability. On the basis of interviews with pilots involved in these investigations, the conclusion was reached that the only method presently developed to the extent that it can be quickly used in operational applications is the last one mentioned above. Augmenting this conclusion is the fact that the Army Corps of Engineers has developed, field validated, and published suitable criteria relating ground vehicle sinkage and light aircraft operational capability (reference 2). Responses to field inquiries indicate that the technique has been accepted and is used satisfactorily by Army pilots.

A natural follow-up to Army experience in correlating light aircraft soil surface operation capability with ground vehicle rut depth is expansion of this technique to develop suitable criteria for heavier Air Force aircraft. The investigation reported herein is part of a larger U. S. Air Force effort to develop a simple effective method to predict the performance of military aircraft on natural soil runways.

2. OBJECTIVES

The primary objectives of this study, paraphrased from the sponsor's Statement of Work, were

a. Develop a simple method to estimate soil strength from the rut produced by a conventional military truck.

b. Develop a straightforward technique to forecast an aircraft tire's multiple-pass rut depth and soil drag resistance from the soil strength estimated by a above, or from the rut produced by one pass of the aircraft.

c. Illustrate the use of techniques from a and b above.

In addition, per the statement of work, major emphasis in the data analysis and reporting was placed on "(a) describing the WES dimensionless numeric system used to predict tire rut depth versus cone index relations for the military vehicles and aircraft tires, and validating the system's usefulness for an extremely wide range of tire-load-soil strength conditions; and (b) showing interrelations among the various measures of soil strength (cone index, airfield index, and California Bearing Ratio, etc.)."

3. SCOPE

Tests were conducted under laboratory conditions in one soil type--highly plastic "buckshot" clay--at a wide range of strengths--cone index values from approximately 110 to slightly over 600. Two aircraft tires were tested singly: 20-20, 22-PR (C130 tire) at 25,000- and 35,000-lb loads and 75- and 100-psi inflation pressures for each load; and the 49-17, 26-PR (heavy A/C tire) at 25,000-lb load and 90- and 110-psi inflation pressures. Three standard military trucks (1-1/4-, 2-1/2-, and 5-ton weight classes) were tested loaded and unloaded, with tire deflection for all truck tests set at 15 percent. All tests were conducted at low speed (approximately 3 ft/sec). Aircraft tire tests consisted of 100 passes and truck tests of 10 passes, except that any given test was terminated when at least a 6-in. tire rut was developed.

A technique was developed to predict aircraft tire rutting and towed force (soil drag) for the range of conditions tested. Evidence is presented to demonstrate that the dimensionless term on which the prediction is based is valid for a very broad range of tire-load-soil strength conditions, at least for soils similar to the test soil used.

Appendix A shows that values of AI estimated from truck rut depth can be converted to California Bearing Ratio values and used as input for a nomograph description of aircraft operation on unsurfaced soil.

4. DEFINITIONS

Many of the terms used in this report are peculiar to the technology of bare-soil, wheeled-vehicle operation, and to the numeric system used in subsequent data analyses, and some terms are given special meaning. To ensure an understanding in the discussion, the more important terms are defined in the list that follows.

a. Pneumatic Tire Terms (See Figure 1)

Carcass diameter (d). Outside diameter, esclusive of tread of the inflated, unloaded tire. Equals the rim diameter plus twice the carcass section height.

Tire diameter. Outside diameter, including tread, of the inflated, unloaded tire. (In figure 1, one half of the tire diameter, i.e. the tire radius, is shown.)

Section width (b). Maximum outside width of the cross section of the inflated, unloaded tire.

Loaded section width. Maximum outside width of the cross section of the loaded tire when the tire rests on an unyielding, horizontal, plane surface.

Tire section height. Distance from the shoulder of the rim to the periphery of the tire, including tread, measured along the vertical center line of the cross section of the inflated, unloaded tire.

Carcass section height (h). Distance from the lip of the rim flange to the periphery of the tire, exclusive of tread, measured along the vertical center line of the cross section of the inflated unloaded tire.

Loaded carcass section height. Minimum distance from the lowest point of the lip of the rim flange to the unyielding level surface on which the tire is resting, less the tread height.

Tire deflection. Displacement of a point on the tire surface from its position on the inflated, unloaded tire.

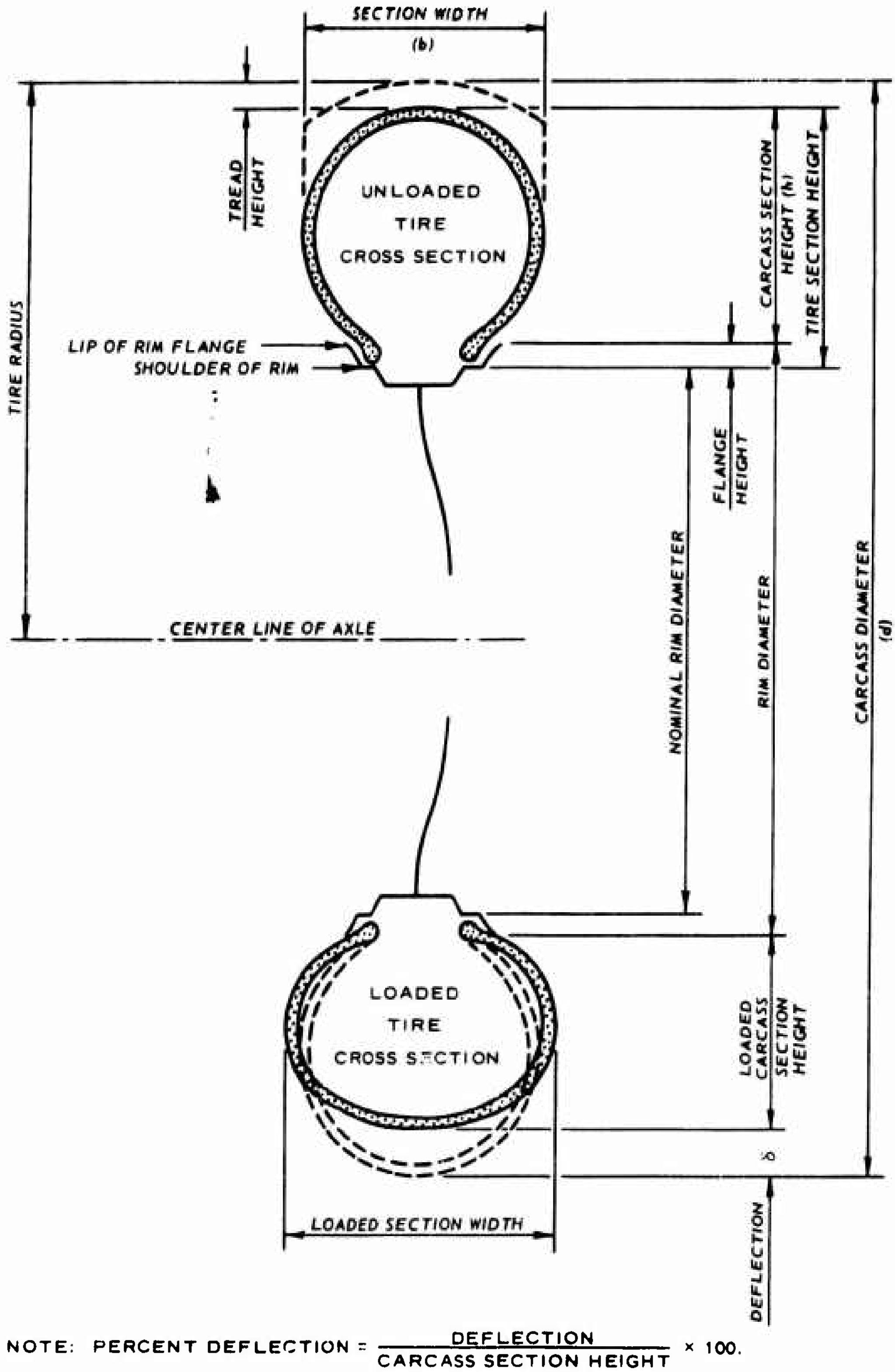

Figure 1. Pneumatic Tire Terms

Maximum hard-surface deflection (δ). Difference between carcass section height and loaded carcass section height.

Percent deflection. Maximum hard-surface tire deflection divided by carcass section height, times 100, i.e., $\frac{\delta}{h} \times 100$.

Tire-print contact area. The portion of the tire in contact with the supporting horizontal, unyielding, plane surface. Interruptions of the contact area due to tread patterns are considered part of the contact area.

Tire-print contact pressure. Load on the tire divided by the print contact area.

Tire-print contact length. Maximum length of the tire-print contact area, measured parallel to the plane of rotation of the tire.

Tire-print contact width. Maximum width of the tire-print contact area, measured perpendicular to the tire-print contact length.

Hard-surface rolling circumference. Forward advance per revolution of the loaded tire when towed on a flat, level, unyielding surface.

Nominal rim diameter. Wheel diameter at the shoulder of the rim. This is the rim diameter value that appears in the designation of the tire size (e.g. the "17" in the "49-17").

Rim diameter. Wheel diameter at the lip of the rim flange.

b. Soil Terms

Cone index (CI). An index of the soil strength obtained with the cone penetrometer. It is the force (in lb) per unit cone base area (in square inches) required to penetrate a soil vertically at 72 in./min with a 30-deg-apex angle, right circular cone of 0.5-in.^{2} base area. Values of CI are expressed without dimensions to avoid the implication that CI measures a specific soil property. These values usually are given for a specified layer of soil several inches thick.

Airfield index (AI). An index of soil strength obtained with the airfield cone penetrometer. Values of AI are read directly from the penetrometer and cover a range of 0 to 15. A reading of AI = 0 is obtained when no force is applied to the penetrometer, and a reading of AI = 15 results when a vertical force of 150 lb is applied. The diameter of the base of the airfield cone is 0.5 in. (0.196-sq-in. area). In use, the airfield cone penetrometer is forced vertically into the soil at a slow, steady rate (about 72 in./min). Values of AI are expressed without dimensions, and usually are given for a specified layer of soil several inches thick.*

California Bearing Ratio (CBR). A measure of soil strength used to evaluate the ability of soils to resist shear deformation. The CBR test is conducted by forcing a 3-in.^{2} circular area piston into the soil at a rate of approximately 0.05 in./min. The load required to force the piston into the soil 0.1 in. is expressed as a percentage of the standard value for crushed stone. This percentage is the CBR. (See reference 3 for standard testing procedures.)

Cohesion (c). The shear strength of a soil at zero normal pressure. It is represented as a parameter in the Coulomb expression, $s = c + p \tan \phi$, relating the shear strength s of a soil to the normal pressure p.

Friction angle (ϕ). A parameter in the Coulomb expression $s = c + p \tan \phi$. It is a measure of the amount that the shear strength s of a soil increases with an increase in pressure p.

c. Tire-Soil Term

Tire-clay numeric (N_c). A term composed of independent variables that describe the tire-clay system, arranged so that the overall term is dimensionless. In this report, $N_c = \frac{\overline{AI}bd}{W} \cdot \frac{1}{\left(1 - \frac{\delta}{h}\right)^2} \cdot \frac{1}{1 + \frac{b}{2d}}$. In this form, N_c can be considered as a ratio of soil strength (in implied units of pressure) to tire loading (W/bd, or units of pressure), times a dimensionless term that reflects tire flexibility, times a dimensionless term associated with tire shape.

d. Wheel Performance Terms

Load (W). The vertical force applied to the tire through the axle.

Torque (M). Torque input at the axle.

Travel ratio. Ratio of the actual wheel advance per revolution to the theoretical advance per revolution, the latter defined as the hard-surface rolling circumference.

---

* In this study, the cone penetrometer and the airfield cone penetrometer were replaced by cone-shaft-load cell arrangements (cone base areas of 0.5 and 0.196 in.^{2}, respectively) that were mechanically driven at 72 in./min. Values of CI were determined as force per unit cone base area (0.5 in.^{2}), and those of AI as force divided by 10. Values of CI and AI determined this way correspond to those of CI and AI defined above.

Slip. Unity minus the travel ratio, usually expressed as a percentage.

Pull (P). The component, acting parallel to the direction of travel, of the resultant of all soil forces acting on the wheel. It is considered positive when the wheel is performing useful work, and negative when an additional force must be applied to maintain motion.

Towed condition. The condition in which torque input to the wheel is zero and the pull is negative.

Towed force (P_T); drag (D). Negative pull at the towed condition, i.e., that additional horizontal force that must be applied to a towed wheel so that it can maintain forward motion (at constant, very low speed). In this report, towed force and drag for the free-rolling condition (i.e., wheel neither powered nor braked) are considered synonymous terms.

Positive-pull condition. The condition in which sufficient torque input is provided for the wheel not only to propel itself, but also to develop positive pull (i.e., to perform useful work).

Immobilization. That condition at which wehel load becomes too large, soil strength too weak, or input torque too small to allow a tire to propel itself.

Sinkage (z). The depth to which the tire penetrates the soil, measured relative to the original soil surface at the instant this depth is achieved.

Rut depth (r). The depth to which the tire penetrates the soil, as indicated by measurement taken relative to the original soil surface at some time after the tire has traveled over (and through) the soil (see figure 2a). For cohesive soils, rut depth values generally are slightly smaller than sinkage values due to soil rebound. The depth illustrated in figure 2b was also measured in this study and is referred to herein as "rut depth relative to rut shoulders."

Rut shoulders. The soil adjacent to and on either side of the tire rut that is displaced above the original soil surface by soil-tire interaction when the tire rut is made (see figure 2).

Hub movement. The in-soil change in elevation of the wheel axle, measured instantaneously and relative to the original soil surface.

Pass (n). In this report, trafficking the same rut with a single tire n number of times results in n passes. For trucks with two tires per axle and all tires on each side of the truck tracking one another

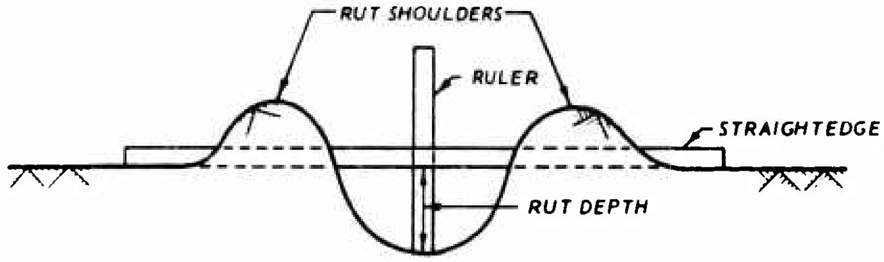

a.

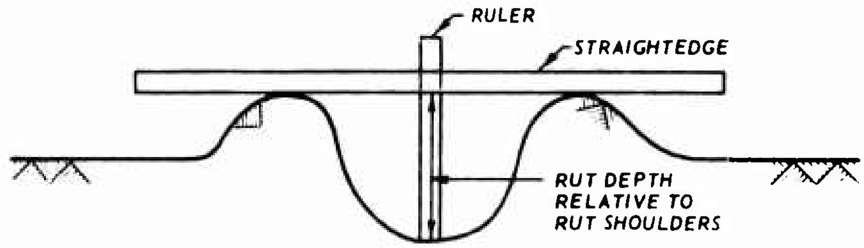

b.

Figure 2. Illustration of Rut Depth and Rut Depth Relative to Rut Shoulders

(following the same straight-line path), pass number n for each truck rut equals number of truck passes times number of axles.

SECTION II

TEST PROGRAM

1. PLAN OF TESTS

a. Aircraft Tires

Two aircraft tires, the 20-20, 22-PR (C130 tire) and the 49-17, 26-PR (heavy A/C tire) were tested singly (i.e., no multiwheel configurations were tested) at the following loads and inflation pressures:

Single Aircraft Tire	Test Load, lb	Inflation Pressures, psi
20-20, 22-PR	25,000 and 35,000	75 and 100
49-17, 26-PR	25,000	90 and 110

Geometries of these tires for the conditions tested are described in table I. Each aircraft tire test consisted of 100 passes, unless a rut depth of at least 6 in. was obtained before pass 100, in which case the test was terminated after the pass in which the 6-in. rut depth occurred.

b. Trucks

Three standard military trucks, chosen to cover a range of weight classes and for their wide-spread availability at United States military bases around the world, were tested at the following loads and tire sizes:

Truck Name	Test Loads, lb	Tire Size
M715, 1-1/4-ton, 4x4*	6,290 and 9,305	9.00-16, 8-PR
M35A2, 2-1/2-ton, 6x6	13,160 and 23,095	9.00-20, 8-PR
M51, 5-ton, 6x6	21,690 and 41,700	11.00-20, 12-PR

The test load is the overall weight of the entire truck plus driver (driver weight taken as 180 lb for all tests). For each truck, the test load listed first is the unloaded truck weight plus driver weight, and the second is driver weight plus maximum recommended truck weight for operation on hard-surfaced roads.**

---

* The first number in the last part of the truck name, e.g., the first "4" in "4x4," designates the total number of wheels (whether single or dual) of that vehicle. The second number, e.g., the second "4" in "4x4," designates the number of these wheels that are driving, or powered.

** The rationale was that for an airfield condition such that operation by a heavy aircraft could be considered, any given truck should be capable of performing the required slow-speed test passes at its hard surface road weight.

TABLE I.--AIRCRAFT TIRE TEST GEOMETRIES

Tire Size Designation	Load W, lb	Loaded Tire Inflation Pressure psi	Carcass Section Height Unloaded h, in.	Carcass Section Height Loaded in.	Maximum Hard-Surface Deflection δ, in.	Deflection, %	Carcass Diameter d, in.*	Section Width Unloaded b, in.	Section Width Loaded in.	Tire Print Contact Length in.	Tire Print Contact Width in.	Tire Print Contact Area $in.^2$	Tire Print Contact Pressure psi	"Dynamic" Correction for Hub Movement in.**
20-20, 22-PR	25,000	75	16.43	11.16	5.27	32.1	56.36	19.59	21.50	25.95	15.80	330.55	75.63	0.35
20-20, 22-PR	25,000	100	16.51	12.25	4.26	25.8	56.52	19.60	21.11	23.10	13.35	249.03	100.39	0.35
20-20, 22-PR	35,000	75	16.43	9.51	6.92	42.1	56.36	19.59	23.00	30.17	17.10	447.58	78.20	0.39
20-20, 22-PR	35,000	100	16.51	10.84	5.67	34.3	56.52	19.60	21.90	27.25	16.80	362.66	96.51	0.39
49-17, 26-PR	25,000	90	12.00	8.23	3.77	31.4	47.50	16.95	18.40	21.00	13.30	243.32	102.75	0.32
49-17, 26-PR	25,000	110	12.95	8.69	3.36	28.0	47.60	16.95	18.20	19.58	13.10	215.32	116.11	0.33

* Each of the two aircraft tires had widely-spaced circumferential ribs of heights that were insignificant compared to the other dimensions of the tire. It was judged not necessary to describe the tire ribs, as they affected the test results negligibly.

** "Dynamic" correction for hub movement is the amount the wheel hub moved upward when the tire was towed slowly on a flat, level, unyielding surface. All measures of tire test geometry listed above, except for "dynamic" correction for hub movement, were obtained with the tire in a static, i.e, a non-rolling, condition.

For all tests reported herein, the outer tires of the second and third axles of the 2-1/2- and 5-ton trucks were removed.* This was done for two reasons: (1) A decrease in the number of tires increased the rut depth attainable by these two trucks, and thereby increased the trucks' ability to provide a sensitive index of soil support capability, particularly at high soil strength levels; and (2) a single-tire arrangement at all wheels simplified data analysis aimed at predicting in-soil tire performance. Sketches of the trucks, showing their tire spacings, dead weight locations, and weight distributions are shown in figure 3.

Note that for each of the three trucks, the distance between tires on the front axle was different from that between tires on the second or second and third axles. Also, for only two of the six test conditions (the unloaded M715 and the loaded M35A2) was the load on each axle approximately equal.

Photographs of the three test trucks, as tested, are shown in figures 4, 5, and 6, and geometries of each truck tire for the conditions tested are described in table II. Note in table II that each tire was inflated to produce 15 percent deflection, a tire condition chosen because it provides safe in-soil operation while providing rut depths reasonably close to the maximum possible (which would be attained at zero percent deflection).

Each truck test consisted of 10 passes (five forward and five reverse), unless a rut depth of at least 6 in. was obtained before pass 10. In that case, the test was stopped after the vehicle pass that produced the 6-in. rut depth.

c. Test Soil

The test soil was a Mississippi River alluvium obtained from the Long Lake area northwest of Vicksburg, Mississippi, and is known locally as "buckshot" clay. It is a highly plastic, essentially purely cohesive soil, classified according to the Unified Soil Classification Systems as fat clay (CH). Information describing the soil's grain-size distribution and its plasticity is presented in figure 7.

---

* In the laboratory tests reported, dead weights were placed in the cargo area of the M35A2 and M51 trucks to simulate the weight of the removed second- and third-axle tires. In field operations, the removed tires should be placed in the cargo area and centered between the second and third axles.

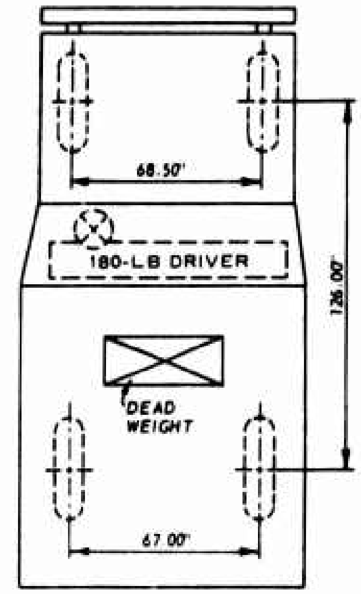

M715, 1-1/4-TON, 4×4 TRUCK

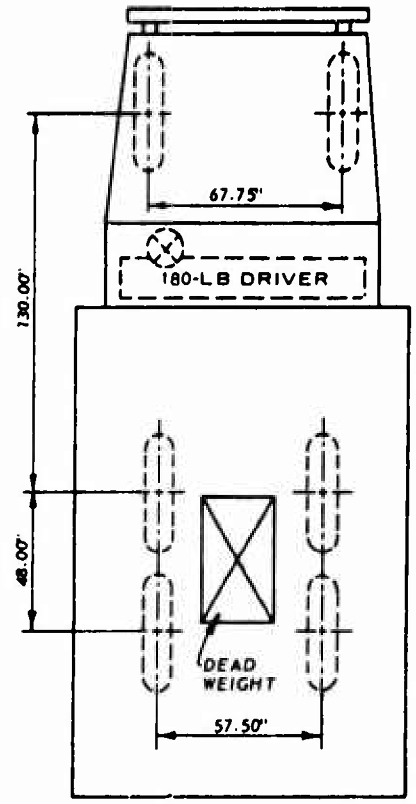

M35A2, 2-1/2-TON, 6×6 TRUCK

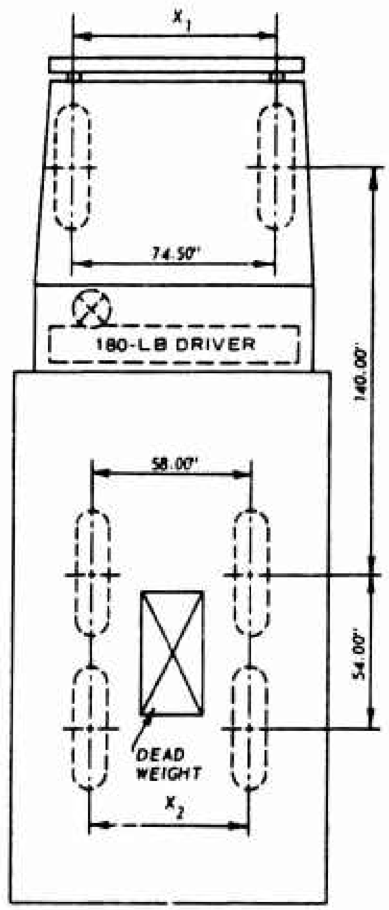

M51, 5-TON 6×6 TRUCK

TRUCK	TOTAL LOAD LBS (W)	FRONT-AXLE LOAD LBS	SECOND-AXLE LOAD LBS	THIRD-AXLE LOAD LBS	NON-TRACKING DISTANCE IN., (S)*
M715	6,290	3,145	3,145	--	0.75
M715	9,305	3,910	5,395	--	0.75
M35A2	13,160	6,040	3,540	3,580	5.125
M35A2	23,095	7,640	7,650	7,805	5.125
M51	21,690	8,220	6,690	6,780	8.25
M51	41,700	11,160	14,975	15,565	8.25

* LET X_1 = DISTANCE BETWEEN CENTER LINES OF FRONT-AXLE TIRES.

LET X_2 = DISTANCE BETWEEN CENTER LINES OF 2ND- OR 2ND-AND 3RD-AXLE TIRES.

THEN, $S = \frac{X_1 - X_2}{2}$

NOTE: THE M35A2 AND M51 TRUCKS WERE TESTED WITH OUTER WHEELS ON THEIR SECOND AND THIRD AXLES REMOVED.

Figure 3. Sketches Showing Test Truck Tire Spacings and Weight Distributions

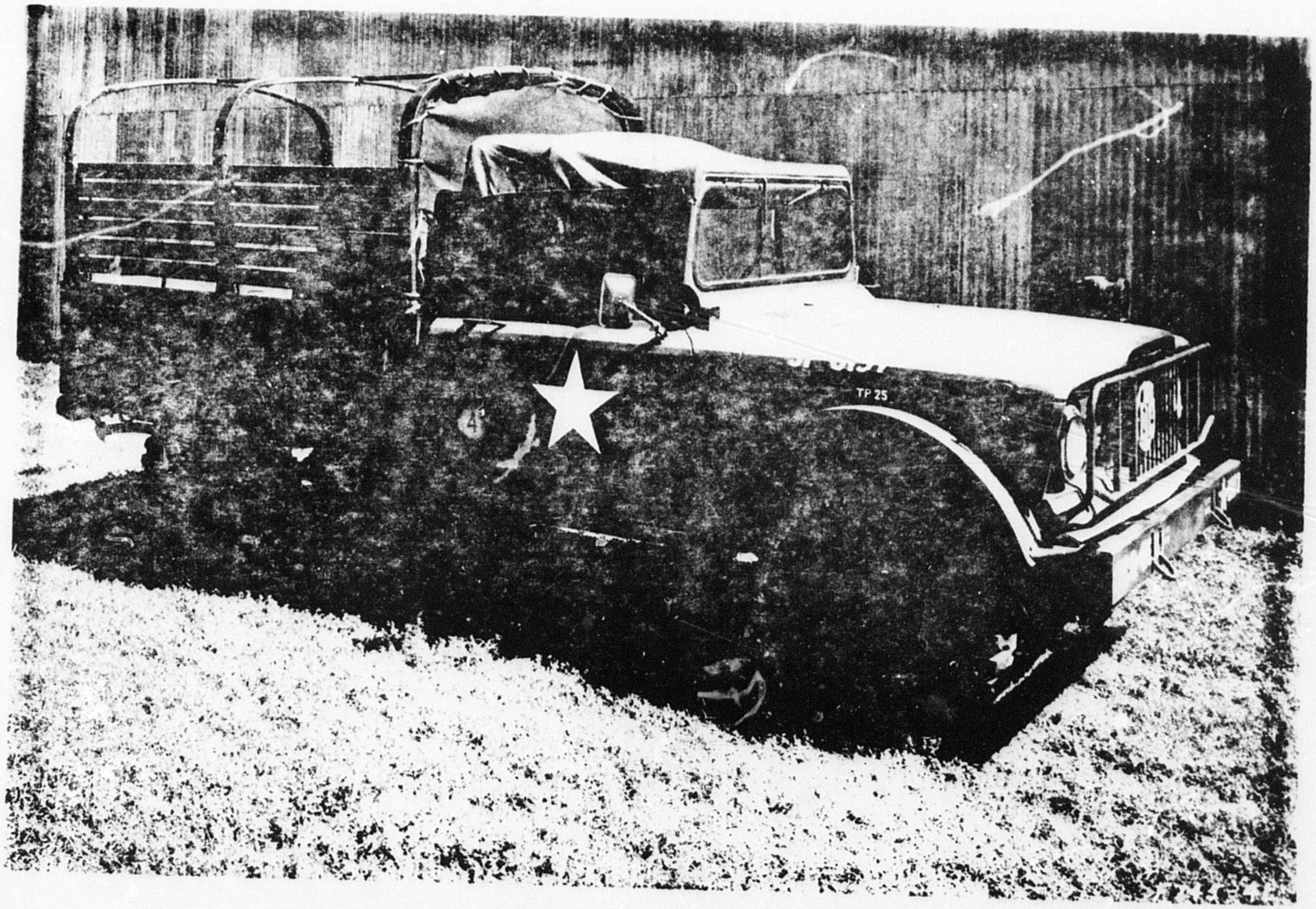

Figure 4. Side View of M715, 1-1/4-Ton Truck

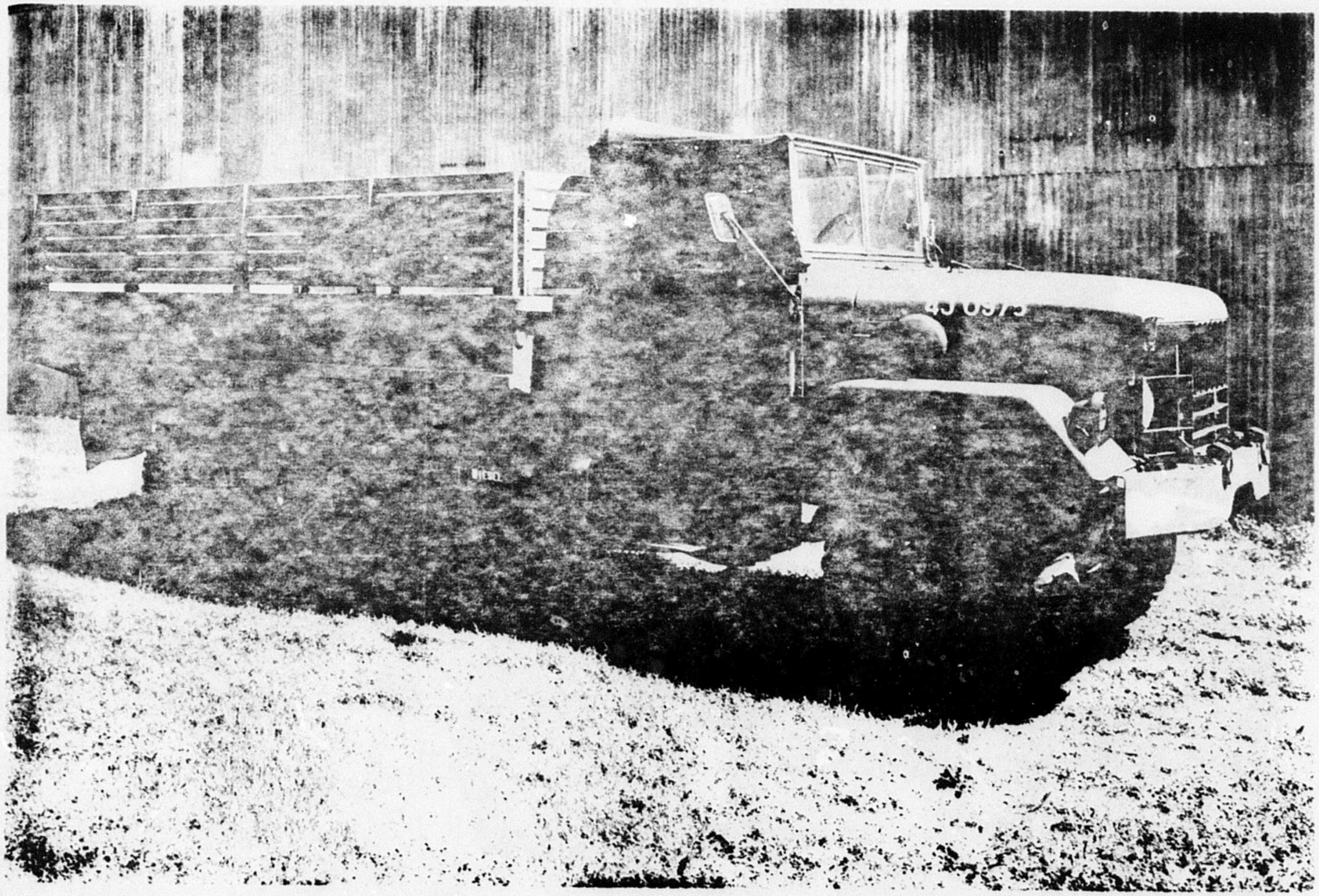

Figure 5. Side View of M35A2, 2-1/2-Ton Truck

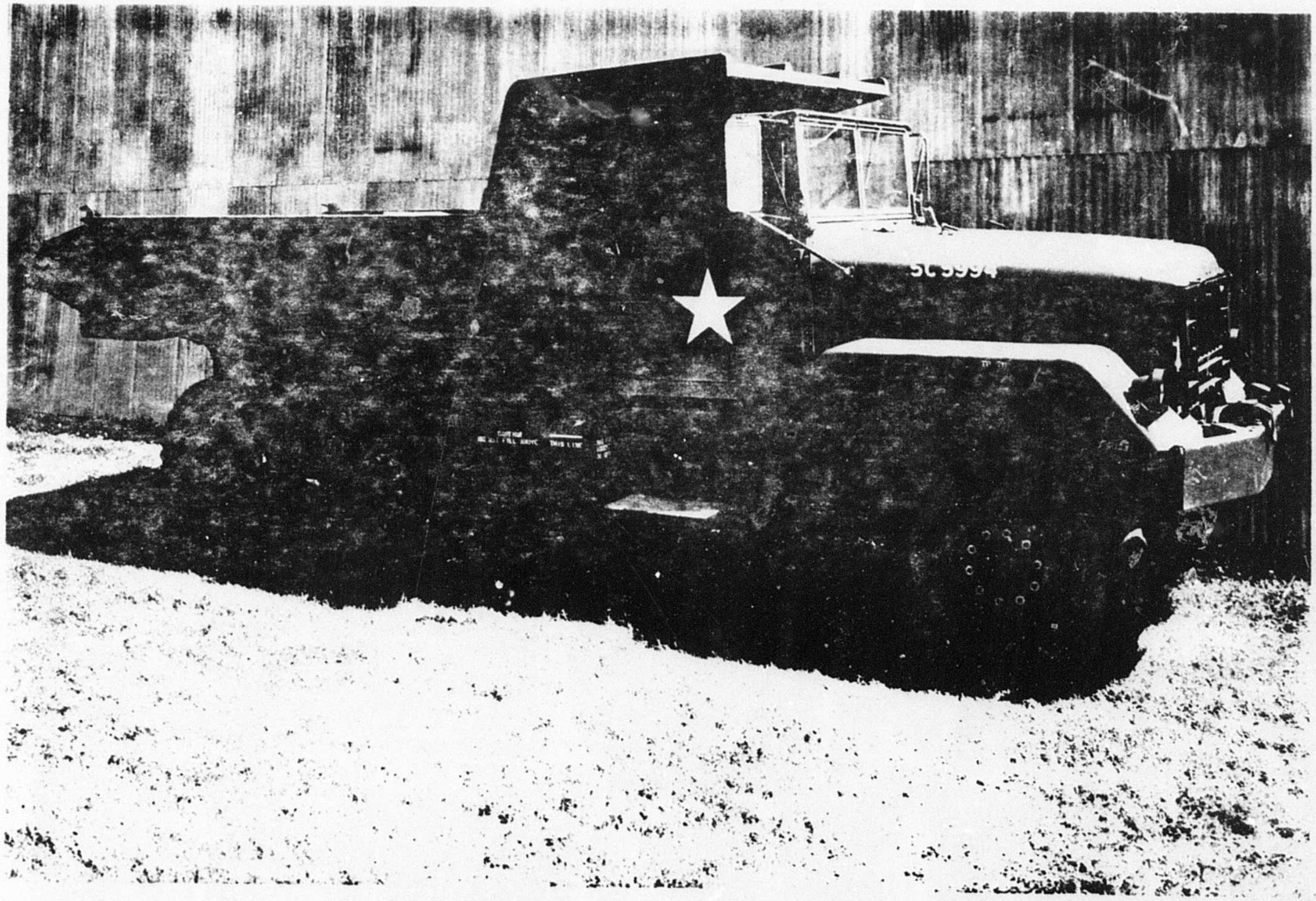

Figure 6. Side View of M51, 5-Ton Truck

TABLE II.--TRUCK TIRE TEST GEOMETRIES

Tire Size Designation	Wheel Location on Truck*	Test Load W, lb	Loaded Tire Inflation Pressure psi	Rim Diameter in.	Average Tread Height in.	Carcass Section Height Unloaded h, in.	Carcass Section Height Loaded in.	Maximum Hard-Surface Deflection δ, in.	Deflection %	Tire Diameter in.**	Carcass Diameter d, in.	Section Width Unloaded b, in.	Section Width Loaded in.	Tire Print Contact Length in.	Tire Print Contact Width in.	Tire Print Contact Area in.^{2}	Tire Print Contact Pressure psi
							M715, 1-1/4-Ton, 4x4 (Unloaded)										
9.00-16, 8-PR	LF	1575	17.3	18.60	0.35	7.60	6.46	1.14	15	34.50	33.80	10.17	10.43	9.70	7.04	65.21	24.15
	RF	1565	15.8			7.30	6.20	1.10		33.90	33.20	9.80	10.10	9.90	7.10	66.96	23.37
	LR	1570	18.0			7.93	6.74	1.19		35.16	34.46	10.30	10.74	9.60	7.40	64.33	24.41
	RR	1580	17.4			7.75	6.59	1.16		34.80	34.10	10.23	10.70	9.40	7.30	62.93	25.11
							M715, 1-1/4-Ton, 4x4 (Loaded)										
9.00-16, 8-PR	LF	1955	28.3	18.60	0.35	7.64	6.49	1.15	15	34.58	33.88	10.23	10.64	9.23	7.08	64.22	30.44
	RF	1955	24.4			7.52	6.39	1.13		34.34	33.64	9.82	10.29	9.00	7.10	58.36	33.50
	LR	2710	45.2			8.04	6.83	1.21		35.38	34.68	10.34	10.98	9.20	7.52	61.30	44.21
	RR	2685	44.7			7.89	6.71	1.18		35.08	34.38	10.32	11.00	9.13	7.55	62.31	43.09
							M35A2, 2-1/2-Ton, 6x6 (Unloaded)										
9.00-20, 8-PR	LF	2970	49.4	23.20	0.50	8.10	6.89	1.21	15	40.40	39.40	10.72	11.38	11.00	6.22	57.01	52.10
	RF	3070	50.4			8.12	6.90	1.22		40.44	39.44	10.76	11.37	11.08	6.70	63.55	48.31
	LFT	1800	30.3			8.19	6.96	1.23		40.58	39.58	10.67	11.27	9.43	5.42	43.25	41.62
	RFT	1740	29.8			8.18	6.95	1.23		40.56	39.56	10.70	11.30	10.05	6.50	54.11	32.17
	LRT	1740	29.2			8.24	7.00	1.24		40.68	39.68	10.61	11.24	8.62	5.85	46.81	37.17
	RRT	1840	30.0			8.21	6.98	1.23		40.62	39.62	10.50	11.20	10.10	5.92	49.60	37.10
							M35A2, 2-1/2-Ton, 6x6 (Loaded)										
9.00-20, 8-PR	LF	3835	72.0	23.20	0.50	8.30	7.06	1.24	15	40.80	40.30	10.90	11.45	11.00	6.24	57.38	66.84
	RF	3805	72.4			8.23	7.00	1.23		40.66	40.16	10.88	11.39	10.93	6.57	61.44	61.93
	LFT	3850	73.0			8.28	7.04	1.24		40.76	40.26	10.75	11.40	11.10	6.20	59.52	64.68
	RFT	3800	74.2			8.27	7.03	1.24		40.74	40.24	10.77	11.41	10.50	6.65	57.35	66.26
	LRT	3910	74.1			8.29	7.05	1.24		40.78	40.28	10.74	11.37	11.05	6.40	59.75	65.44
	RRT	3895	73.2			8.33	7.08	1.25		40.86	40.36	10.68	11.40	11.00	6.32	58.75	66.30
							M51, 5-Ton, 6x6 (Unloaded)										
11.00-20, 12-PR	LF	4075	51.0	23.10	0.40	9.45	8.03	1.42	15	42.80	42.00	11.91	12.63	12.30	7.75	81.06	50.27
	RF	4145	52.0			9.55	8.12	1.43		43.00	42.20	12.10	12.72	11.42	7.77	78.10	53.07
	LFT	3330	40.6			9.53	8.10	1.43		42.96	42.16	11.93	12.62	11.20	7.80	77.73	42.84
	RFT	3360	38.7			9.40	7.99	1.41		42.70	41.90	11.92	12.74	10.90	7.50	72.34	46.45
	LRT	3375	39.5			9.40	7.99	1.41		42.70	41.90	11.97	12.44	11.42	8.10	83.24	40.55
	RRT	3405	38.3			9.42	8.01	1.41		42.74	41.94	11.90	12.42	11.21	8.04	82.00	41.52
							M51, 5-Ton, 6x6 (Loaded)										
11.00-20, 12-PR	LF	5560	82.0	23.10	0.40	9.60	8.16	1.44	15	43.10	42.30	11.93	12.74	12.35	7.80	83.16	66.86
	RF	5600	83.0			9.70	8.25	1.45		43.30	42.50	12.11	12.80	11.36	7.80	78.65	71.20
	LFT	7540	97.0			9.75	8.29	1.46		43.40	42.60	11.90	12.80	12.97	8.30	96.25	78.34
	RFT	7435	98.0			9.63	8.19	1.44		43.16	42.36	11.93	12.77	12.58	8.23	92.46	80.41
	LRT	7780	99.0			9.61	8.17	1.44		43.12	42.32	12.02	12.60	12.72	8.72	101.80	76.42
	RRT	7785	98.0			9.58	8.14	1.44		43.06	42.26	11.92	12.65	12.70	8.60	99.20	78.48

* LF = left front, RF = right front, LR = left rear, RR = right rear, LFT = left front tandem, RFT = right front tandem, LRT = left rear tandem, RRT = right rear tandem.

** Tire diameter = rim diameter + 2 (carcass section height unloaded + average tread height). Carcass diameter = tire diameter - 2 (average tread height). Average tread heights were sufficiently large for tires of the three test trucks to take tread height into account in determining values of tire diameter and carcass diameter.

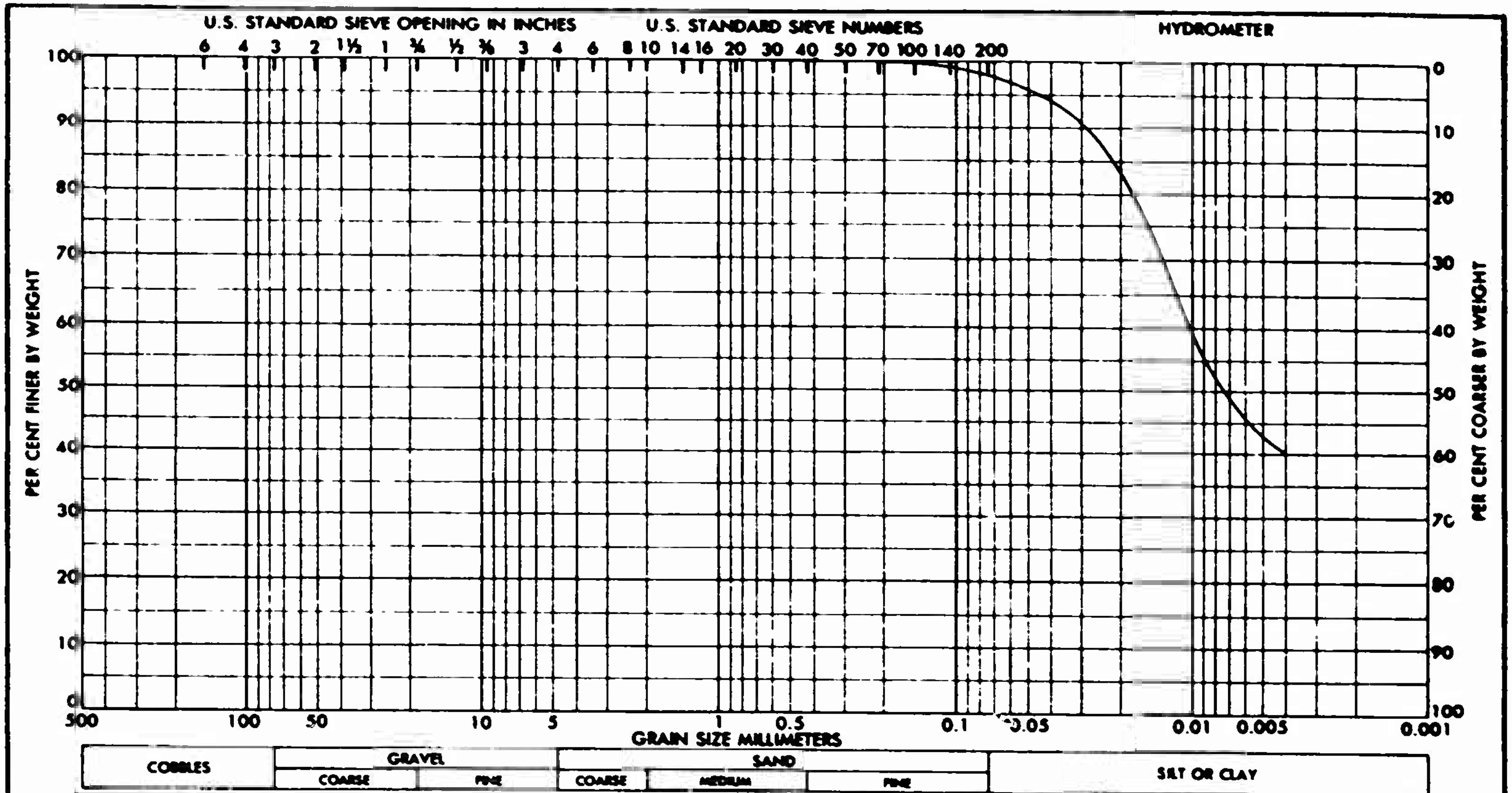

SAMPLE NO	ELEV OR DEPTH	CLASSIFICATION	NAT W%	LL	PL	PI
		FAT CLAY (CH)		62	24	38

Figure 7. Test Soil Gradation and Classification Data

Initial plans called for testing each combination of aircraft tire, load, and inflation pressure and each combination of truck and test load at three levels of soil strength--CI values of about 150, 350, and 600. The primary intent was to test over a range of soil strengths such that (1) the lowest strength would allow test results to be compared with tire performance data from a large block of WES tests conducted at CI values in the 8-68 range, and (2) the highest strength would not be too great to allow at least one of the truck test conditions to produce a 10-pass rut deep enough to use in predicting aircraft tire performance. The total number of tests initially called for was 36 (6 aircraft tire tests and 6 truck tests in each of 3 soil strengths). Conditions that arose as testing progressed required some departure from this format;* sufficient data were developed, however, in slightly fewer tests (34) to satisfy intents (1) and (2) above, as well as all objectives set forth for this study.

d. Test Responses

For the aircraft tires, the test responses measured were rut depth (after passes 2, 10, 20, 50, and 100), and hub movement and towed force (each measured during passes 2, 10, 20, 50, and 100). In routine tests of the three military trucks, the only test response measured was rut depth after vehicle passes 2, 6, and 10. In those few tests where 6-in. ruts were obtained before 10 truck passes or 100 aircraft tire passes, rut depth was measured after the last pass (i.e., the pass that produced the 6-in. rut depth). For those aircraft tire tests that clearly could be conducted to only a few passes, rut depth, towed force, and hub movement were also measured for pass 1.

2. TEST EQUIPMENT AND PROCEDURES

a. Test Pit and Soil Preparation

All tests were conducted indoors in a soil-filled, concrete-lined pit 6 ft deep by 11.7 ft wide, using 130 ft of the 180-ft overall pit length--see figure 8. (A service platform at one end of the pit and an entrance-exit ramp at the other reduced the usable pit length by about 50 ft.) A subgrade of high-strength clay (cone index of about 700) was placed to within 24 in.

---

* Departures from the original test conditions, and the reasons for these departures, are described in the fourth paragraph of Section I.2.a.

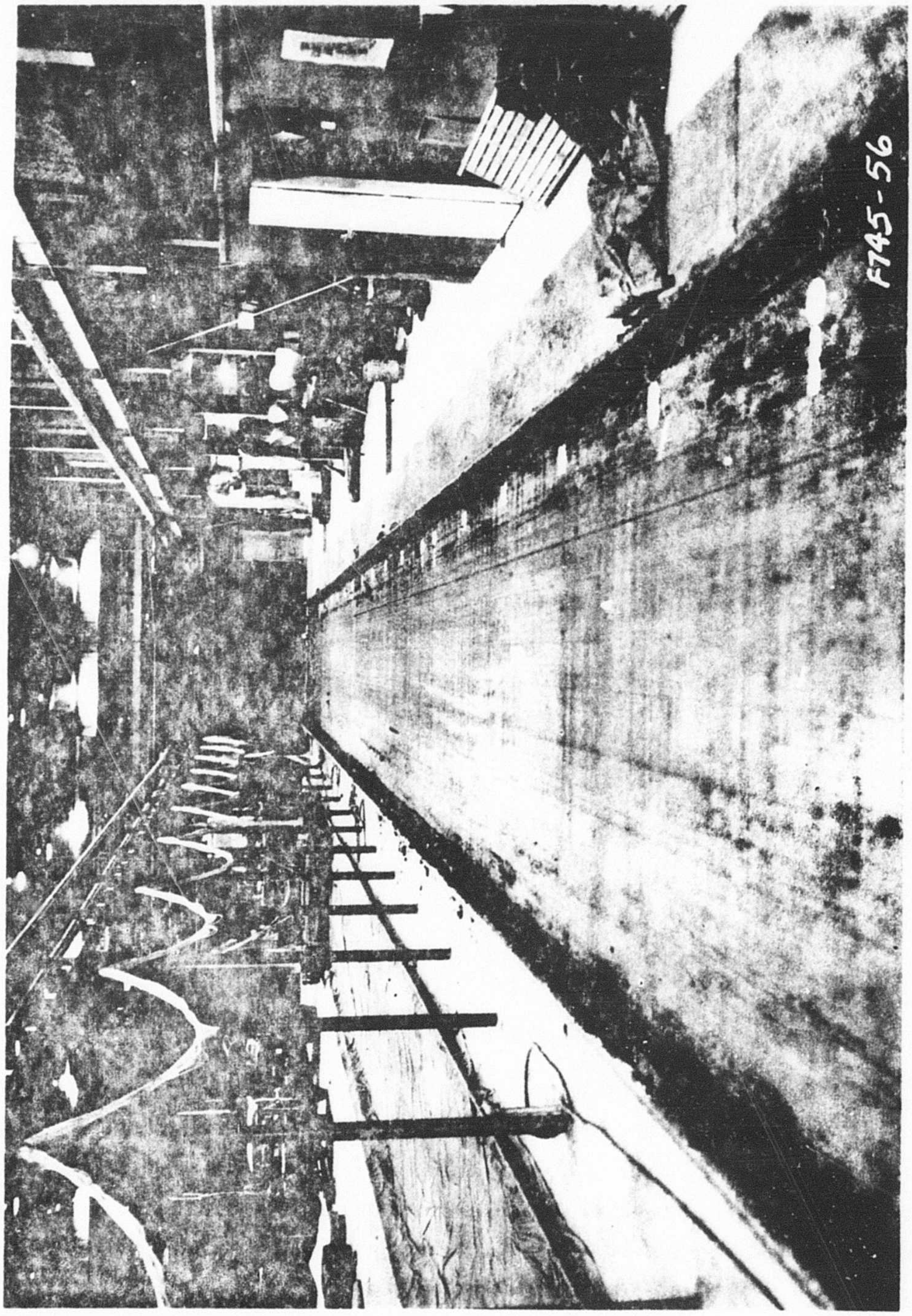

Figure 8. Soil Test Pit

of the top of the pit over the full pit length. Enough soil to fill the top 24 in. was then processed to a prescribed moisture content and placed in the test pit in 6-in. lifts (or layers), the soil in each layer being first pulvimixed (thoroughly cut, aerated, and mixed by the pulvimixer's rotating tines) and then compacted to desired density by trafficking with a 40,000-lb, self-propelled, multiwheeled roller. After the full 24 in. of test soil was in place and compacted, its surface was bladed smooth and level to about the same height as the top of the soil pit.

Uniformity of soil moisture content was essential in the clay test beds, and sufficient measurements of this variable were taken in each stage of soil preparation to assure that moisture content varied only slightly throughout the volume of test soil. In the placement stage, for example, values of moisture content were measured at at least three locations within the 130-ft test length in each of the four 6-in. lifts to assure uniformity of moisture content both over the length and depth of the soil volume.

For the tests reported herein, the measure used to specify soil strength during clay test bed construction was CI. For all strengths tested, the CI value remained nearly constant with depth (see figure 9, for example). Unless specified differently, each value of CI (and of AI) cited hereafter was measured in the 0- to 6-in. soil layer. This does <u>not</u> suggest that this layer had the most influence on the performance of the aircraft tires and the trucks. Choice of this layer was arbitrary, since essentially the same value described the average CI in any buckshot clay layer in the 24 in. of soil above the subgrade.

Plans called for constructing, in order, clay test beds of about 350, 600 and 150 CI. The first two beds were constructed as planned. Tests in the second test bed produced unimportantly small rut depths at 100 passes for both the 20-20 and the 49-17 tires at their most severe test conditions, and hardly measurable 10-pass rut depths with even the loaded 5-ton truck. A third test section was then constructed and tested at a strength level intermediate between the first two (CI of about 475). The value of CI for the fourth test bed was adjusted downward slightly from original plans (from about 150 to 120) to allow test results to be more closely compared with those from a large block of WES tests conducted at lower CI values. The low-strength clay test bed was reworked in place (i.e., the same soil was mixed and compacted in the top 24 in. of the test pit with no new soil required from

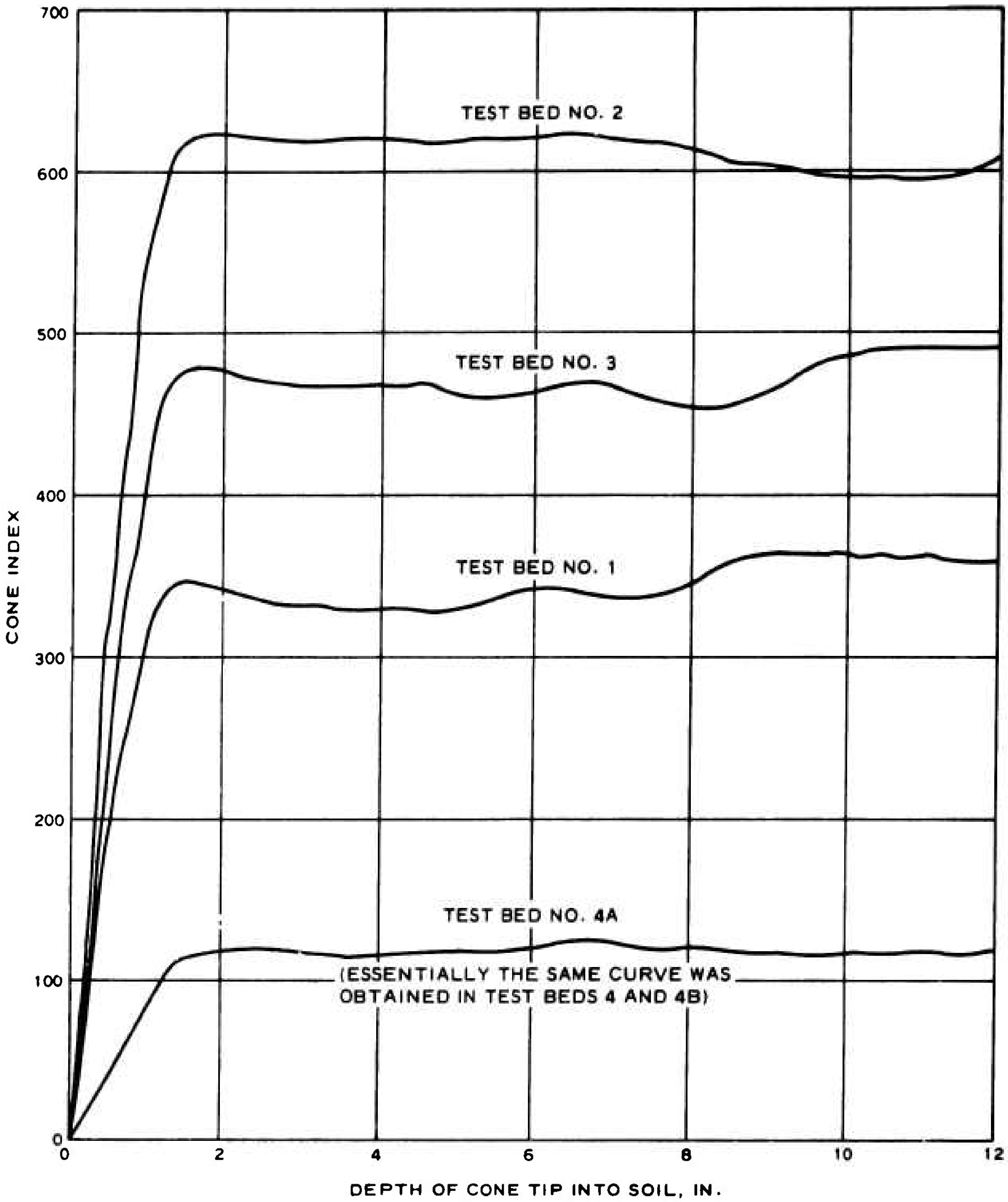

Figure 9. Representative Cone Index Versus Depth Curves for the Four Soil Strength Levels Tested

the storage area) to provide three successive test beds (4, 4A, and 4B) of about 120 CI. This was necessary because the low-strength test condition allowed considerably fewer independent aircraft tire and truck tests (i.e., tests not influenced by others conducted in the same general area) than were possible in the three higher-strength beds.

The primary factors that control the strength of a given soil in the test bed are its density and moisture content and the compactive effort applied. For each test bed, an estimate was made of the moisture content needed to provide the desired CI, and sufficient coverages were made with a 40,000-lb roller to accomplish this objective. Figure 10 shows the relation achieved in the test beds among soil moisture content, dry density, and percent saturation.* The dashed line through the data points has the shape typical of laboratory soil tests at constant compactive effort (as in standard optimum density tests). The data demonstrate that the test pit preparation methods, including compactive effort available, were adequate to achieve 90 percent or greater saturation in the soil whenever moisture content was 22 percent or more.

The relation of cone index to moisture content for the four cone index levels tested is indicated by the data points in figure 11.** The slope of the curve in figure 11 becomes increasingly steep as moisture content decreases. Thus, for small values of moisture content, substantial differences in CI are produced by very small differences in moisture content. Within the length of the soil bed used for any given test, CI values proved to be very uniform, reflecting the care used in maintaining moisture content nearly constant.

b. Dynamometer and Its Instrumentation

Each aircraft tire was tested in a large four-wheeled dynamometer test carriage that rides on two railroad rails that are accurately leveled and spaced 12.7 ft apart. Each rail is set in concrete at ground level

---

* Percent saturation is the ratio, expressed as a percentage, of the volume of water in a given soil mass to the total volume of voids. It is computed from measured moisture content and dry density and the specific gravity of dry soil particles.

** Each data point reflects the average of at least three measurements of each of the two variables taken in the 0- to 6-in. soil layer just after preparation of the soil bed was completed.

NOTE: IN BOTH FIGS., NOS. 1 THROUGH 4B DESIGNATE CLAY TEST BEDS. IN FIG. 10, THE REMAINING NOS. INDICATE PERCENT SATURATION.

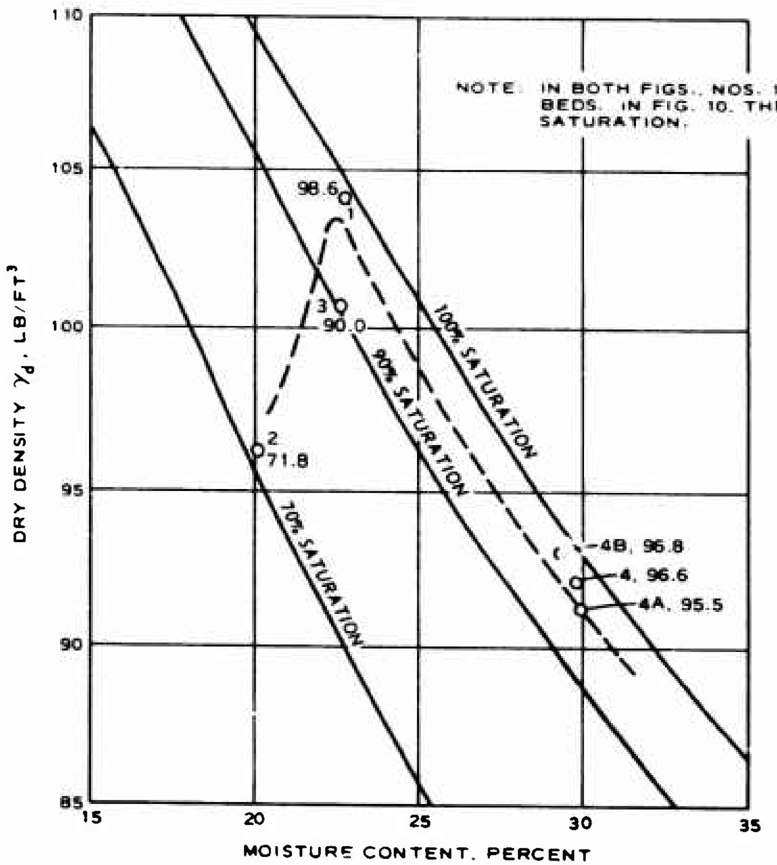

Figure 10. Relation of Dry Density to Moisture Content

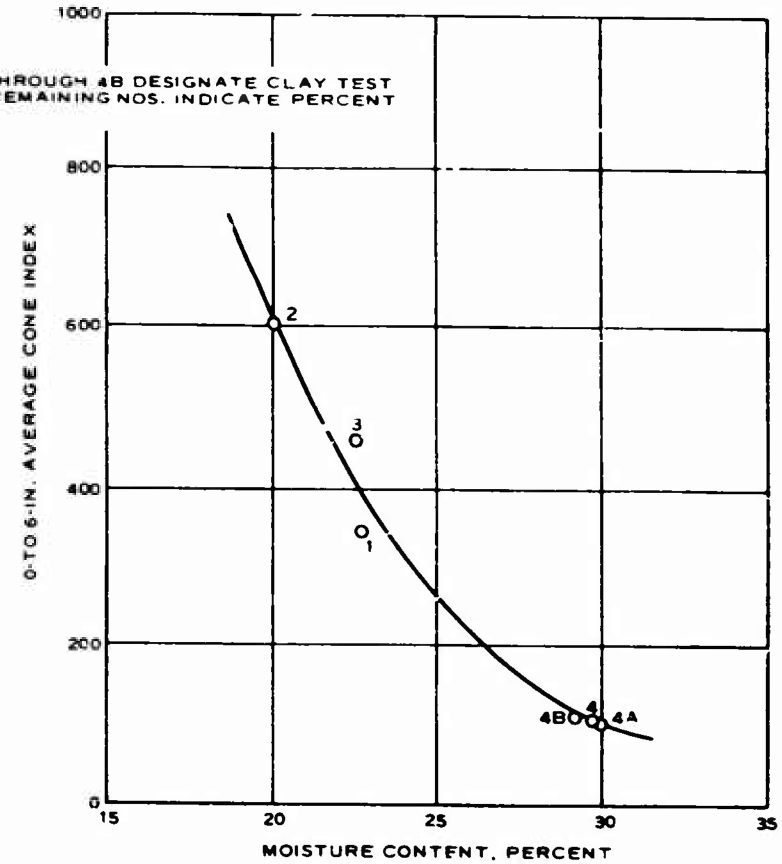

Figure 11. Relation of Cone Index to Moisture Content

6 in. outside the vertical sidewalls of the test pit over which the carriage travels. Each wheel of the test carriage is powered by a 7-1/2-hp d-c electric motor; all four motors are powered by a generator located near the rear of the test frame on which the dynamometer carriage rides. The carriage carries a loading frame which is free to float vertically while applying an adjustable, predetermined vertical load to a test tire or wheel assembly (see figure 12). Test items are mounted to the loading frame through a rigid measurement subframe which attaches to the loading frame by means of two free pivots and two horizontal links. The two pivots (one on each side) define a transverse axis directly above and parallel to the axle of the test wheels, and are instrumented to measure vertical forces. The two horizontal links (also one on each side) restrain the measurement subframe from motion under the influence of forces in the direction of carriage travel, and are instrumented to measure necessary restraining forces. These forces may be readily translated to the test axle axis, while, due to the measurement subframe configuration, vertical forces measured at the pivots may be directly translated to the axis.

Test loads of 25,000 and 35,000 lb were applied by a combination of the weight of the loading frame and measurement subframe* plus sufficient dead weights placed directly atop the measurement subframe and centered above the wheel axle to bring the weight to the desired value. Test weight and pull (vertical and horizontal forces, respectively) acting on the tire were continuously measured during each test. Test load varied slightly during the course of each aircraft tire test because of minor load frame friction and lag in the pneumatic load system response. For a given pass of any given aircraft tire test, the value of load reported is the average value measured during that pass.

Hub movement was continuously measured during each test by a potentiometer that measured vertical movement of the tire's frame-and-axle assembly relative to the carriage. For all tests in the first three soil beds (CI values of 350, 600, and 475), the at-rest zero hub movement condition was obtained when the tire was loaded to its test value in soil just

---

* The combined weight of the dynamometer loading and measurement frames is approximately 11,000 lb. However, some pressure must be maintained in the test carriage pneumatic lift cylinders that regulate net test load. 8670 lb of carriage weight was used in each aircraft tire test.

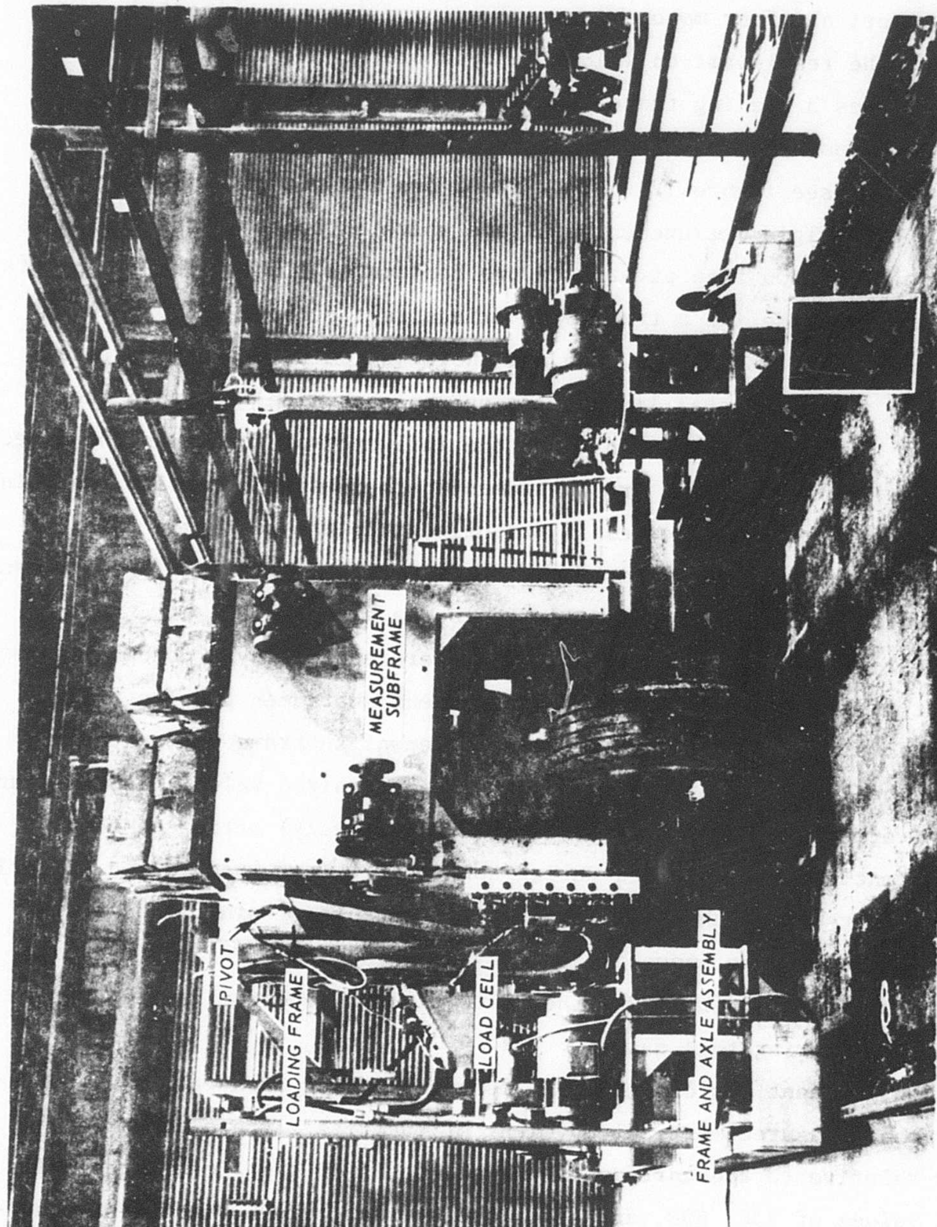

Figure 12. 20-20, 22-PR Tire Mounted in Test Dynamometer Carriage

prior to the start of the test. In the low-strength test beds (4, 4A, and 4B), test load was applied to the tire just prior to in-soil testing as the tire rested on a 1-in.-thick, 3-ft-square steel plate. At-rest zero hub movement was then taken as the value indicated by the potentiometer for the plate-loaded condition minus the difference in elevation between the test soil and the loaded plate. Pretest loading on the steel plate was necessary only in the low-strength test beds because essentially no settling of the aircraft tires into the clay occurred during static pretest loading in the high-strength beds.

During the course of testing, it was determined that account had to be taken of the fact that apparently negative hub movement was caused by travel of the aircraft tires--i.e., the tire hub moved upward relative to its at-rest zero because of in-motion tire flexure. A "dynamic" correction to account for this was developed by measuring on a flat, level concrete surface the amount of upward hub movement associated with each test combination of aircraft tire size, load, and inflation pressure.* Values of dynamic correction are listed in table 1. For a given test, the appropriate correction value was added to the at-rest zero hub movement (described in the preceding paragraph) to produce the zero (or datum) from which in-soil, moving-tire hub movement was measured.

In each aircraft tire test, measurements of load, pull, and hub movement were continuously and simultaneously recorded on an oscillograph chart and on magnetic tape. Operations by a digital computer later transformed the magnetic tape data to the printed numerical form used in the final data analysis. The oscillograph recordings were used both in a backup role (i.e., to provide a check on the digital readings) and in visual checks after each test to determine whether all systems were operating properly and the test appeared to be a valid one.

c. Soil Measurements

Measurements of CI and soil moisture content and density that were

---

* For each aircraft tire size-load-inflation pressure combination, the tire was towed at in-soil test speed (approximately 3 ft/sec) four times (two forward and two reverse) over a 25-ft concrete floor length. (Note that 25 ft is more than 1.5 rolling circumferences for each tire test condition.) The average value of upward hub movement that occurred during the middle 20 ft of each hard-surface test run was measured. No significant variation in this vlaue occurred from pass to pass for any condition tested.

were made during construction of each clay test bed are described in Section II.2.a. Values of moisture content and density were also measured just after the last aircraft tire or truck test in all but two beds (4 and 4B) at at least three locations spaced over the test bed length for each of the four strength levels tested. Before-test and after-test moisture contents and densities are listed in table III.

Measurements of CBR also were taken in test beds of each of the four soil strengths tested. Values of CBR and of CI and AI that were measured very near the CBR locations are listed in table III.

Finally, three samples were taken from each of three test beds (1, 3, and 4A) and subjected to unconsolidated, undrained, triaxial "Q" testing. Major results of the Q tests are listed in table III.

All of the above soil measurements were taken either before or after the aircraft tire and truck tests. During testing, values of both CI and AI were measured before traffic; after aircraft tire passes 2, 10, 20, 50, and 100; and after truck passes 2, 6, and 10 (or after the last aircraft tire or truck pass when less than 100 or 10 passes, respectively, could be accomplished).* Before-traffic measurements were made along the same line followed subsequently by the center line of the aircraft tire, or by the center line of the truck rear tire whose rut was later measured, and as close as practicable to station numbers where rut depths were measured in the test that followed. During-test measurements of CI and AI were located in the bottom of the tire rut and as near as possible to station numbers where rut cross sections were measured. Before- and during-test values of CI and AI appear in tables IV and V.

The equipment used to measure CI and AI consisted of a cone (either 0.5- or 0.196-$in.^2$ base area), shaft, and load cell mounted within a wheeled test carriage that traveled over the two rails mounted outside the soil pit walls. (This carriage was separate from the dynamometer carriage described in Section I.2.b.) The cones were mechanically driven at a soil penetration speed of 72 in./min, and values of CI (or AI) versus soil depth for each soil penetration were recorded simultaneously by an X-Y plotter and on magnetic tape. The X-Y records were used in monitoring

* In those few aircraft tests where it was obvious that very few passes could be made, values of CI and AI were also measured after pass 1.

TABLE III.--PRE-TEST AND POST-TEST SOIL MEASUREMENTS

Test Bed No.	Before-Test* Sta-tion No.	Before-Test* Moisture Content %	Before-Test* Dry Density pcf	Before-Test* Cone Index CI	Before-Test* Airfield Index AI	After-Test Station No.	After-Test Moisture Content %	After-Test Dry Density pcf	After-Test Cone Index CI	After-Test Airfield Index AI	California Bearing Ratio** Sta-tion No.	California Bearing Ratio** CBR %	California Bearing Ratio** Cone Index CI	California Bearing Ratio** Airfield Index AI	Unconsolidated, Undrained Triaxial "Q" Tests Sta-tion No.	Unconsolidated, Undrained Triaxial "Q" Tests Cohe-sion c psi	Unconsolidated, Undrained Triaxial "Q" Tests Angle of Internal Friction ϕ	Unconsolidated, Undrained Triaxial "Q" Tests Specific Gravity G_s
1	12	21.6	105.8			14	21.9	105.5			14	13	395	8.59	20	23.3	5.1	2.67
	20	22.2	105.1			23	22.4	104.4			53	10	318	7.00	72	15.3	6.1	2.67
	60	23.0	103.4			54	23.8	102.9			106	11	324	6.75	119	19.7	6.1	2.71
	94	23.0	103.6			72	24.2	102.7			Avg	11.3	346	7.45	Avg	19.4	5.8	2.68
	124	23.0	103.1			100	23.3	104.1										
	Avg	22.6	104.2	354	7.60	112	23.2	102.9										
						Avg	23.1	103.8	362	7.46								
2	12	19.9	97.0			20	20.2	97.4			20	20	625	12.12	No measurements taken			
	60	20.3	95.1			64	19.3	95.0			64	21	600	11.75				
	94	19.9	96.4			104	19.5	97.1			104	20	651	12.22				
	120	20.0	96.7			Avg	19.7	96.5	634	12.77	Avg	20.3	625	12.03				
	Avg	20.0	96.3	603	12.47													
3	12	22.7	100.4			20	22.1	100.9			10	12	491	10.25	16	32.6	0.0	2.68
	60	22.1	101.4			64	22.0	101.1			60	10	494	10.22	70	32.8	0.0	2.68
	102	22.7	100.6			104	22.1	101.1			108	13	449	10.19	110	33.3	0.0	2.68
	Avg	22.5	100.8	465	9.80	Avg	22.1	101.0	478	10.44	Avg	11.7	478	10.22	Avg	32.9	0.0	2.68
4	20	29.5	92.8			No measurements taken					No measurements taken				No measurements taken			
	64	30.1	91.0															
	100	29.6	92.5															
	Avg	29.7	92.1	114	2.48				116	2.48								
4A	24	29.3	92.2			30	29.7	89.8			24	2.2	104	2.30	18	9.4	0.0	2.66
	68	30.5	90.5			74	30.0	89.3			76	2.2	106	2.36	76	8.8	0.0	2.66
	108	29.9	91.5			108	28.9	90.0			106	2.3	109	2.36	110	9.7	0.0	2.66
	Avg	29.9	91.4	111	2.44	Avg	29.5	89.7	114	2.51	Avg	2.2	106	2.34	Avg	9.3	0.0	2.66
4B	40	29.0	93.2			No measurements taken					No measurements taken				No measurements taken			
	68	29.0	92.9															
	110	29.2	93.2															
	Avg	29.1	93.1	118	2.49				124	2.71								

* All values tabulated for moisture content, dry density, cone index, and airfield index were measured in the 0- to 6-in. soil layer. Single values shown for cone index and airfield index in conjunction with the moisture content/dry density listings are the average values of CI and AI from all penetrations made before- or after-traffic in the truck and aircraft tire tests within a given test bed.

** Values of CI and AI tabulated under "Californis Bearing Ratio" were measured in locations very near those of the CBR's, and at about the same time.

TABLE IV.--AIRCRAFT TIRE TEST RESULTS

Test Bed No.	Test No.	Tire Size Designation	Load W, lb	Inflation Pressure psi	Pass No.	0- to 6-in. Average Cone Index, CI	0- to 6-in. Average Airfield Index, AI	Towed Force P_T lb	Rod-and-Level Rut Depth: Original Soil Surface r, in.	Rod-and-Level Rut Depth: Rut Shoulders in.	Straightedge Rut Depth; Original Soil Surface, in.	Hub Movement in.	Rut Depth Coefficient r/d	Towed Force Coefficient P_T/W	Tire-Clay Numeric N_c *
1	E-73-0004-3	49-17, 26-PR	-	110	0	369	7.85	-	-	-	-	-	-	-	-
			25,092		2	316	6.03	NM†	0.45	0.62	0.62	0.16	0.0094	NM	0.413
			25,597		10	328	6.22		1.29	2.13	1.75	0.74	0.0271		0.405
			25,316		20	342	6.76		2.17	4.51	2.50	1.39	0.0456		0.410
			25,411		50**	394	7.95		5.78	11.22	NM	4.30	0.1214		0.408
1	E-73-0005-3	49-17, 26-PR	-	90	0	294	6.26	-	-	-	-	-	-	-	-
			25,026		2	272	5.71	NM	0.84	1.10	1.06	0.29	0.0177	NM	0.363
			25,132		10	276	5.77		2.28	4.68	2.38	1.10	0.0480		0.362
			25,132		20	296	5.66		3.68	8.04	4.04	2.93	0.0775		0.362
			NM		40**	300	5.60		6.94	11.41	7.21	NM	0.1461		0.362
1	E-73-0008-3	20-20, 22-PR	-	100	0	316	7.02	-	-	-	-	-	-	-	-
			25,661		2	321	7.49	1647	0.71	0.94	NM	0.34	0.0126	0.0642	0.469
			25,931		10	348	6.20	1608	1.55	2.32		0.79	0.0274	0.0620	0.464
			26,219		20	336	6.53	1862	2.14	3.60		1.74	0.0379	0.0710	0.459
			26,482		50	370	7.24	2362	4.25	6.48		2.68	0.0752	0.0892	0.455
			25,980		72**	307	7.44	NM	5.97	-††		4.00	0.1056	NM	0.461
1	E-73-0009-3	20-20, 22-PR	-	75	0	323	7.07	-	-	-	-	-	-	-	-
			26,552		2	295	5.44	1101	0.29	0.36	NM	0.18	0.0051	0.0415	0.561
			26,608		10	274	5.75	1197	0.68	0.95		0.45	0.0121	0.0450	0.562
			26,627		20	318	6.44	1142	0.93	1.44		0.48	0.0165	0.0429	0.542
			26,650		50	300	5.74	1114	1.50	2.46		0.72	0.0266	0.0418	0.541
			26,537		100	316	6.49	1142	2.10	3.89		0.78	0.0373	0.0430	0.544
1	E-73-0010-3	20-20, 22-PR	-	75	0	382	7.73	-	-	-	-	-	-	-	-
			35,007		2	335	7.29	1445	0.18	0.21	0.19	0.32	0.0032	0.0413	0.620
			35,029		10	338	7.59	1445	0.40	0.50	0.46	0.46	0.0071	0.0413	0.619
			35,082		20	362	6.70	1468	0.55	0.68	0.50	0.49	0.0089	0.0418	0.618
			35,143		50	399	7.19	1486	0.88	1.17	1.06	0.65	0.0156	0.0423	0.617
			35,203		100	335	6.64	1517	1.22	1.95	1.54	0.87	0.0216	0.0433	0.616
1	E-73-0011-3	20-20, 22-PR	-	100	0	438	9.13	-	-	-	-	-	-	-	-
			35,390		2	451	9.93	1406	0.22	0.23	0.16	0.01	0.0039	0.0397	0.564
			35,405		10	429	10.47	1418	0.59	0.60	0.59	0.21	0.0104	0.0401	0.564
			35,389		20	438	9.09	1504	0.86	0.91	0.81	0.25	0.0152	0.0425	0.564
			35,356		50	449	8.99	1603	1.28	1.46	1.31	0.46	0.0226	0.0453	0.565
			35,382		100	453	9.53	1813	1.77	2.72	1.91	0.71	0.0313	0.0512	0.564
2	E-73-0012-3	49-17, 26-PR	-	110	0	618	12.74	-	-	-	-	-	-	-	-
			25,570		2	648	12.95	772	0.07	0.08	0.00	0.04	0.0015	0.0302	0.658
			25,091		10	644	12.97	785	0.15	0.19	0.19	0.09	0.0032	0.0313	0.671
			24,931		20	658	13.21	802	0.22	0.28	0.27	0.17	0.0046	0.0322	0.675
			24,999		50	657	13.35	850	0.37	0.48	0.42	0.26	0.0078	0.0340	0.673
			24,908		100	647	13.11	865	0.50	0.65	0.54	0.31	0.0105	0.0347	0.676
2	E-73-0014-3	20-20, 22-PR	-	100	0	625	12.84	-	-	-	-	-	-	-	-
			35,166		2	674	13.65	915	0.04	0.08	0.00	0.06	0.0007	0.0260	0.799
			35,248		10	646	13.80	990	0.10	0.16	0.00	0.08	0.0018	0.0281	0.797
			35,238		20	670	14.12	1016	0.15	0.19	0.00	0.20	0.0027	0.0288	0.797
			35,217		50	667	13.95	1032	0.21	0.28	0.13	0.25	0.0037	0.0293	0.798
			35,262		100	686	14.43	1039	0.26	0.33	0.38	0.33	0.0046	0.0295	0.796
3	E-73-0017-3	20-20, 22-PR	-	100	0	457	10.54	-	-	-	-	-	-	-	-
			35,020		2	444	9.88	1151	0.18	0.30	NM	NM	0.0032	0.0329	0.658
			35,048		10	464	9.29	1304	0.35	0.59		0.04	0.0062	0.0372	0.658
			35,037		20	451	9.01	1338	0.41	0.77		0.03	0.0073	0.0382	0.658
			35,025		50	470	10.35	1390	0.61	1.06	0.75	0.12	0.0108	0.0397	0.658
			34,909		100	506	10.30	1417	0.81	1.47	0.96	0.22	0.0143	0.0406	0.661
3	E-73-0018-3	20-20, 22-PR	-	75	0	438	9.01	-	-	-	-	-	-	-	-
			35,002		2	467	9.83	1008	0.07	0.33	NM	0.08	0.0012	0.0288	0.722
			35,513		10	476	9.96	1307	0.18	0.45		0.05	0.0032	0.0368	0.712
			35,458		20	436	9.31	1307	0.26	0.60	0.44	0.19	0.0046	0.0369	0.713
			35,329		50	455	9.78	1308	0.35	0.74	0.56	0.20	0.0062	0.0370	0.715
			35,329		100	466	10.73	1304	0.43	0.85	0.58	0.20	0.0076	0.0369	0.715
3	E-73-0019-3	20-20, 22-PR	-	75	0	483	9.67	-	-	-	-	-	-	-	-
			24,922		2	444	11.07	785	0.13	0.24	NM	0.14	0.0023	0.0315	0.792
			25,061		10	432	9.90	860	0.24	0.38		0.32	0.0043	0.0343	0.787
			25,024		20	463	10.77	824	0.28	0.56	0.54	0.29	0.0050	0.0329	0.788
			24,994		50	428	8.75	893	0.39	0.67	0.67	0.35	0.0069	0.0357	0.789
			25,041		100	470	10.48	875	0.50	0.90	0.79	0.56	0.0089	0.0349	0.788
3	E-73-0020-3	20-20, 22-PR	-	100	0	477	9.82	-	-	-	-	-	-	-	-
			24,880		2	445	10.10	897	0.23	0.29	NM	0.14	0.0041	0.0361	0.677
			25,099		10	494	9.72	892	0.32	0.44		0.15	0.0057	0.0355	0.671
			25,095		20	476	10.58	919	0.43	0.61	0.59	0.15	0.0076	0.0366	0.671
			25,148		50	471	10.68	952	0.62	0.94	0.78	0.17	0.0110	0.0379	0.669
			25,169		100	460	10.28	991	0.80	1.42	NM	0.25	0.0142	0.0394	0.669
3	E-73-0021-3	49-17, 26-PR	-	110	0	475	10.82	-	-	-	-	-	-	-	-
			25,106		2	526	9.36	1046	0.06	0.32	0.00	0.19	0.0013	0.0417	0.569
			25,379		10	497	9.97	1245	0.30	0.61	0.47	0.36	0.0063	0.0491	0.563
			25,112		20	500	8.63	1331	0.47	0.84	0.69	0.34	0.0099	0.0530	0.569
			25,058		50	509	10.07	1412	0.95	1.96	1.50	0.65	0.0200	0.0563	0.570
			25,166		100	540	11.39	1363	2.01	4.69	2.00	1.65	0.0422	0.0542	0.568
3	E-73-0022-3	49-17, 26-PR	-	90	0	511	10.08	-	-	-	-	-	-	-	-
			25,111		2	424	10.71	1036	0.08	0.28	NM	0.14	0.0017	0.0413	0.583
			25,244		10	463	10.28	1180	0.18	0.48		0.46	0.0038	0.0467	0.580
			25,263		20	460	10.06	1195	0.34	0.91	0.75	0.47	0.0072	0.0473	0.579
			25,385		50	422	10.04	1311	0.60	1.37	0.81	0.56	0.0126	0.0516	0.577
			25,252		100	494	10.96	1315	1.07	2.44	1.34	0.84	0.0225	0.0521	0.580

(Continued)

* $N_c = \frac{AIbd}{W} \cdot \frac{1}{\left(1 - \frac{\delta}{h}\right)^{2}} \cdot \frac{1}{1 + \frac{b}{2d}}$. Each N_c value is based on the before-traffic (0 pass) AI value, and the load W for the particular pass number of interest.

** Last pass.

† NM means "not measured."

†† Top of rut shoulder was scraped by bottom of carriage used for AI and CI measurements.

1 of 2 Sheets

TABLE IV. (CONCLUDED)

Test Bed No.	Test No.	Tire Size Designation	Load W, lb	Inflation Pressure psi	Pass No.	0- to 6-in. Average Cone Index, CI	0- to 6-in. Average Airfield Index, AI	Towed Force P_T lb	Rod-and-Level Rut Depth: Original Soil Surface r, in.	Rod-and-Level Rut Depth: Rut Shoulders in.	Straightedge Rut Depth: Original Soil Surface, in.	Hub Movement in.	Rut Depth Coefficient r/d	Towed Force Coefficient P_T/W	Tire-Clay Numeric N_c *
4B	E-73-0030-3	20-20, 22-PR	-	75	0	116	2.48	-	-	-	-	-	-	-	-
			35,183		1*	128	2.60	-*	4.10	6.22	4.25	2.40	0.0727	-	0.198
4B	E-73-0031-3	20-20, 22-PR	-	75	0	112	2.42	-	-	-	-	-	-	-	-
			25,217		1	118	2.70	3555	3.03	5.08	3.33	2.14	0.0538	0.1410	[illegible]
			25,247		2	120	2.62	3190	4.60	7.67	4.92	3.75	0.0816	0.1264	[illegible]
			25,279		4	117	2.79	-	6.67	11.27	6.83	-	0.1183	-	0.195
4B	E-73-0032-3	20-20, 22-PR	-	100	0	116	2.45	-	-	-	-	-	-	-	-
			24,942		1	119	2.56	4338	3.73	5.67	3.81	2.75	0.0660	0.1739	0.168
			25,172		2	121	2.77	4031	5.73	9.10	5.63	4.60	0.1014	0.1601	0.167
4B	E-73-0033-3	49-17, 26-PR	-	90	0	125	2.71	-	-	-	-	-	-	-	-
			25,045		1	130	2.73	5851	4.40	6.85	4.81	3.16	0.0926	0.2336	0.157
			24,836		2	130	7.68	5481	7.00	11.24	7.43	5.33	0.1474	0.2207	0.158
4B	E-73-0034-3	49-17, 26-PR	-	110	0	121	2.39	-	-	-	-	-	-	-	-
			25,069		1**	-	-	-	-	-	-	-	-	-	0.176

* Test was stopped during first pass when dynamometer carriage was unable to tow tire beyond about 10 ft. Towed force exceeded the range for which its electrical signal gain was set and was, therefore, not recorded.

** Negligible forward movement was obtained because dynamometer carriage was unable to tow the tire for this test condition.

2 of 2 Sheets

TABLE V. --TRUCK TEST RESULTS

Test Bed No.	Test No.	Truck Name	Over-all Test Load lb	Pass No. Truck	Pass No. Single Tire	0- to 6-in. Aver-age Cone Index CI	0- to 6-in. Average Air-field Index AI	Rod-and-Level Rut Depth: Original Soil Surface r', in.	Rod-and-Level Rut Depth: Rut Shoulders in.	Straight-edge Rut Depth; Orig-inal Soil Surface in.	Rut Depth Coeffi-cient r'/d	Truck-Clay Numeric* N_c	Front-Tire Rut Depth; Original Soil Surface r , in.	Rut Depth Coeffi-cient r/d	Single Front Tire-Clay Numeric** N_c
1	E-73-0001-3	M715	9,305	0	0	385	8.22	-	-	-	-	-	-	-	-
		(L)+		2	4	352	8.35	0.05	0.06	N.M.++	0.0015	1.479	N.M.	-	-
				6	12	375	7.90	0.06	0.07	↓	0.0018	↓	↓	-	-
				10	20	382	8.19	0.06	0.09		0.0018			-	-
1	E-73-0002-3	M35A2	23,095	0	0	318	7.00	-	-	-	-	-	-	-	-
		(L)		2	6	314	7.05	0.19	0.23	N.M.	0.0047	0.964	0.13	0.0032	0.979
				6	18	342	7.06	0.28	0.37	↓	0.0070	↓	0.15	0.0037	↓
				10	30	345	7.20	0.31	0.46		0.0077		0.19	0.0047	
1	E-73-003-3	M51	41,700	0	0	324	6.75	-	-	-	-	-	-	-	-
		(L)		2	6	347	6.74	0.25	0.39	0.24	0.0059	0.598	0.06	0.0014	0.747
				5	18	326	6.65	0.42	0.86	0.47	0.0099	↓	0.13	0.0031	↓
				10	30	353	7.00	0.53	1.17	0.68	0.0125		0.17	0.0040	
1	E-73-006-3	M51	21,690	0	0	395	8.59	-	-	-	-	-	-	-	-
		(U)+		2	6	452	9.49	0.03	0.11	0.00	0.0007	1.446	0.05	0.0012	1.280
				6	18	419	8.71	0.06	0.13	0.00	0.0014	↓	0.10	0.0024	↓
				10	30	416	9.08	0.07	0.13	0.00	0.0017		0.12	0.0029	
1	E-73-0007-3	M35A2	13,160	0	0	354	8.07	-	-	-	-	-	-	-	-
		(U)		2	6	371	7.85	0.14	0.16	N.M.	0.0035	1.899	0.05	0.0013	1.378
				6	18	368	7.57	0.17	0.19	↓	0.0043	↓	0.11	0.0028	↓
				10	30	383	6.99	0.19	0.24		0.0048		0.13	0.0033	
2	E-70-0013-3	M51	41,700	0	0	565	11.85	-	-	-	-	-	-	-	-
		(L)		2	6	598	12.03	0.03	0.05	0.00	0.0007	1.049	0.03	0.0007	1.312
				5	18	607	12.70	0.06	0.06	0.00	0.0014	↓	0.02	0.0005	↓
				10	30	569	10.78	0.08	0.09	0.00	0.0020		0.02	0.0005	

(Continued)

* Truck-clay numeric $N_c = \frac{AIbd}{W} \cdot \frac{1}{(1 - \frac{\delta}{h})^2} \cdot \frac{1}{1 + \frac{b}{2d}}$, where values of W, b, and d are average values for the whole truck.

** Single front tire-clay numeric $N_c = \frac{AIbd}{W} \cdot \frac{1}{(1 - \frac{\delta}{h})^2} \cdot \frac{1}{1 + b/2d}$, where values of W, b, and d are average values for the front-axle tires only.

\+ (L) means "loaded," (U) means "unloaded."

++ N.M. means "not measured."

1 of 3 Sheets

TABLE V. (Continued)

Test Bed No.	Test No.	Truck Name	Over-all Test Load lb	Pass No. Truck	Pass No. Single Tire	0- to 6-in. Aver-age Cone Index CI	0- to 6-in. Average Air-field Index AI	Rod and Level Rut Depth: Original Soil Surface r', in.	Rod and Level Rut Depth: Rut Shoulders in.	Straight-edge Rut Depth; Orig-inal Soil Surface in.	Rut Depth Coeffi-cient r'/d	Truck-Clay Numeric N_c	Front-Tire Rut Depth; Original Soil Surface r, in.	Rut Depth Coeffi-cient r/d	Single Front Tire-Clay Numeric N_c
3	E-73-0015-3	M51 (L)	41,700	0	0	444	9.14	-	-	-	-	-	-	-	-
				2	6	392	7.94	0.10	0.12	0.00	0.0024	0.809	0.02	0.0005	1.012
				6	18	466	9.99	0.15	0.21	0.17	0.0035		0.04	0.0009	
				10	30	445	9.24	0.21	0.27	0.23	0.0050	↓	0.10	0.0024	↓
3	E-73-0016-3	M35A2 (L)	23,095	0	0	438	9.34	-	-	-	-	-	-	-	-
				2	6	464	10.09	0.14	0.23	0.00	0.0035	1.286	0.05	0.0012	1.306
				6	18	479	10.26	0.17	0.23	0.00	0.0042		0.05	0.0012	
				10	30	442	10.13	0.16	0.22	0.00	0.0040	↓	0.06	0.0015	↓
4	E-73-0023-3	M715 (U)	6,290	0	0	115	2.53	-	-	-	-	-	-	-	-
				2	4	116	2.53	0.30	0.31	0.25	0.0089	0.665	N.M.	-	-
				6	12	116	2.54	0.46	0.61	0.44	0.0136			-	-
				10	20	130	2.79	0.57	0.87	0.54	0.0168	↓	↓	-	-
4	E-73-0024-3	M715 (L)	9,305	0	0	112	2.49	-	-	-	-	-	-	-	-
				2	4	114	2.41	0.59	0.91	0.56	0.0173	0.448	0.16	0.0047	0.520
				6	12	114	2.57	1.06	1.87	0.96	0.0310		0.46	0.0136	
				10	20	125	2.48	1.38	2.58	1.52	0.0404	↓	0.57	0.0169	↓
4	E-73-0025-3	M35A2 (U)	13,160	0	0	115	2.53	-	-	-	-	-	-	-	-
				2	6	105	2.19	0.54	0.92	0.58	0.0136	0.595	0.68	0.0173	0.432
				6	18	102	2.29	1.04	1.98	1.25	0.0257		1.00	0.0254	
				10	30	105	2.27	1.42	2.92	1.58	0.0358	↓	1.39	0.0353	↓
4	E-73-0026-3	M25A2 (L)	23,095	0	0	109	2.28	-	-	-	-	-	-	-	-
				2	6	112	2.51	1.56	2.85	2.21	0.0387	0.314	1.11	0.0276	0.319
				6	18	110	2.62	2.80	5.92	2.88	0.0695		1.80	0.0447	
				10	30	111	2.42	3.62	7.71	4.21	0.0899	↓	2.42	0.0602	↓
4	E-73-0027-3	M51 (U)	21,690	0	0	120	2.59	-	-	-	-	-	-	-	-
				2	6	106	2.28	0.69	1.07	0.69	0.0150	0.436	0.84	0.0200	0.386
				6	18	105	2.49	1.10	2.55	1.04	0.0245		1.30	0.0309	
				10	30	110	2.45	1.86	3.94	2.15	0.0443	↓	1.84	0.0463	↓

(Continued)

2 of 3 Sheets

TABLE V. (Concluded)

Test Bed No.	Test No.	Truck Name	Over-all Test Load lb	Pass No. Truck	Pass No. Single Tire	0- to 6-in. Aver-age Cone Index CI	0- to 6-in. Average Air-field Index AI	Rod-and-Level Rut Depth: Original Soil Surface r', in	Rod-and-Level Rut Depth: Rut Shoulders in.	Straight-edge Rut Depth inal Soil Surface in.	Rut Depth Coeffi-cient r'/d	Truck-Clay Numeric N_c	Front-Tire Rut Depth; Original Soil Surface r, in.	Rut Depth Coeffi-cient r/d	Single Front Tire-Clay Numeric N_c
4A	E-73-0038-3	M51 (L)	41,700	0	0	110	2.48	-	-	-	-	-	-	-	-
				2	6	115	2.50	3.69	5.72	3.83	0.0870	0.220	1.36	0.0321	0.275
				6*	18	116	2.56	7.09	9.37	7.63	0.1673		2.40	0.0566	
4A	E-73-0029-3	M35A2 (L)	23,095	0	0	112	2.38	-	-	-	-	-	-	-	-
				2	6	105	2.37	1.56	2.68	1.69	0.0387	0.328	1.01	0.0251	0.333
				6	18	108	2.30	4.39	6.56	4.67	0.1090		2.06	0.0512	
				10	30	112	2.45	5.82	8.52	6.15	0.1445		2.75	0.0684	

*Last pass.

3 of 3 Sheets

each test as it progressed and as backup for the digital records on magnetic tape. Numerical values developed from the magnetic tape records were used in the final data analysis.

d. Aircraft Tire Tests

Each aircraft tire was tested by (1) loading the tire in the dynamometer test carriage; (2) adjusting tire-inflation pressure to the prescribed level; (3) establishing zero levels (datums) for load, towed force, and hub movement; and (4) continuously recording values of these three variables as the tire was slowly towed forward and backward for a total of 100 passes (or until at least a 6-in. rut was developed). The distance traveled during each pass was approximately 20-23 ft.* Test speed was approximately 3 ft/sec. Test values of load, towed force, and hub movement are listed in table IV.

The aircraft tires were tested in clay beds 1, 2, 3, and 4B (strength levels of about 350, 600, 475, and 120 CI, respectively). All aircraft tire tests in beds 2 and 4B and 2 of the 6 tests in bed 3 were made along the longitudinal center line of the test pit in a test bed length that included no truck tests. All 6 aircraft tire tests in bed 1, and 4 of the 6 in bed 3 were made along the longitudinal line that centered the widest soil bed space untouched by the previously conducted truck tests. (See Section II.2.e for more details.) Each aircraft tire test that was enclosed between ruts of a truck test covered a longitudinal distance equal to half that of the truck test.

A profile of soil test bed elevation along the center line of the straight path followed by the aircraft tire was measured by rod and level before traffic and after passes 2, 10, 20, 50, and 100 (or after the last pass when a 6-in. rut was produced). Cross-section elevations of the tire rut also were measured by rod and level at three stations in the middle 8 ft of the test length before traffic and after the tire passes just mentioned. Values of rut depth were determined from each cross-section record relative both to the original soil surface and to the top of the rut shoulders (as in figures 2a and 2b, respectively). For each test and pass number sampled, average values of these two rut

*See Sections II.1.a. and II.2.b. for more details.

depths are listed in table IV.

Rut depth was also measured at each cross-section location "by hand" using a straightedge (a thick, metal yardstick), a ruler, and a rubber hammer to force the straightedge into the position illustrated in figure 2a. Average values of these measurements also appear in table IV.

e. Truck Tests

A given test was conducted by moving the truck slowly forward and then backward for a total of 10 truck passes, or until at least a 6-in. rut was developed. Test speed was approximately 3 ft/sec. The driver was able to maintain very nearly the same straight-line path on each truck pass with the aid of voice signals from other test personnel, and by keeping the tip of a truck-mounted pointer in a position directly above one of the rails on the side of the test pit (see figure 13).

Only CI, AI, rut depth, and rut depth relative to rut shoulders were measured during tests of the three military trucks (results listed in table V). Each of these variables was measured in one tire rut, as described below.

Truck tests were conducted in clay beds 1 (CI $\approx$ 350), 2 (CI $\approx$ 600), 3 (CI $\approx$ 475), 4 and 4A (CI $\approx$ 120 for each). In these beds, the test lengths used by the M715, M35A2, and M51 trucks were approximately 40, 44, and 46 ft, respectively. In clay beds 1, 2, and 3 both aircraft tire and truck tests were conducted; in beds 4 and 4A, only truck tests. More than one set of passes (either truck or truck and aircraft tire) were run only in beds 1, 3, and 4. In the other two truck test beds--2 and 4A--each truck was tested with its left front tire about 2 ft in from the soil pit sidewall, and measurements of AI, CI, and tire rut were made in the right-side rut.

In clay bed 3 (CI $\approx$ 475), only two truck tests were conducted (loaded M51 and loaded M35A2 trucks produced 10-pass rut depths of 0.21 in. and 0.16 in., respectively), and the same procedure described for beds 2 and 4A was used. In bed 4 (CI $\approx$ 120) the procedure for the first test in a given length of bed was the same as in beds 2 and 4A; the second test of the same truck in a given bed length was run with the truck's left tires centered on the space between ruts made by the first test (see figure 13, for example). Second-test AI, CI, and tire ruts were measured in the left-side rut.

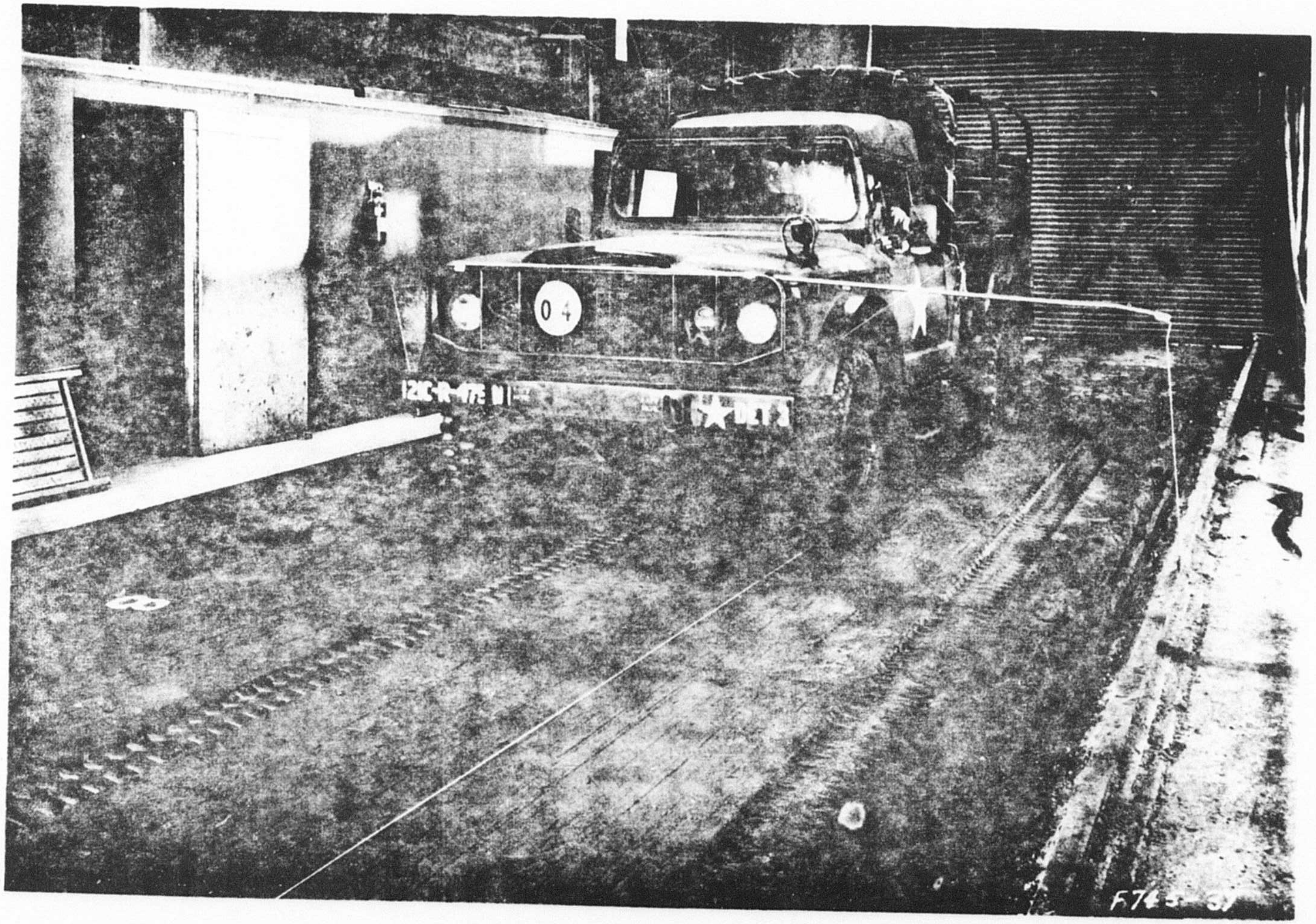

Figure 13. Front View of M715 Truck in Position to Begin Test Run

In clay bed 1 (CI · ·350), each of the three trucks was tested loaded, and the M51 and M35A2 trucks were subsequently tested unloaded. (The M715 truck was not tested unloaded since its loaded test produced a 10-pass rut of only 0.06 in.) Each of the first three truck tests was conducted with the front left tire approximately 12 in. in from the soil pit sidewall, with AI, CI, and tire rut measured in the right-side rut. The second test of the M35A2 truck (test 6) was conducted in the same bed length as the first test of tha‿ truck; the M51 was tested unloaded (test 7) in the same length as was the loaded M715. For tests 6 and 7, the left rear truck tires were positioned such that their right side was 6 in. to the left of the rut made by the right-side tires of the previous truck test. Measurements of AI, CI, and tire rut for these two tests were made in the right-side rut.

For each truck test, cross section elevations were measured before traffic and after truck passes 2, 6, and 10 (or after the pass that produced a 6-in. rut) at three stations within the middle 16 ft of test length trafficked by the full truck length. From these records, average values were determined of maximum rut depth relative both to the original soil surface and to the top of the rut shoulders. Maximum truck rut depth relative to the original soil surface was also measured by the straightedge-and-ruler method at the same stations and after the same passes just mentioned. The maximum rut depth produced by only the truck's front tires was determined from soil profiles measured at the times mentioned above. Values of each of these four descriptors of the tire rut are listed in table V.

For all three trucks, the distance between tires on the front axle was different from that on the second or second and third axles. This caused maximum rut depths to occur over a range of locations relative to the center line of the front tire. Figure 14 illustrates, from cross-section records, two of the rut patterns obtained.

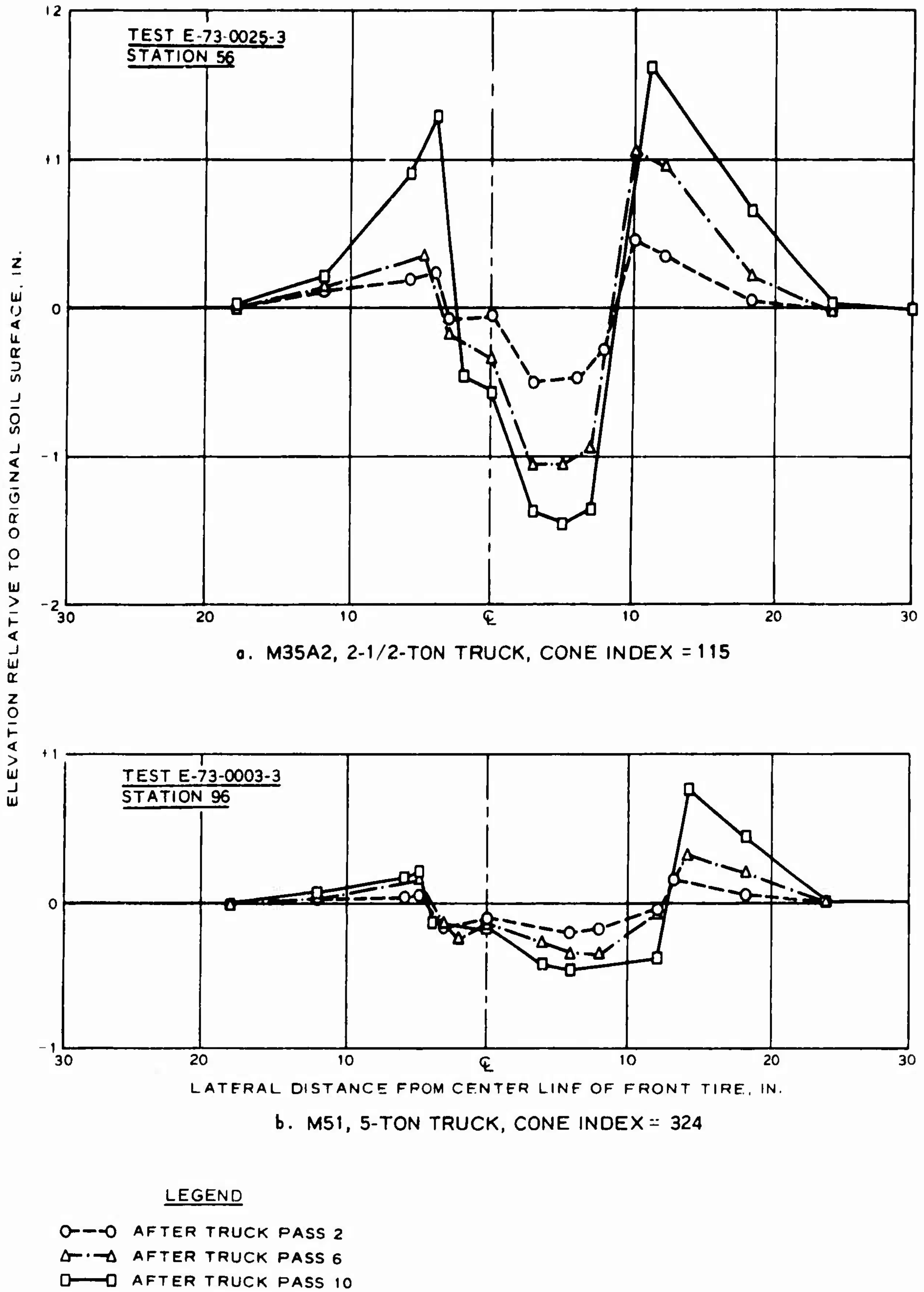

Figure 14. Representative Rut Cross Sections for the M35A2 and M51 Trucks

SECTION III

DATA ANALYSIS

1. SOIL STRENGTH CHARACTERIZATION

a. Cone Index, Airfield Index, and CBR

Because CI, AI, and CBR are often used to describe the strength of fine-grained soils in the field, it was considered useful to describe the relations among them for the test buckshot clay. The relation, in fine-grained soils,

$$CI = 50 \quad AI$$

was deliberately designed into the instruments, scales, and procedures for obtaining these two quantities. Examination of the data developed in the present program indicates that this relation is appropriate for use in this study.

The scale for AI was, moreover, selected to provide an index whose numerical value in fine-grained soil is of the same order as that of the CBR. Because of the more extensive difference between CBR and AI tests (than between two conceptually similar cone penetration tests), there is no single, broadly applicable correlation between AI (or CI) and CBR. It is possible, however, to establish a useable correlation for specific soils (references 4 and 5). This is done in figure 15, in which each data point represents the average of three measurements of the variables of interest from test beds 1, 2, 3, and 4A (see table III). Though based on only four data points, the solid curve in figure 15 is considered to provide a reasonable description of the CI versus CBR and AI versus CBR relations for buckshot clay (only).

b. Effect of Tire Traffic

The buckshot clay was effectively remolded by its preparation process so that tire traffic was expected to produce very little change in soil strength. Values of AI and CI presented in tables IV and V for the aircraft tire and truck tests, respectively, show no significant changes with pass number. Only before-traffic values of soil strength are used in the remainder of this report to establish the basic relations required to fulfill the objectives of this study.

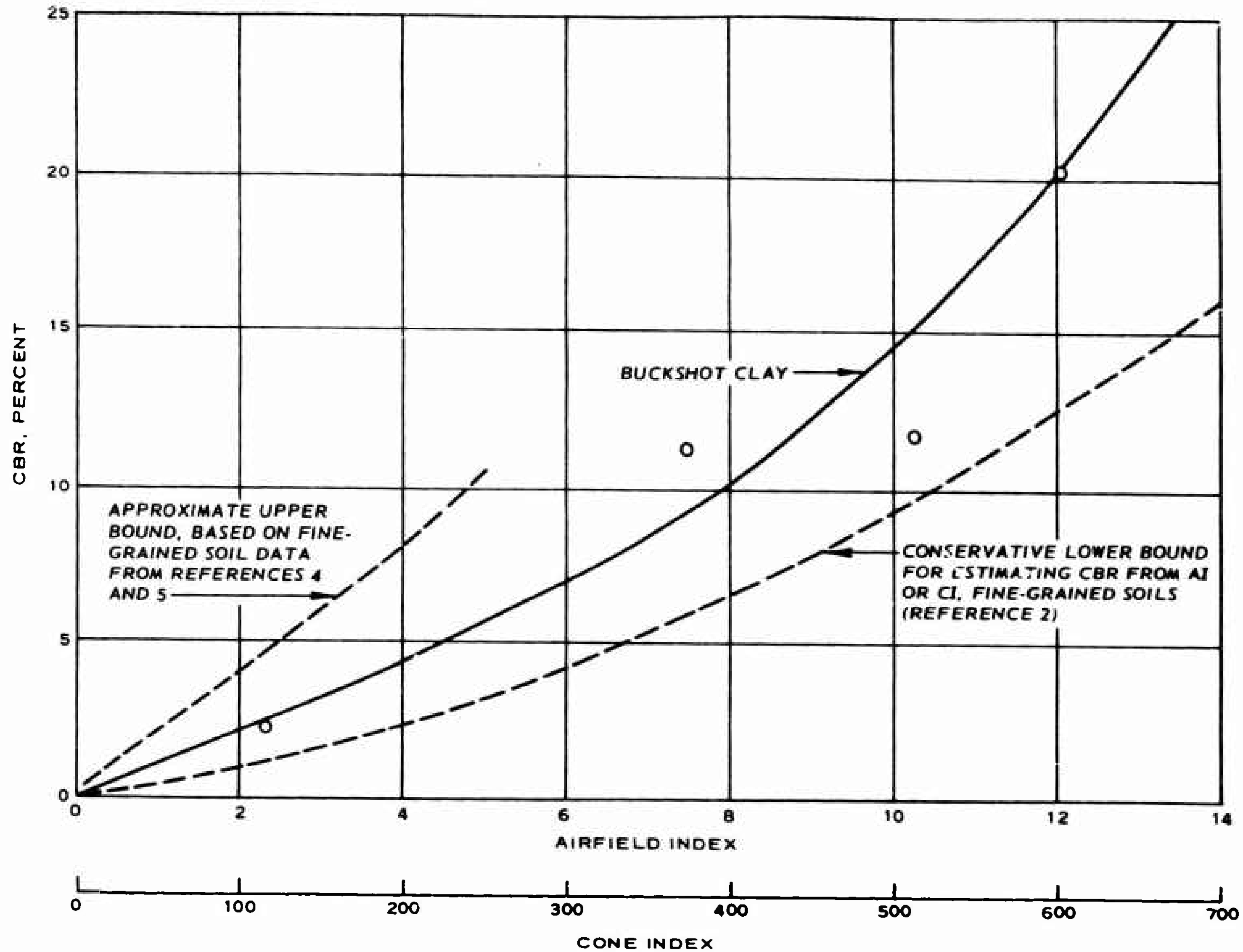

Figure 15. Relations of CBR to Cone Index and to Airfield Index for Homogeneous (Laboratory Test Pit) Buckshot Clay

2. CONSOLIDATING AIRCRAFT TIRE PERFORMANCE DATA

a. General Approach

Dimensionless prediction terms, or "numerics," have been successfully used by WES for several years to describe the performance of pneumatic tires in soil. These terms were developed by means of dimensional analysis.

For example, in reference 6 it was found that a single independent dimensionless variable was a sufficient basis for developing reliable, unique relations to predict the slow-speed sinkage, towed force, pull, and torque performance for a wide variety of tire sizes, proportions, and deflections, in a given soil type over a large range of soil strengths and loads. For tires operating in saturated, highly plastic, essentially purely cohesive clay, this dimensionless variable took the form $\frac{\overline{CI}bd}{W}\left(\frac{\delta}{h}\right)^{1/2}$, where CI = cone index, b = tire section width, d = tire carcass diameter, W = wheel load, δ = maximum hard-surface deflection, and h = tire carcass section height. Of direct interest in the present study is the fact that the towed force (P_T) and cumulative rut depth (r) (which is closely related to sinkage z) can both be predicted by use of this relatively simple numeric, or prediction term: i.e., for the type of clay soil of present interest:

$$\frac{P_T}{W} = f_{P_T}\left[\frac{\overline{CI}bd}{W}\left(\frac{\delta}{h}\right)^{1/2}\right]$$

and

$$\frac{r}{d} = f_z\left[\frac{\overline{CI}bd}{W}\left(\frac{\delta}{h}\right)^{1/2}\right]$$

Note that, at least within the range of test conditions under which this prediction term was developed, a single value of P_T/W and a single value of r/d is predicted for each particular value of $\frac{\overline{CI}bd}{W}\left(\frac{\delta}{h}\right)^{1/2}$, no matter what values CI , b , d , W , δ , and h take.

b. Range of Application of Numerics

The prediction term developed in reference 6 was demonstrated to be applicable for conventional toroidal-shaped, pneumatic tires operating at low speed (5 ft/sec or less). The largest value of load considered was 4,500 lb. Tire section widths ranged from 4.2 to 11.4 in., carcass diameters from 14.1 to 41.2 in., soil strengths from 14 to 67 CI, aspect ratios (d/b values) from 3 to 7, and deflections from 15 to 35 percent.

In a later report (reference 7), an improved alternative prediction term, $\frac{\overline{CI}bd}{W} \cdot \frac{1}{(1 - \frac{\delta}{h})^2} \cdot \frac{1}{1 + \frac{b}{2d}}$, was developed that has the advantages of (a) predicting the in-soil performance of tires with d/b values from 1 to 15, and (b) predicting the performance of tires of very small deflection (to as little as 1 percent) with better accuracy than can $\frac{\overline{CI}bd}{W} \cdot \frac{\delta}{h}^{1/2}$. A still more recent report (reference 8) shows that the WES numeric system can predict with useful accuracy the in-soil performance of very small-scale tires (to as small as 8 in. in diameter).

The dimensionless prediction term used in all considerations from this point on is $\frac{\overline{AI}bd}{W} \cdot \frac{1}{(1 - \frac{\delta}{h})^2} \cdot \frac{1}{1 + \frac{b}{2d}}$, hereafter referred to as the tire-clay numeric N_c. Good agreement was obtained between test results listed in reference 7 and those produced in this study (for much larger tire sizes, wheel loads, and AI values), as will be demonstrated.

c. Rut Depth

Figure 16 shows two of the widely different combinations of rut depth and pass number that were produced in this test program. Note that, for the same tire (20-20, 22-PR), more severe values of load and inflation pressure are shown for the test in figure 16a. However, the test in figure 16b developed a much larger rut depth because its soil was prepared to a much weaker condition (AI = 12.84 in figure 16a, AI = 2.42 in figure 16b).

To determine in equation form the relations among aircraft tire rut depth coefficient r/d, tire pass number n, and tire-clay numeric N_c, it was necessary first to ascertain the relation between r/d and N_c for each pass on which rut depth r* was measured (normally passes 2, 10, 20, 50, and 100). In figure 17, arithmetic plots of r/d versus N_c

* Unless otherwise noted, rut depth r is the average value of maximum rut depth measured relative to the original soil surface, as computed from rod-and-level cross-section measurements.

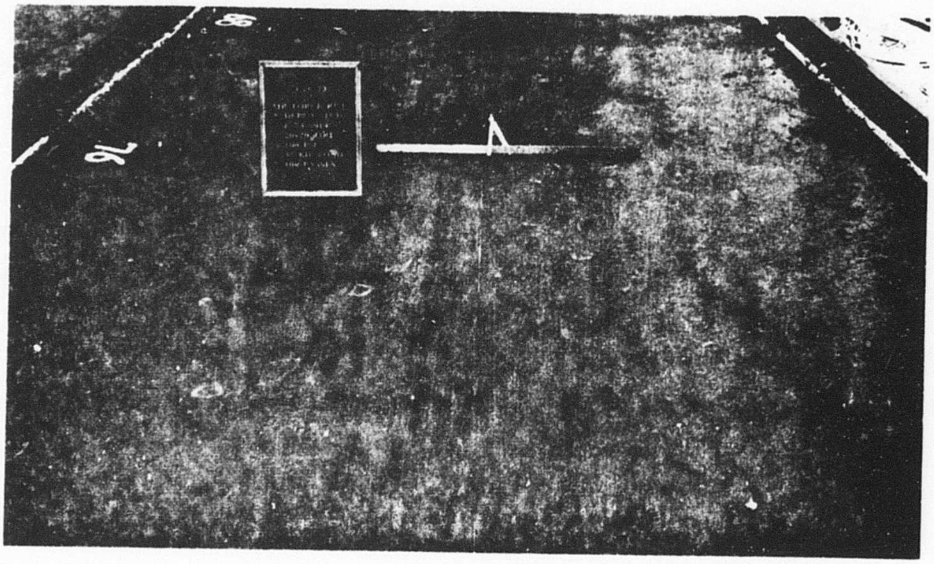

a. AFTER 100 PASSES; AI = 12.84; TIRE INFLATION PRESSURE = 100 PSI; TIRE LOAD = 35 KIPS

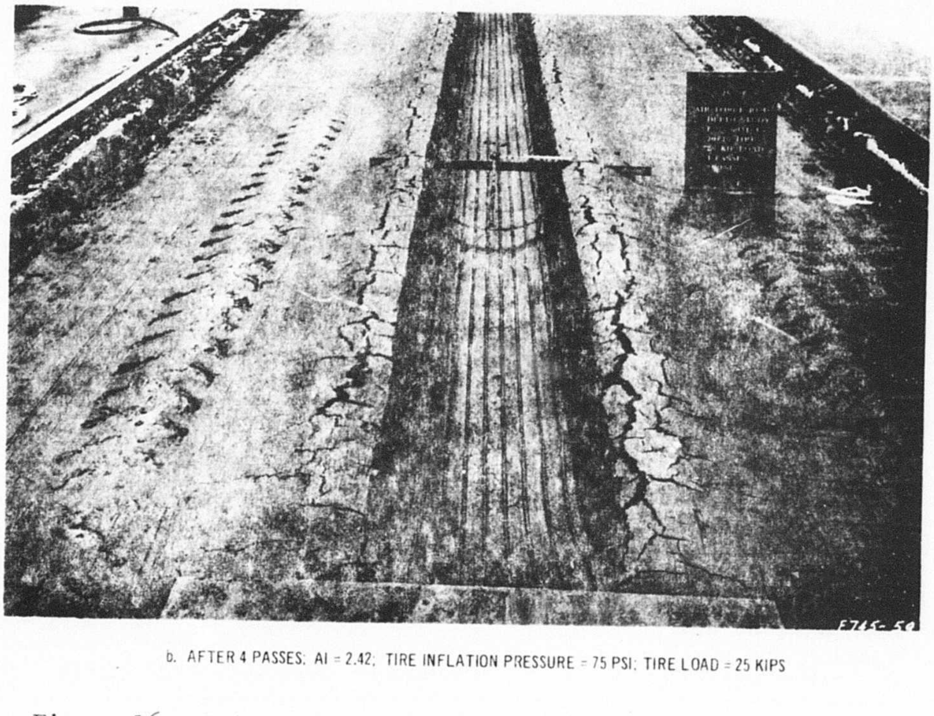

b. AFTER 4 PASSES; AI = 2.42; TIRE INFLATION PRESSURE = 75 PSI; TIRE LOAD = 25 KIPS

Figure 16. Ruts Produced by the Towed 20-20, 22-PR Aircraft Tire in Buckshot Clay

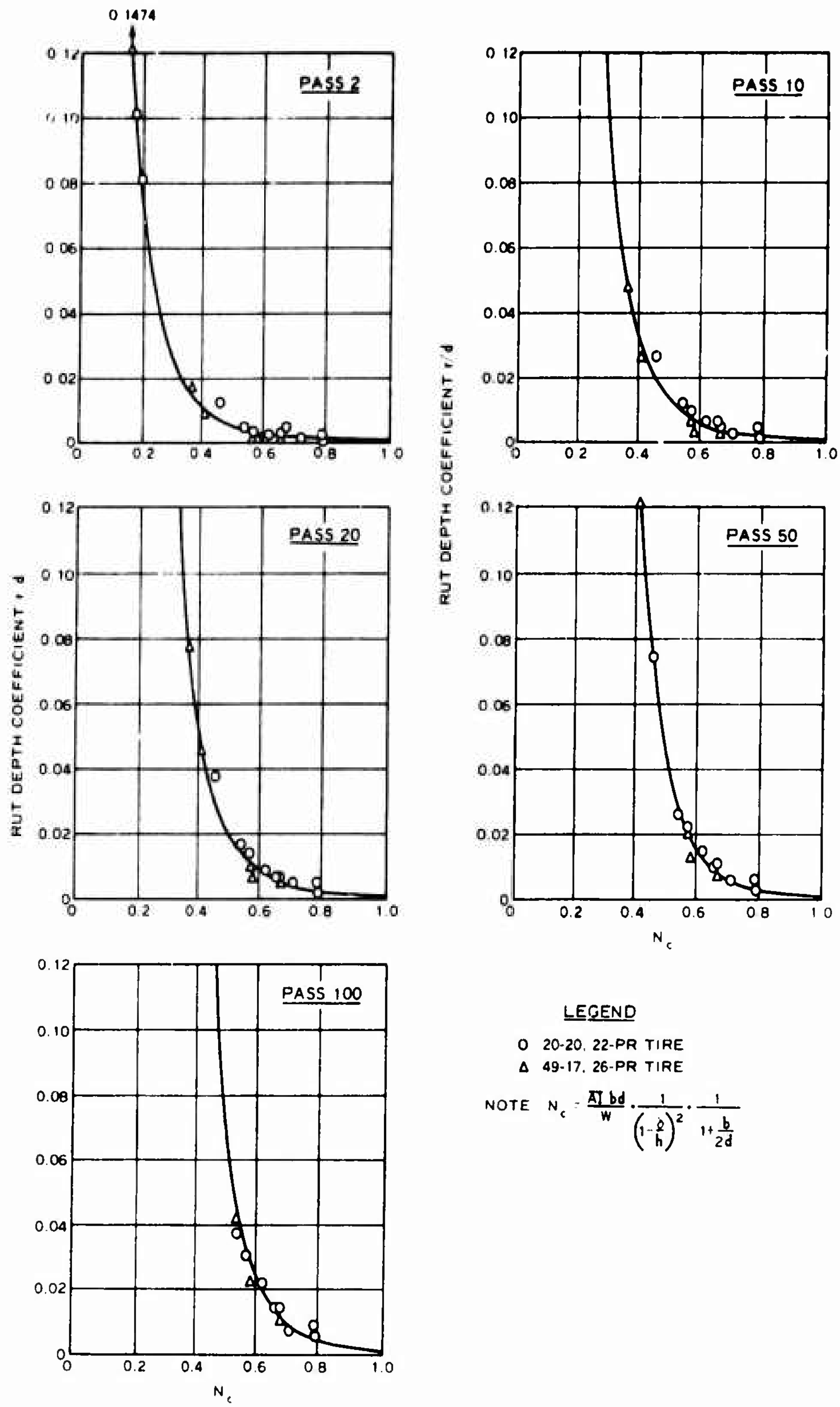

Figure 17. Arithmetic Plots of r/d Versus N_c for Passes 2, 10, 20, 50, and 100 of Two Towed Aircraft Tires

show that for a given value of N_c , values of r/d increases with pass number n . Note, also, that as the number of passes increases, the general shape of the curves is maintained, but the degree of curvature becomes increasingly severe. These data plotted in logarithmic form indicate that for each pass number considered, r/d is related to N_c by an equation of the form

$$r/d = a\, N_c^{\,b} \tag{1}$$

For the relations in figure 17, values of a and b are

$$a = 0.001 \tag{2}$$

and

$$b = -2.27\, n^{0.220} \tag{3}$$

where n is tire pass number.

From equations 1, 2, and 3 the equation to describe rut depth for multiple passes of a towed (free-rolling, nonpowered) tire is

$$r/d = 0.001\, N_c^{\,-2.27n^{0.220}} \tag{4}$$

The family of curves described by equation 4 is presented graphically in figure 31* for passes 1-1000 and values of N_c up to 0.9. The relation described by equation 4 is mathematically suitable only for values of N_c less than 1.0. At N_c values of the order of 1.0 or larger, corresponding rut depth coefficients have values so small as to cause no practical concern. To illustrate, from equation 4 for $N_c = 0.9$ and pass numbers of 100 and 1000, values or r/d are 0.00193 and 0.00298, respectively. For a 5-ft-diam tire, these are rut depths of only 0.12 in. after 100 passes and 0.18 in. after 1000 passes. A cumulative rut depth of 3 in. is currently accepted as the failure criterion for unsurfaced airstrips (reference 1). Thus values of N_c of 0.9 and larger appear to pose hardly any problem insofar as unsurfaced airstrips are concerned.

---

*Found on page 68.

The relation defined by equation 4 from results of the aircraft tire tests also applies over a very wide range of smaller loads and lower soil strengths (in the same buckshot clay), and for many tire sizes, shapes, and deflection conditions. This is illustrated in figure 18, where data from table 7, reference 7, are presented. Values of AI were not measured for tests in reference 7; these were computed from measured CI values as AI = CI/50. The ordinate variable in figure 18 is first-pass sinkage coefficient z/d, rather than the rut-depth coefficient r/d. Each data point reflects a sinkage value that was instantaneously measured at time of occurrence. (Rut depths were not measured in the tests of reference 7.) For clays, sinkage has a value slightly larger than rut depth because the soil rebounds before rut depth is measured.

The lower and upper curves in figure 18 define the r/d versus N_c relation for passes 1 and 2, respectively (from equation 4). The pass 2 r/d curve describes the pass 1 z/d data quite well for z/d values less than about 0.04. Most of the data points in figure 18 whose z/d values are larger than about 0.04 lie between the pass 1 and pass 2 r/d curves. For z/d values of this order, this indicates tire sinkage takes a value somewhere between one- and two-pass rut depth. This is consistent with the expectation that the relative amount by which soil rebound subtracts from sinkage to produce rut depth becomes larger as sinkage decreases.

d. Towed Force

First-pass towed force was measured only in cases where it was clear, a priori, that only a few passes would be possible before excessive sinkage would halt the test. In all other tests towed force was measured, in accordance with the test plan, on passes 2, 10, 20, 50, and 100 (or until a prior halt). As a result, first-pass towed force measurements were attempted on only five tests, and data obtained in three.* Examination of the multipass records showed that, all other conditions being the same, towed force increases monotonically with pass numbers from 2 to 100. The three first-pass measurements, however, indicated that first-pass towed force might not follow this pattern. Accordingly, and because first-pass

---

* Measurements were attempted in tests 30-34. Mechanical problems interfered with recording towed force in test 30, and immediate immobilization effectively cancelled test 34.

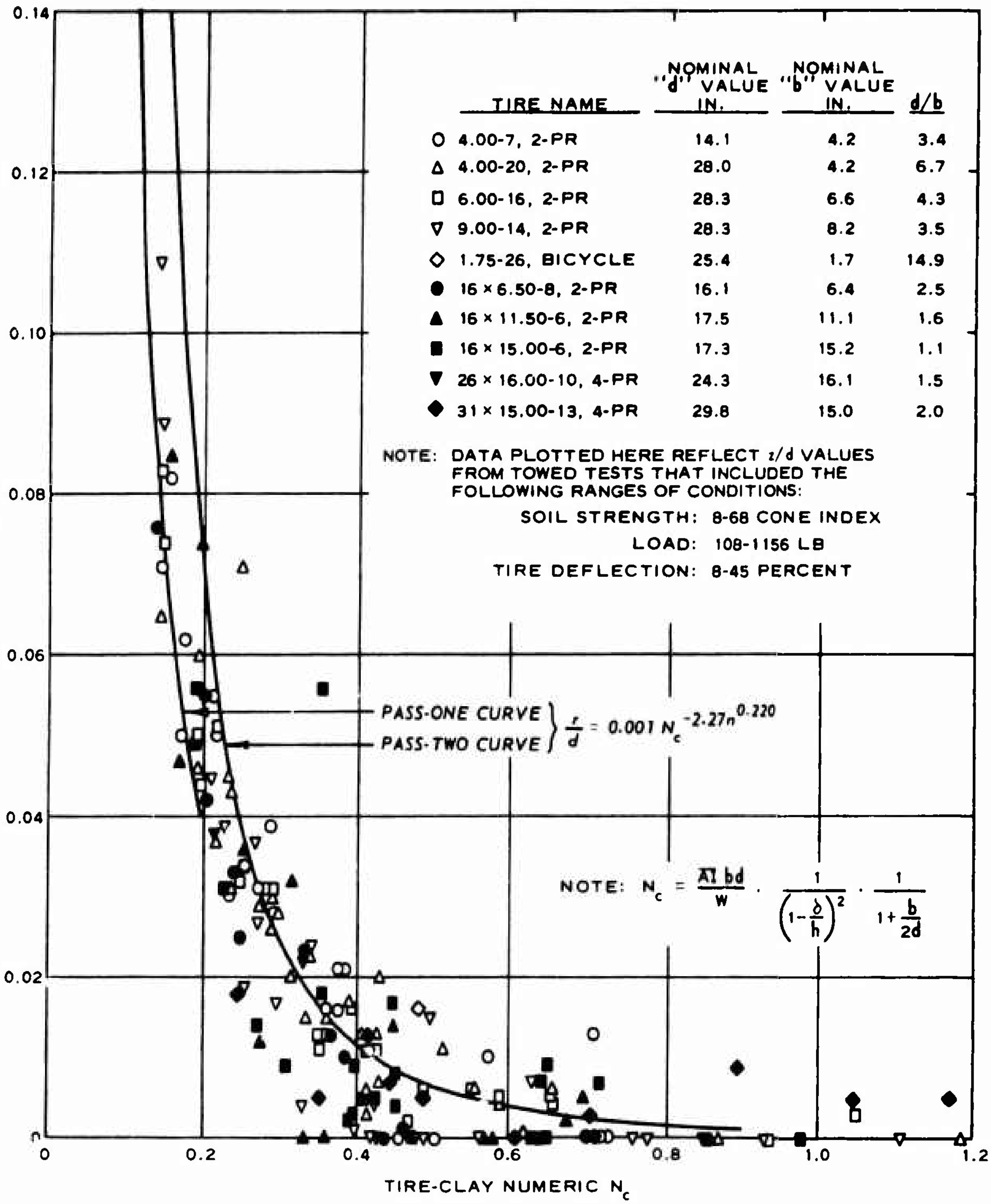

Figure 18. Relation of Sinkage Coefficient (At the Towed Point) to Tire-Clay Numeric N_c for Small and Aircraft Size Tires

data available from current tests were limited, towed force on the first pass was considered apart from that on subsequent passes.

The same procedure used to develop a description of rut depth for the multipass towed aircraft tire tests was also used to obtain a description of towed force for passes two on up. Figure 19 presents logarithmic plots of towed force coefficient P_T/W versus tire-clay numeric N_c for 2, 10, 20, 50, and 100 passes. Values of the slopes of the lines are related to pass number n by the equation

$$\text{slope} = -1.23\ n^{0.076} \tag{5}$$

The family of curves in figure 19 is then described by

$$P_T/W = 0.02\ N_c^{-1.23n^{0.076}} \qquad (n > 1) \tag{6}$$

To describe the first-pass towed force situation, the few aircraft tire measurements obtained as a part of the present test program were compared to the large body of data available in reference 7 on other tires and loads and in the same soil over a range of lower soil strengths. Figure 20 presents first-pass P_T/W versus N_c using data from reference 7, with the aircraft tire test results superimposed. These three points lie slightly on the low side of the scatter band, but clearly within it.

In view of the limited first-pass towed force data from the present tests, a relation describing towed force was fitted to the pooled data. A number of equations in P_T/W and N_c could have been used, and the apparent qualitative differences in the rut formation process on the first and successive passes might serve to justify some change in form of the equation if this proved necessary. However, it readily appeared that equation 6, with n = 3, fit the pooled data quite well, as can be seen in figure 20. This convenient expression was accepted for first-pass towed force, i.e.,

$$P_T/W = 0.02\ N_c^{-1.337} \qquad (n = 1) \tag{6a}$$

The family of P_T/W versus N_c curves defined by equation 6 and 6a is plotted in figure 32.* The figure demonstrates that after a small

*Found on page 69.

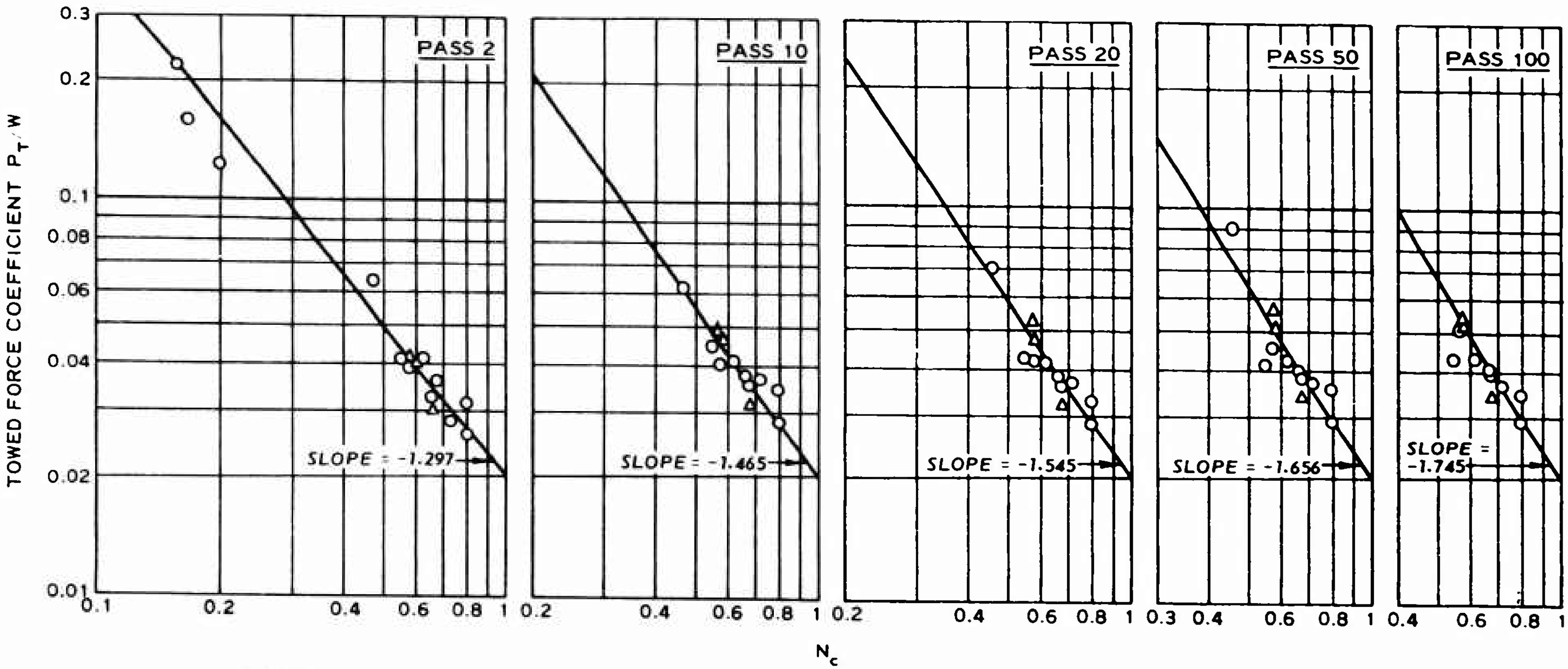

LEGEND

O 20-20, 22-PR TIRE

Δ 49-17, 26-PR TIRE

NOTE: TIRE-CLAY NUMERIC $N_c = \frac{\overline{AI}\, bd}{W} \cdot \frac{1}{\left(1-\frac{\delta}{h}\right)^2} \cdot \frac{1}{1+\frac{b}{2d}}$

Figure 19. Logarithmic Plots of P_T/W Versus N_c for Passes 2, 10, 20, 50, and 100 of Two Towed Aircraft Tires

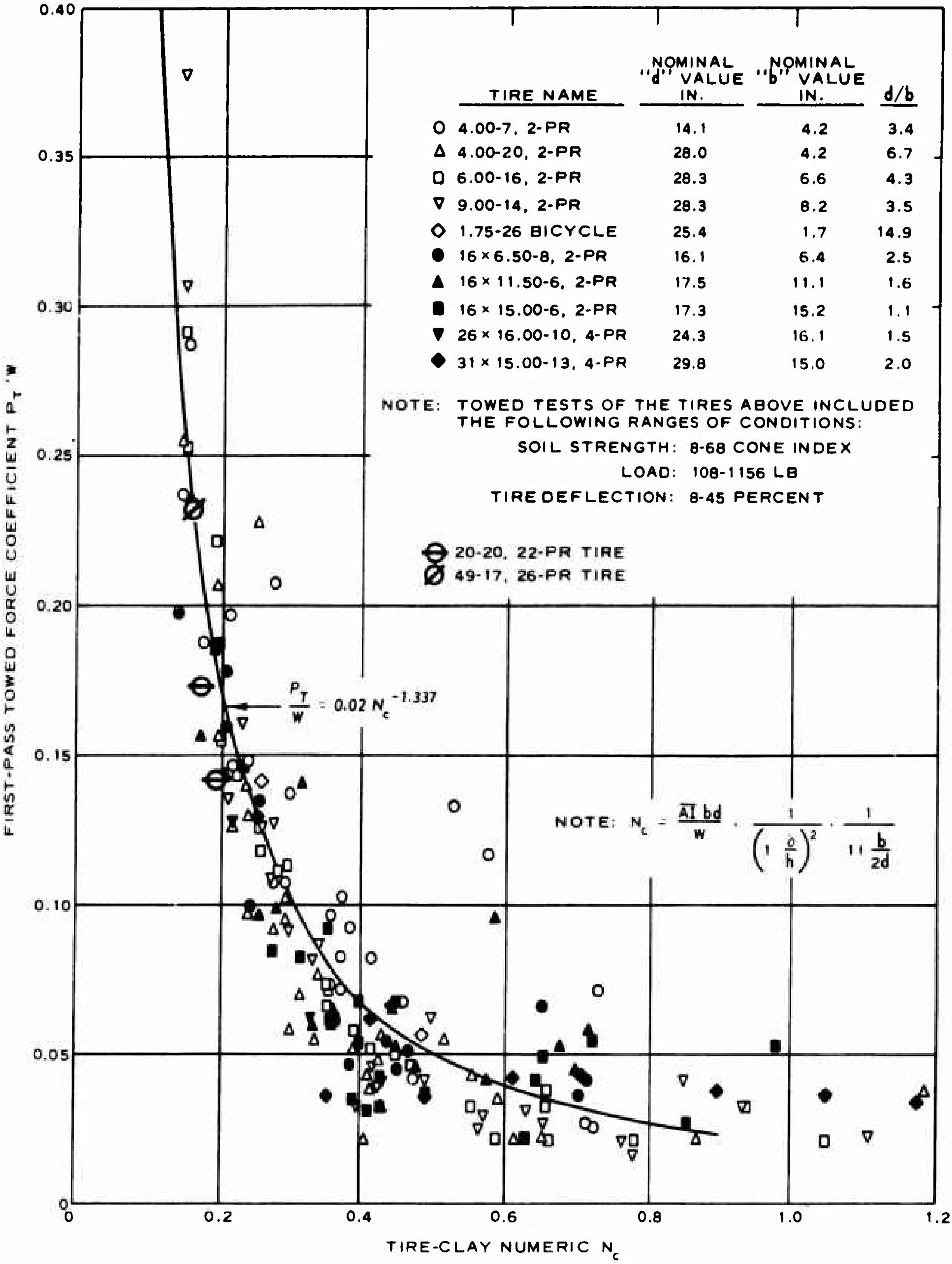

Figure 20. Relation of Towed Force Coefficient to Tire-Clay Numeric N_c for Small and Aircraft Size Tires

decrease in towed force coefficient from pass 1 to pass 2, the coefficient increases very slowly with pass number. The curves are plotted only for N_c values through 0.9. Larger N_c values produce unimportantly small P_T/W values.

e. Hub Movement

One of the secondary interests of this study was to relate aircraft tire hub movement to rut depth. Figure 21 shows the relation between these two variables using data from multipass towed tests of the 20-20 and 49-17 tires. [Hub movement is important to the description of tire-soil interactions primarily in considerations of the dynamic effects transmitted to the aircraft by movement of the aircraft tires' hubs (or axles).] Figure 21 shows that hub movement can be estimated roughly as 0.73 times rut depth, at least for hub movements of substantial magnitude (say, 2 in. and larger). No significant separation by tire size or pass number is noted, and a very wide range of tire-clay numeric values (0.16 to 0.80) is included in the data.

Hub movement is usually smaller than rut depth because of dynamic effects associated with pneumatic tire operation in soil. A detailed description of these effects is included in Appendix A of reference 9 for pneumatic tires in sand. The same relations developed there apply equally as well for tires in clay. For the purposes of this study, the relation of figure 21 is sufficiently well defined to allow useful prediction of hub movement from rut depth for the conditions of these tests.

3. CONSOLIDATING TRUCK PERFORMANCE DATA

a. General Approach

The same approach used in consolidating the aircraft tire performance data was also employed for the truck test data. That is, relations were sought to describe tire performance as a function of the tire-clay numeric N_c and pass number n. It should be recalled that, for the truck tests, the only test response measured was rut depth [measured relative to original soil surface (r) and relative to rut shoulders].

b. Front-Tire Rut Depth

In all but two of the 15 truck tests, the tire rut was measured after truck passes 2, 6, and 10 within that length of one of the ruts trafficked

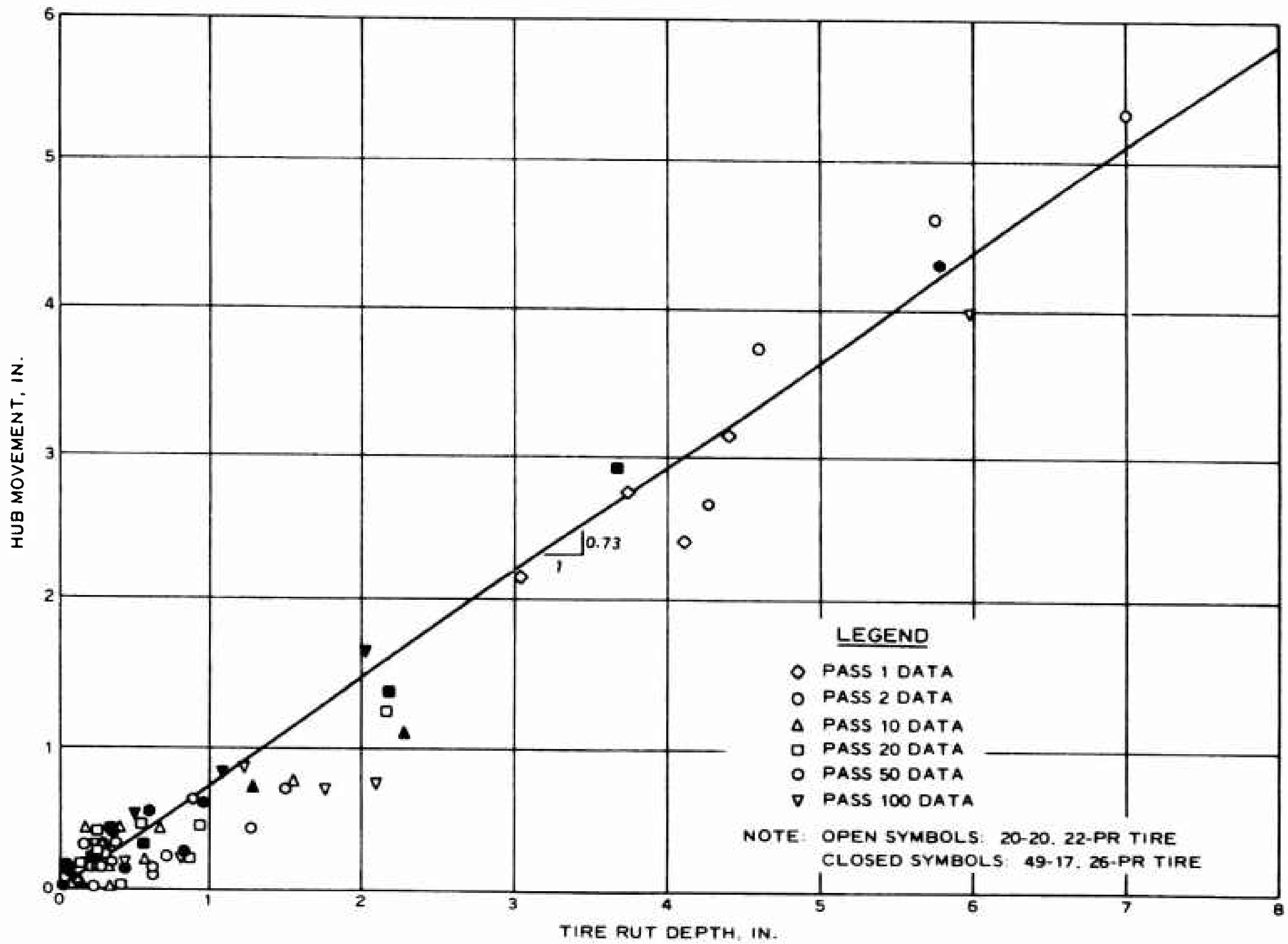

Figure 21. Relation of Hub Movement to Rut Depth for Multipass Tests of Towed Single Aircraft Tires

(a) only by one of the truck's front tires and (b) by the whole truck. An illustration of the difference between front-tire and whole-truck ruts is shown in figure 22 for the loaded M35A2, 2-1/2-ton truck after two truck passes in one of the low-strength test beds (test E-73-0029-3). Notice in this figure that each front-tire rut was produced under conditions of near-perfect tracking. Also, the load acting on each front tire was known (half the front-axle load). On the other hand, the whole-truck ruts in figure 22 are wider than the front-tire ruts because the space between tires on the front axle was different from that between tires on the second and third axles. Whole-truck rut depths in figure 22 were also influenced by the fact that each truck axle carried a different load. (See figure 3 for values of non-tracking distance s and weight distributions of the three test trucks.)

A quantitative description of front-tire rut depth was selected to serve as a datum against which comparisons could be made for rutting developed by the truck as a whole. This datum served to illustrate (a) whether rut depth is related to tire-clay numeric N_c and pass number n in the same way whether or not nontracking distance s and uneven load distributions are considerations, and (b) how much less well defined this relation is (if it is the same) when distance s and uneven load distribution influence the test results.

Logarithmic plots of r/d versus N_c in figure 23 indicate that the front-tire data can be described by

$$r/d = p\, N_c^{\,q} \tag{7}$$

where

$$p = 0.00107n^{0.50}$$

and

$$q = -2.60$$

The family of parallel lines described by equation 7 is shown in figure 33, page 70. Note that while the form of equations 1 and 7 is the same, the parameters a and b of equation 1, which refers to freely towed wheels,

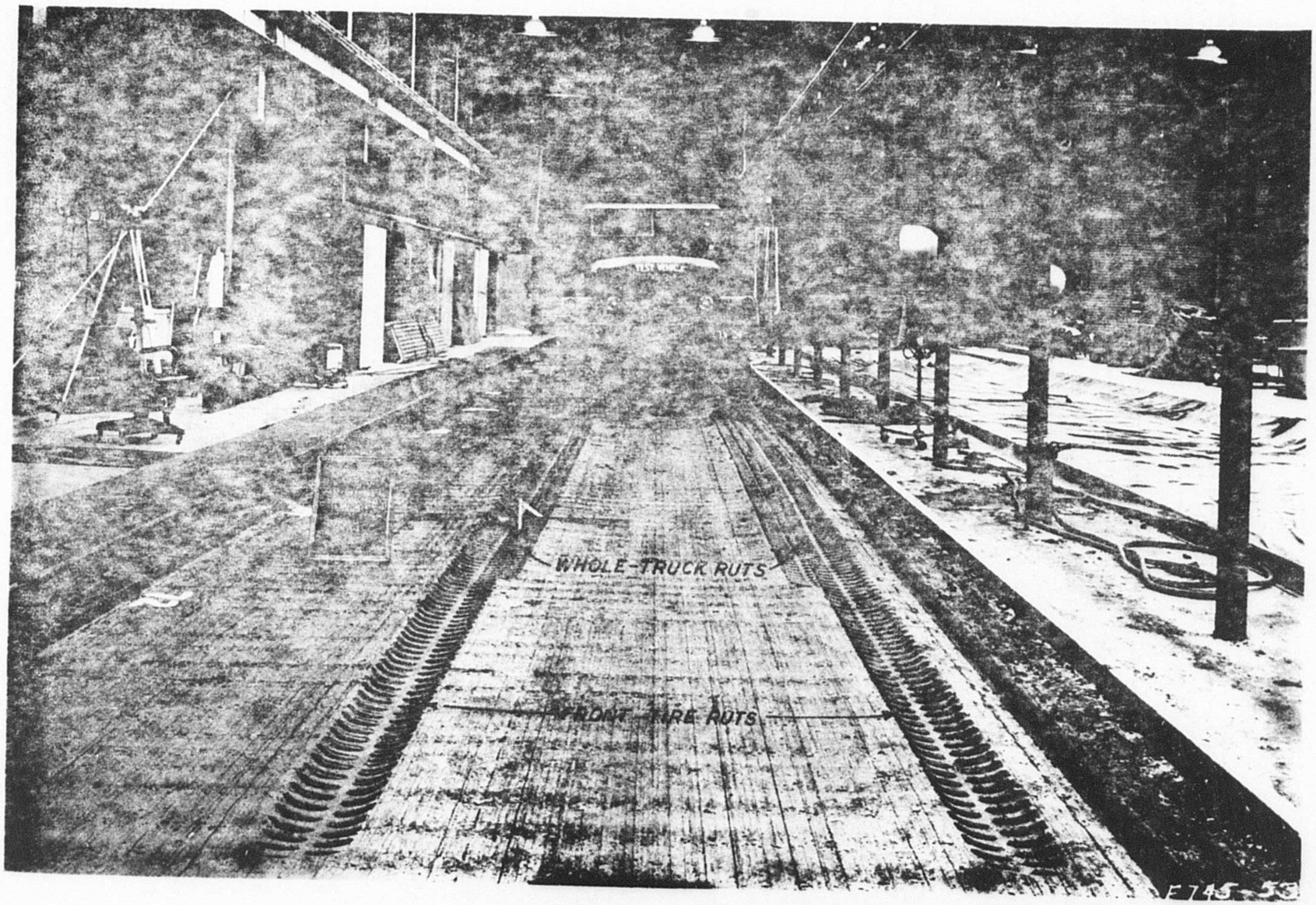

Figure 22. Rut Produced by Multiple Passes of the M35A2 Powered M35A2 Truck

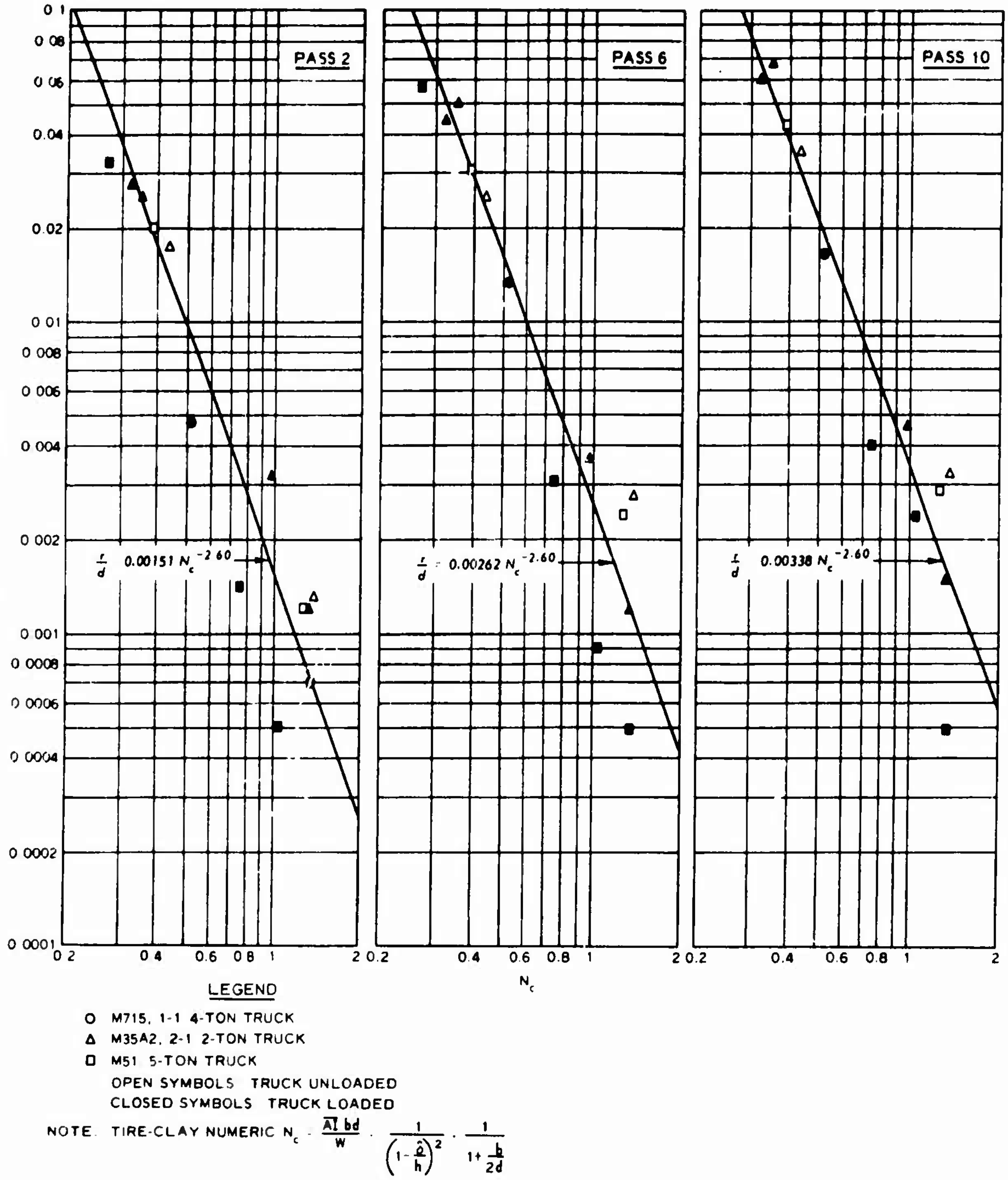

Figure 23. Logarithmic Relation of Front-Axle Rut Depth Coefficient to Tire-Clay Numeric N_c for Multiple Passes of Powered Trucks

are quite different from parameters p and q of equation 7 for driven wheels.

c. Whole-Truck Rut Depth

To describe rut depth for the whole vehicle requires an expression relating rut depth to characteristics of the vehicle as a whole. As a starting point, equation 7 was used by defining load W as total truck load ÷ number of truck tires and unloaded tire section width b as the average value of b for all tires of a given truck; and by interpreting pass number n as truck pass number × number of truck axles. These conventions ignored the uneven load distribution among a given truck's axles, and the fact that each truck's front tires followed a straight-line path different from that of the trailing tires. (See figure 3 for a description of these factors.)

For all 15 truck tests, average maximum tire rut depth was computed from cross-section measurements taken at three locations within the middle 16 ft of the rut length trafficked by the whole truck. Figure 24 compares these average measurements with values computed using equation 7 and the redefinition of terms just discussed. Correlation on the whole is good, and is best for the M715, 1-1/4-ton truck for which nontracking of front and rear axles is least. Efforts to improve upon the relation given by equation 7 through the introduction of measures of nontracking were unsuccessful due to limitations in the variation in truck geometry.

4. PREDICTING AIRCRAFT TIRE RUT DEPTH AND TOWED FORCE

a. Measurement of the Rut

In all the analysis to this point, the rut depth values used have been those computed from rod-and-level cross-section measurements. This was done because the rod-and-level technique provides a very precise measurement of soil elevation, leading to precise measurement of tire rut depth. In forward-area field situations, however, considerations of time and available equipment often will require that measurement of the rut be made with less sophisticated equipment, such as straightedge and ruler. It was of significant interest, then, to determine how values of rut depth measured with straightedge and ruler are related to those measured by rod and level. Figure 25 shows this relation, using data from both the aircraft

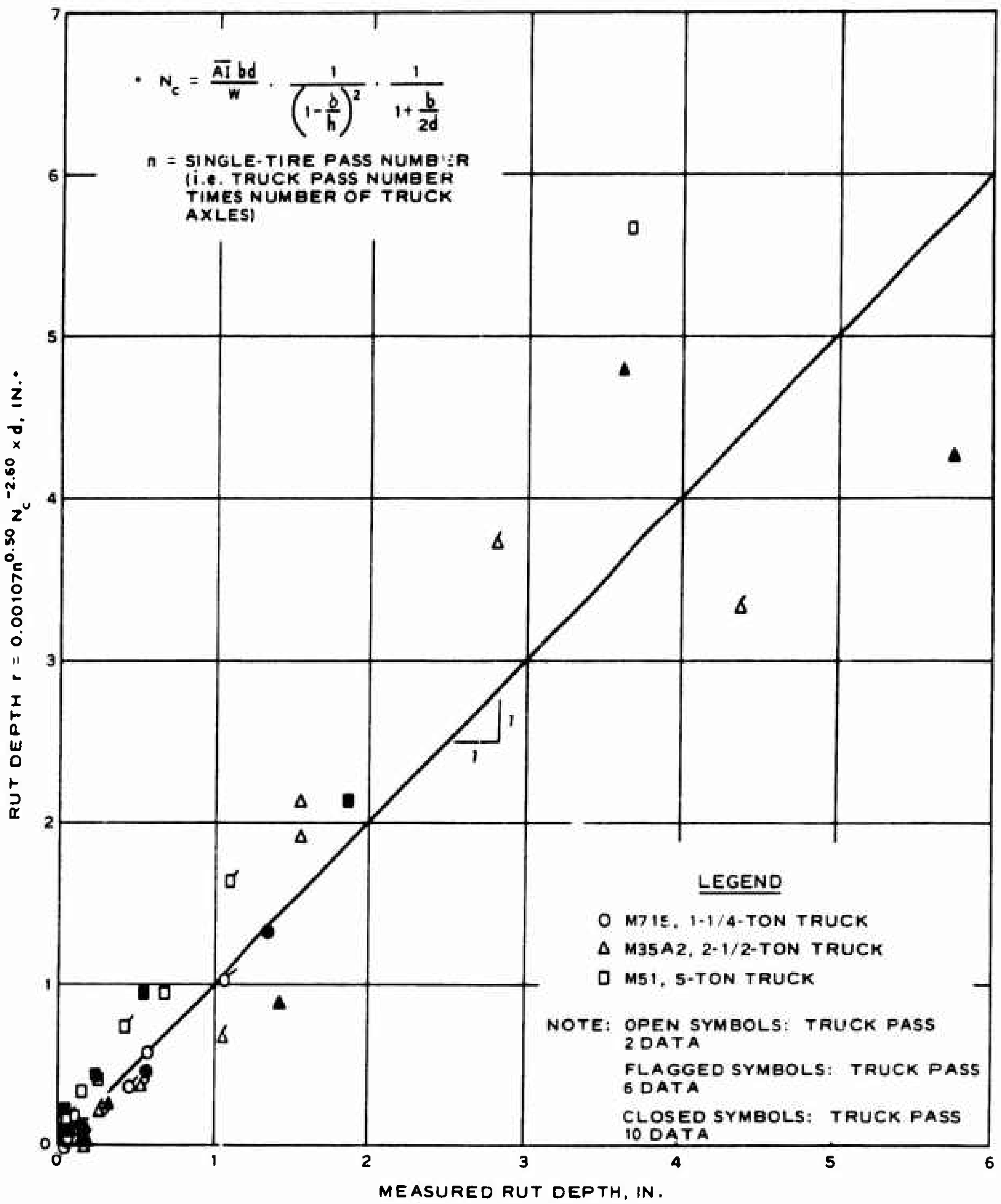

Figure 24. Consolidation of Whole-Truck, Multipass Rut Depth Data

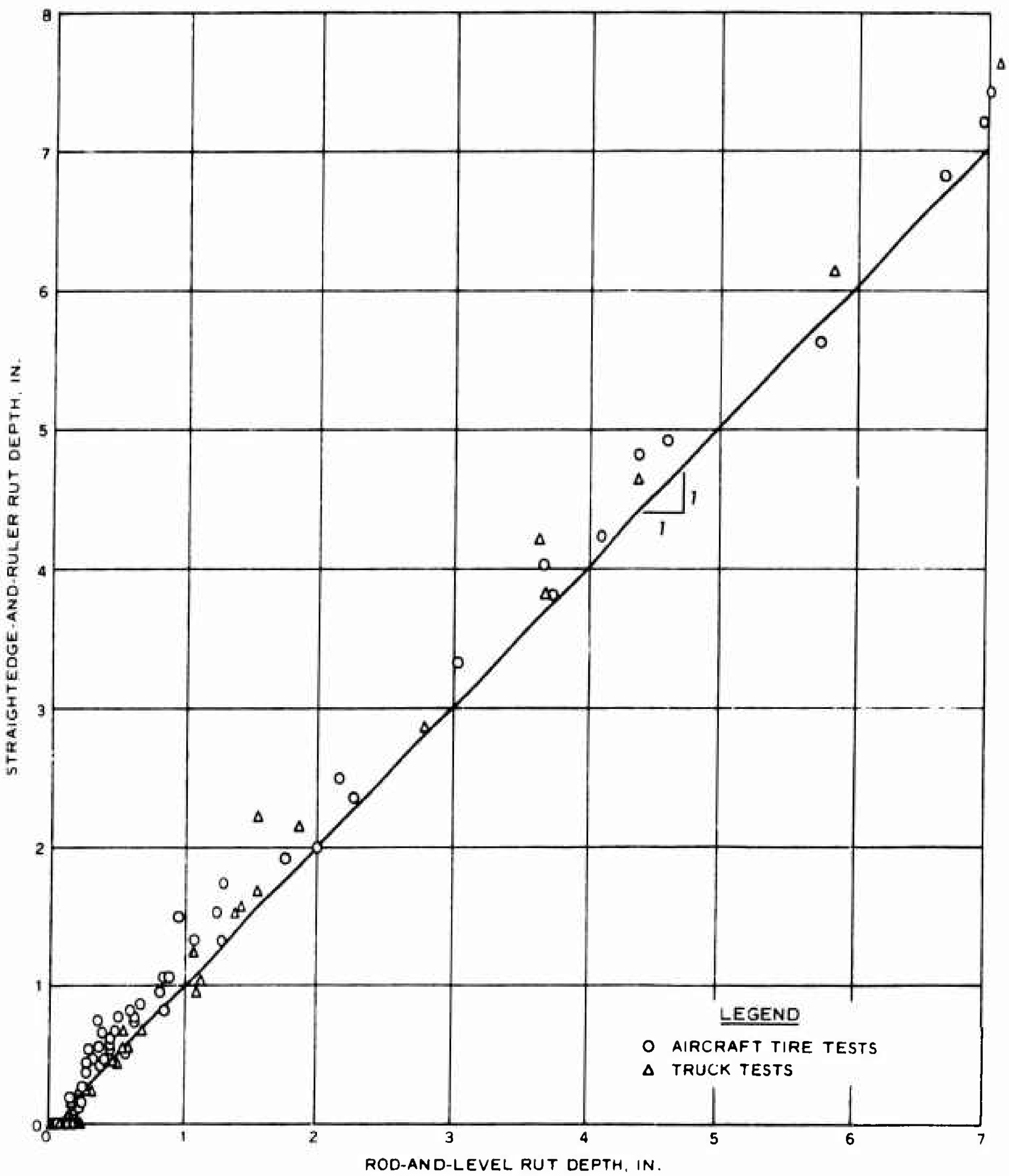

Figure 25. Comparison of Rod-and-Level and Straightedge-and-Ruler Rut Depths

tire and the truck tests.

In figure 25, no significant data separation by aircraft tire or truck is noted. Even under laboratory conditions, however, it is clear that 1:1 agreement was not obtained between the rod-and-level and the straightedge-and-ruler measurements. To establish a datum for comparison purposes, let the rod-and-level measurements be considered to describe rut depth precisely. Figure 25 shows that the straightedge-and-ruler method produces values of rut depth consistently larger than actual (i.e. larger than rod-and-level values) for rod-and-level measurements of about 0.3 in. and larger. The difference between rut depth values measured by the two methods is fairly constant at about 0.2 in. for rod-and-level rut depths of 0.5 in. and larger. The larger straightedge-and-ruler values are explained by one or both of the following: (a) human tendency causes the measurer of rut depth not to force the straightedge down far enough into the soil to cause its bottom edge to coincide with the elevation of the undisturbed soil surface, or (b) the elevation of the soil surface at the ends of the straightedge is higher than it was before traffic due to soil upheaval in the vicinity of the tire rut shoulders.

For rod-and-level rut depths smaller than about 0.3 in., data in figure 25 show that straightedge-and-ruler values of rut depth tend to be smaller than actual. This indicates that for very small rut depths, the straightedge-and-ruler method is unable to distinguish part of rut depth that is actually present.

The most important conclusion to be drawn from figure 25 is that for actual rut depths of about 0.3 in. and larger, the straightedge-and-ruler method usually estimates rut depth too large by a small amount (about 0.2 in.). In the context of this study this tendency is conservative, since it leads to predictions of aircraft tire rut depth and towed force that are equal to or slightly larger than actual. Thus, the straightedge-and-ruler technique can be used as an expedient technique for measuring rut depth in the field, with no correction being made to the measured value if it is at least 0.3 in. For measured rut depths less than 0.3 in., a conservative approach would be to estimate soil strength as if a 0.3 in. rut were present. Using this conservative procedure can be important since for a combination of light truck (say, the M715) and heavy aircraft (say, the C130), the AI value indicated for $r = 0.3$ in. and several truck passes can be too small to forecast even one pass of the aircraft.

In all considerations to this point, the rut depth values used have been those measured relative to the original soil surface (figure 2a). This rut depth is descriptive of soil displacement very near the tire, and takes a value closely associated with tire sinkage. On the other hand, values of rut depth relative to the rut shoulders (figure 2b) reflect to a high degree the cross-sectional shape of the rut shoulders. Quite often, this shape is irregular or is influenced by breakup of the soil at the top of the rut shoulders (see figure 16b, for example). Thus, values of rut depth relative to the rut shoulders can be expected not to follow as consistent a pattern as values of rut depth relative to the original soil surface.

In the literature, values of rut depth have been reported both relative to the original soil surface and relative to the rut shoulders (reference 1, for example). At the sponsor's request, values of rut depth in this study were measured relative to both of these datums; the relation between these two types of measurements is shown in figure 26. This figure shows that ruts measured relative to the rut shoulders are roughly 12/7 times larger than those measured relative to the original soil surface, both for the aircraft tires and for the trucks. Scatter of the data is sufficiently large, however, to recommend using measurements taken only relative to the original soil surface.

b. Predicting Airfield Index from Truck Rut Depth

One of the basic objectives of this study was to develop a simple method to estimate soil strength from the rut produced by a conventional military truck. Equation 7 is ideally suited to satisfy this objective, since this equation defines the interrelations among airfield index, rut depth, and single-tire pass number for single or multiple passes of powered tires. Solved explicitly for AI, equation 7 becomes

$$AI = \left(\frac{0.00107\ n^{0.5}}{r/d} \right)^{0.385} \div F_t \tag{8}$$

where F_t = (truck-tire N_c) $\div$ AI $= \frac{bd}{W} \cdot \frac{1}{(1 - \frac{\delta}{h})^2} \cdot \frac{1}{1 + \frac{b}{2d}}$, which is a

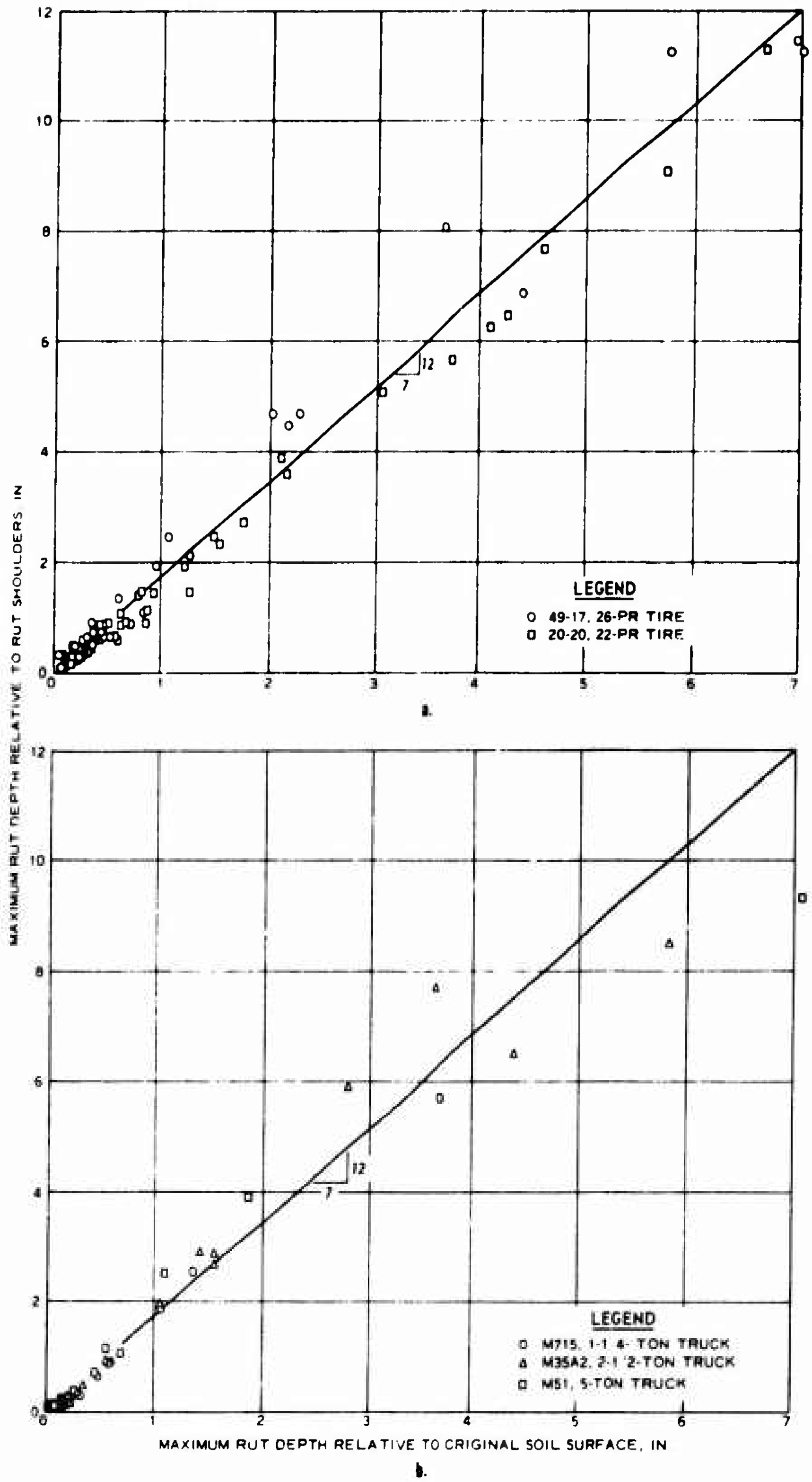

Figure 26. Comparison of Rut Depths Measured Relative to the Original Soil Surface and to the Rut Shoulders

function only of the characteristics of the truck tires used for the rut depth test, and their loading. Comparison of direct measurements of AI with values computed using equation 8 indicates that, at the 95-percent confidence level, the equation describes the data from which it was derived within limits of ±17 percent when front-tire rut depth data are used, or ±24 percent when whole-truck data are used. Families of curves of AI versus rut depth separated by pass number were developed from equation 7 for the three trucks tested in this study, as shown in figures 27-29.

c. The Numeric Prediction Relations

The primary object of predicting AI in this study was to permit forecasting of an aircraft tire's multiple-pass rut depth and soil drag resistance (towed force). This is accomplished by using AI, along with measured or estimated values of b, d, W, and δ/h for the aircraft tire to compute the aircraft tire-clay numeric N_c. The value of N_c is then entered in figures 31 and 32 to determine values of r/d and P_T/W for the aircraft tire pass number of interest.*

A practical concern is that values for tire geometric and loading characteristics are sometimes difficult to obtain. To facilitate use of the numeric system, aircraft tires which might be expected to operate from earthen airstrips could be tabulated along with the value for

$$F_a = (\text{aircraft-tire } N_c) \div AI = \frac{bd}{W} \cdot \frac{1}{\left(1 - \frac{\delta}{h}\right)^2} \cdot \frac{1}{1 + \frac{b}{2d}}$$

corresponding to each of several possible operating loadings. (A similar tabulation of F_t values could be provided for standard truck tires and loads which might be used in rut depth tests.) A less precise alternate is to simplify the numeric by consideration of the fact that most aircraft tires are designed for a fixed percentage tire deflection, 32 percent, and that most have b/d values nearly constant at 0.35. Thus, for most conventionally shaped aircraft tires operated at their design deflection

* Families of curves in figures 31 and 32 were defined by equations 4 and 6, respectively.

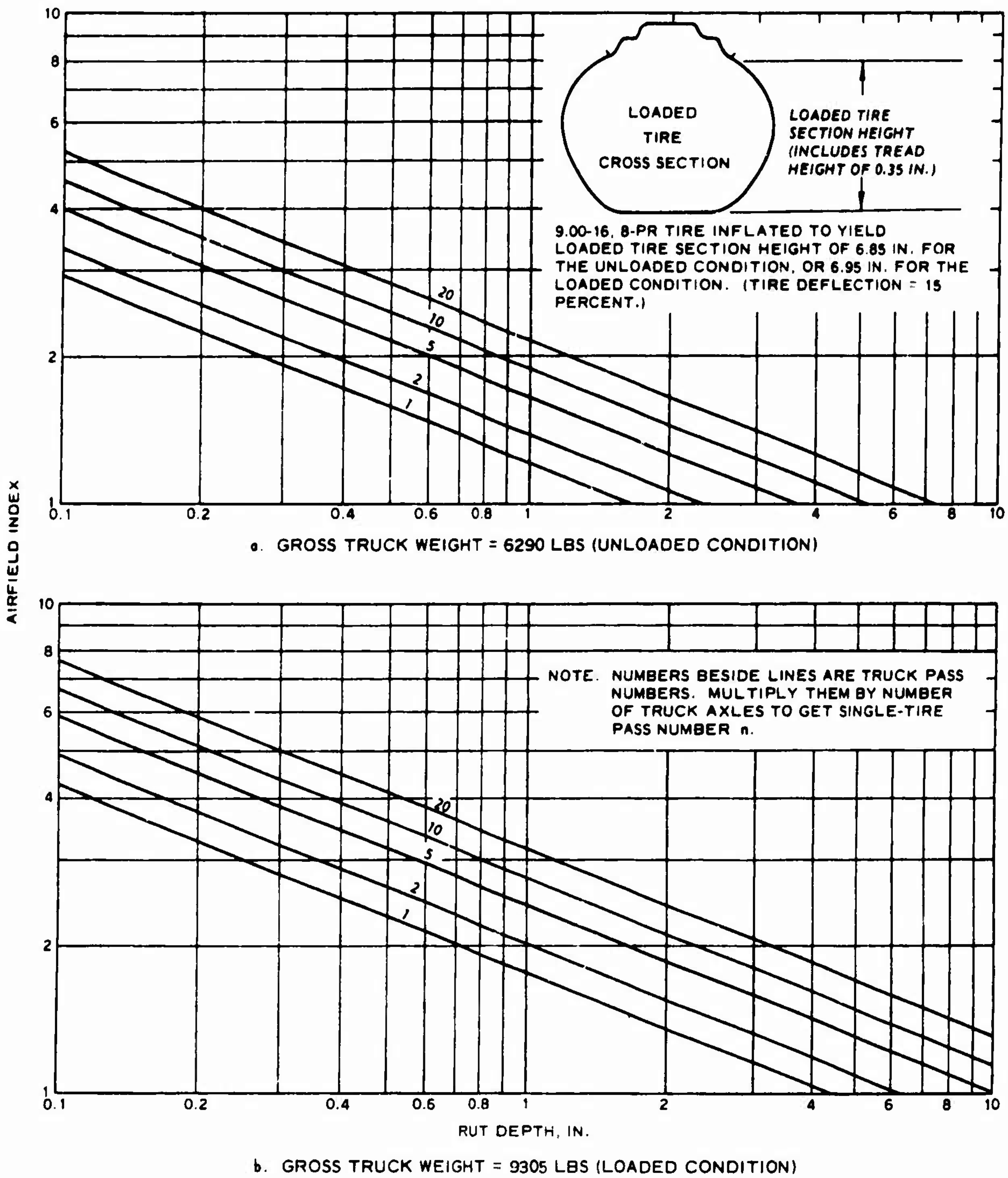

Figure 27. Relation of Airfield Index to Rut Depth for Multiple Passes of the Unloaded and Loaded M715, 1-1/4-Ton Truck

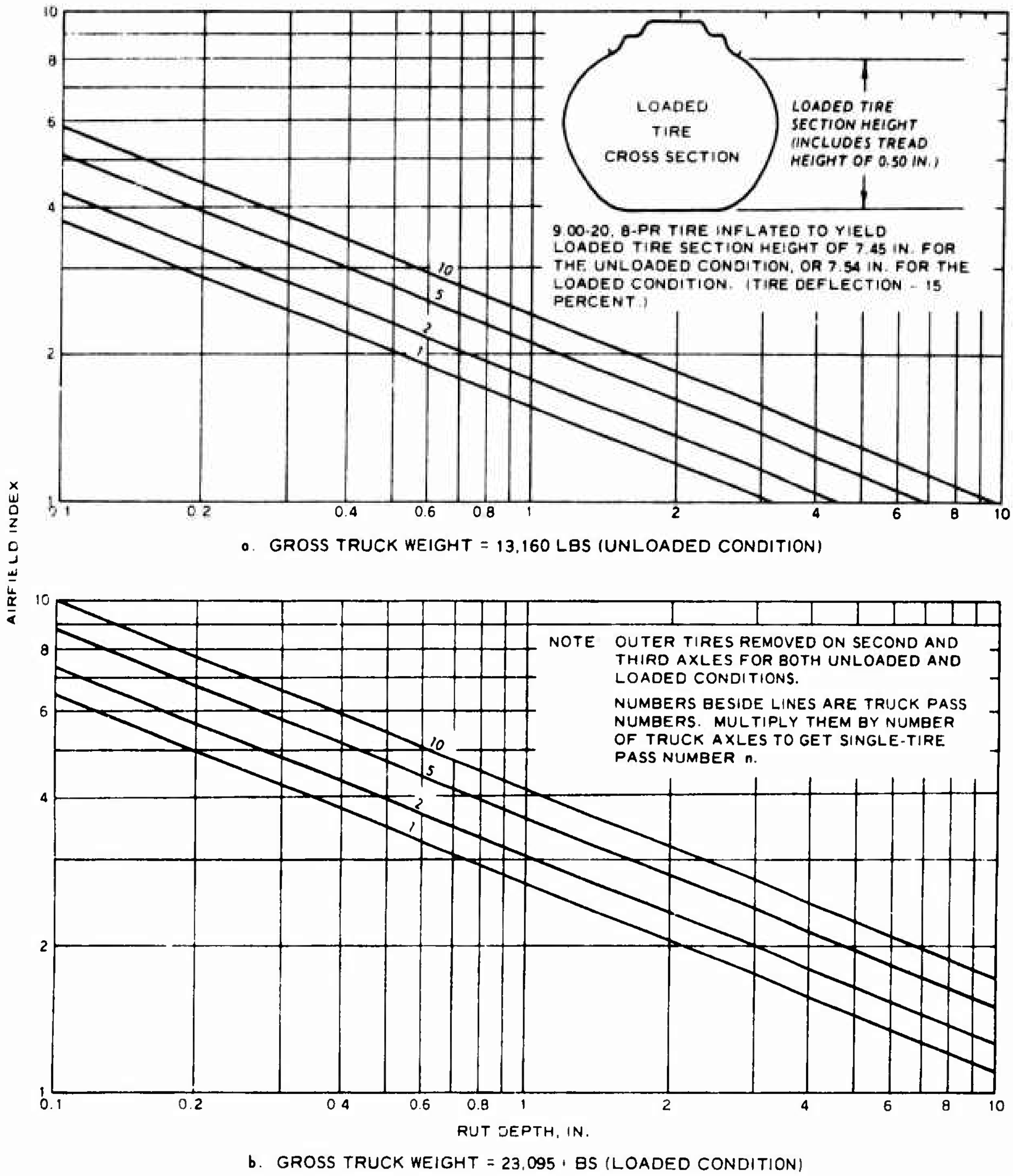

Figure 28. Relation of Airfield Index to Rut Depth for Multiple Passes of the Unloaded and Loaded M35A2, 2-1/2-Ton Truck

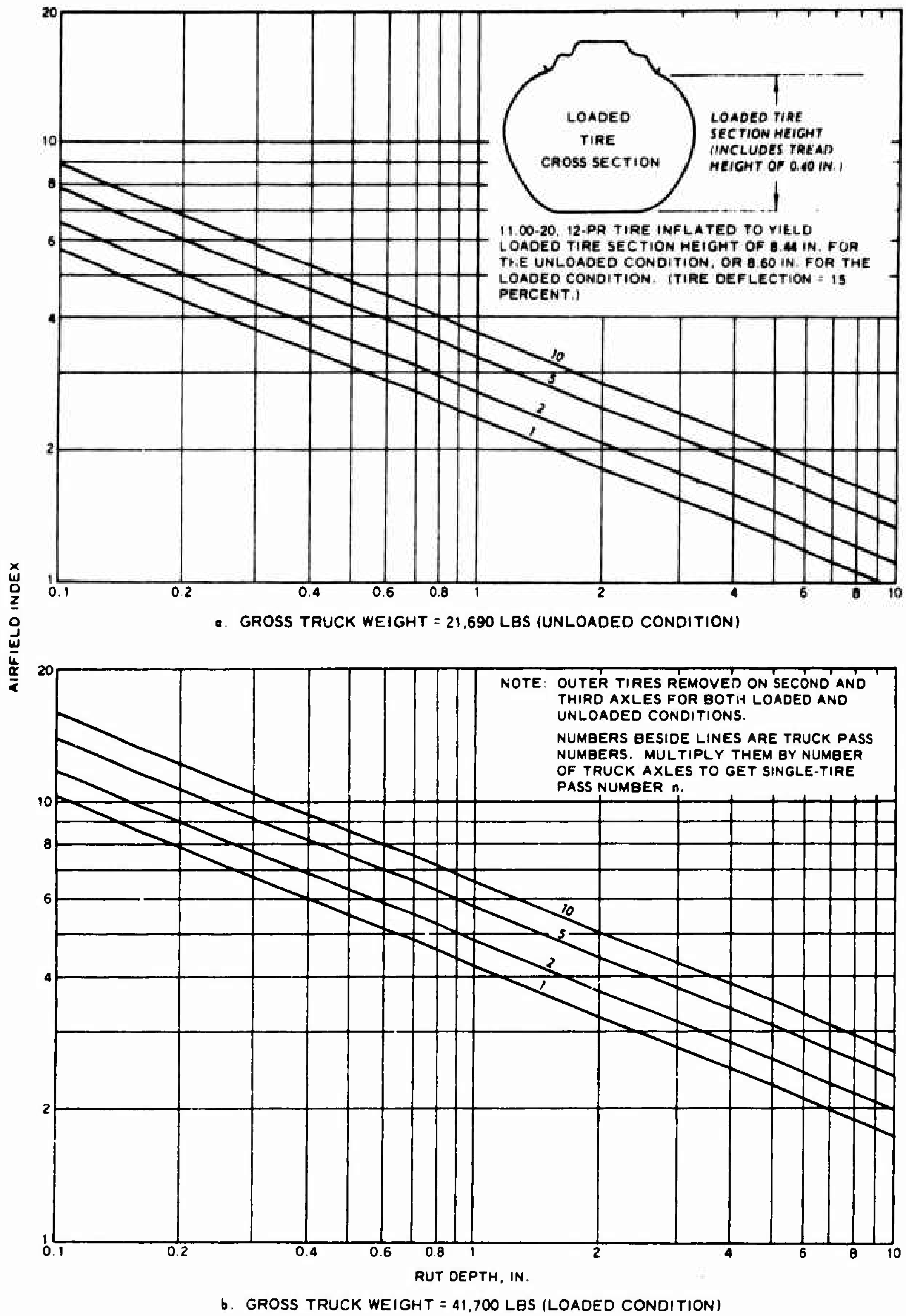

Figure 29. Relation of Airfield Index to Rut Depth for Multiple Passes of the Unloaded and Loaded M51, 5-Ton Truck

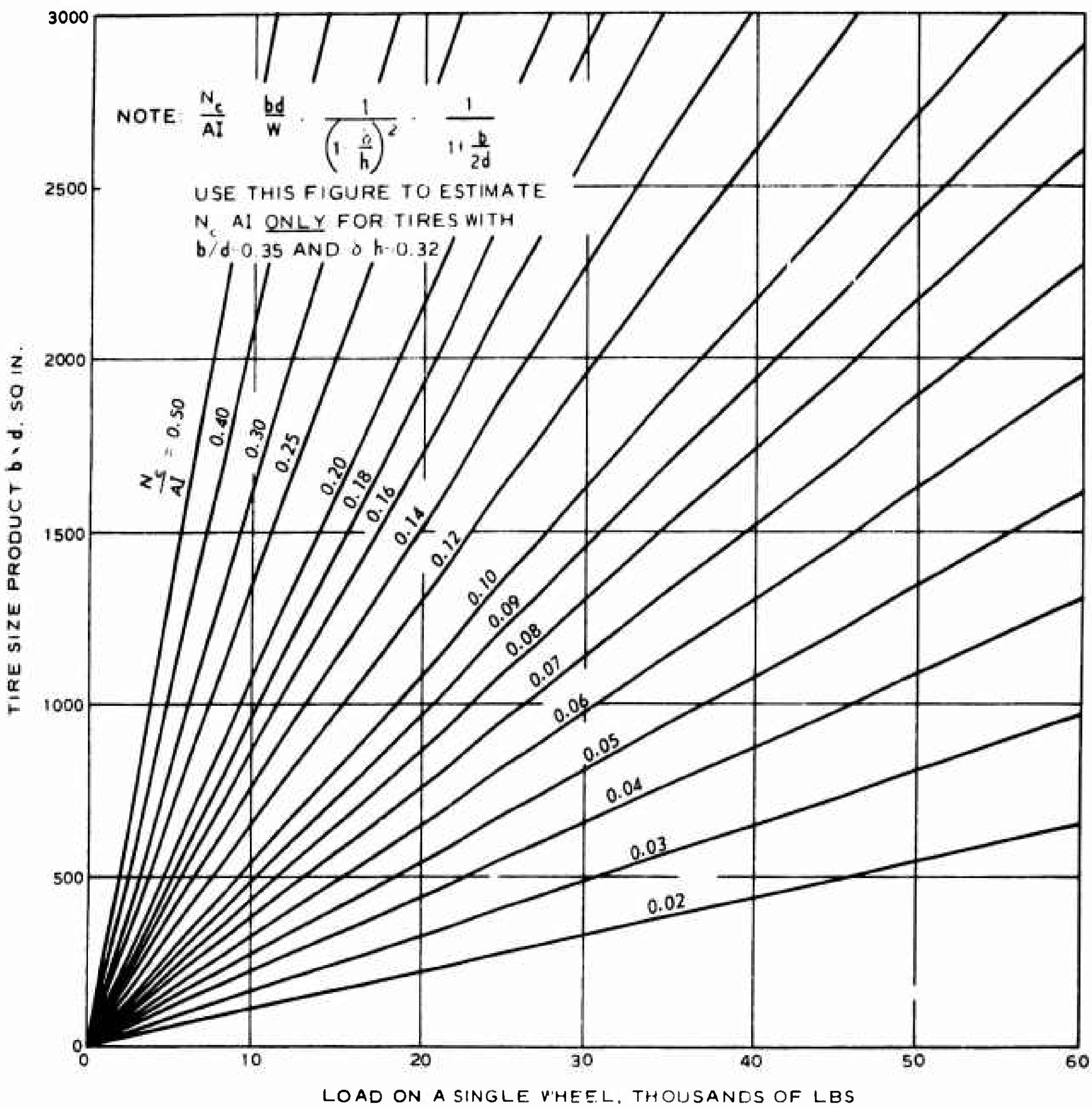

Figure 30. Estimate of N_c/AI for Towed Tires with $b/d \approx 0.35$ and $\delta/h \approx 0.32$

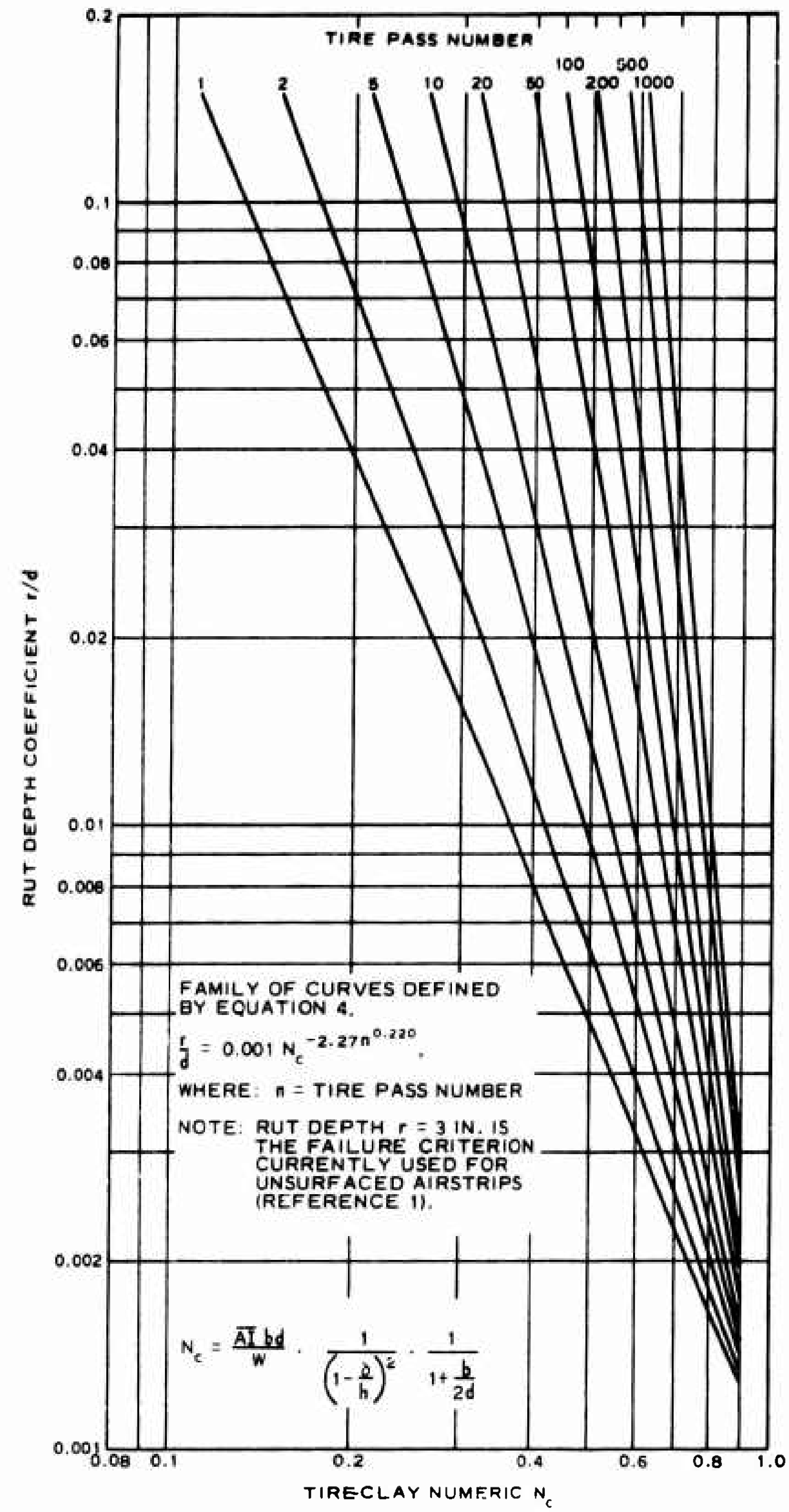

Figure 31. Relation of Rut Depth Coefficient to Tire-Clay Numeric N_c for Towed, Slow-Moving Tires

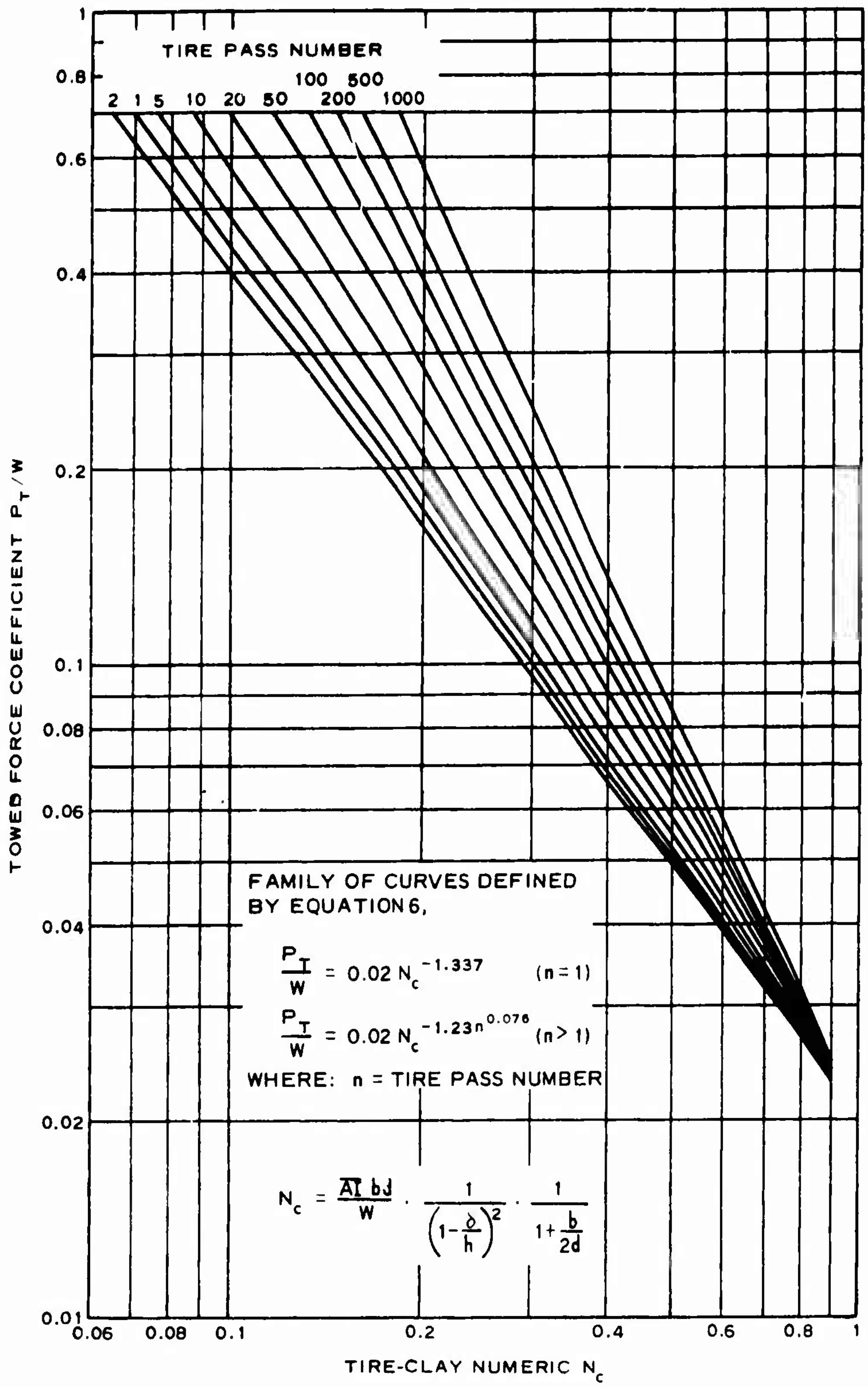

Figure 32. Relation of Towed Force Coefficient to Tire-Clay Numeric N_c for Slow-Moving Tires

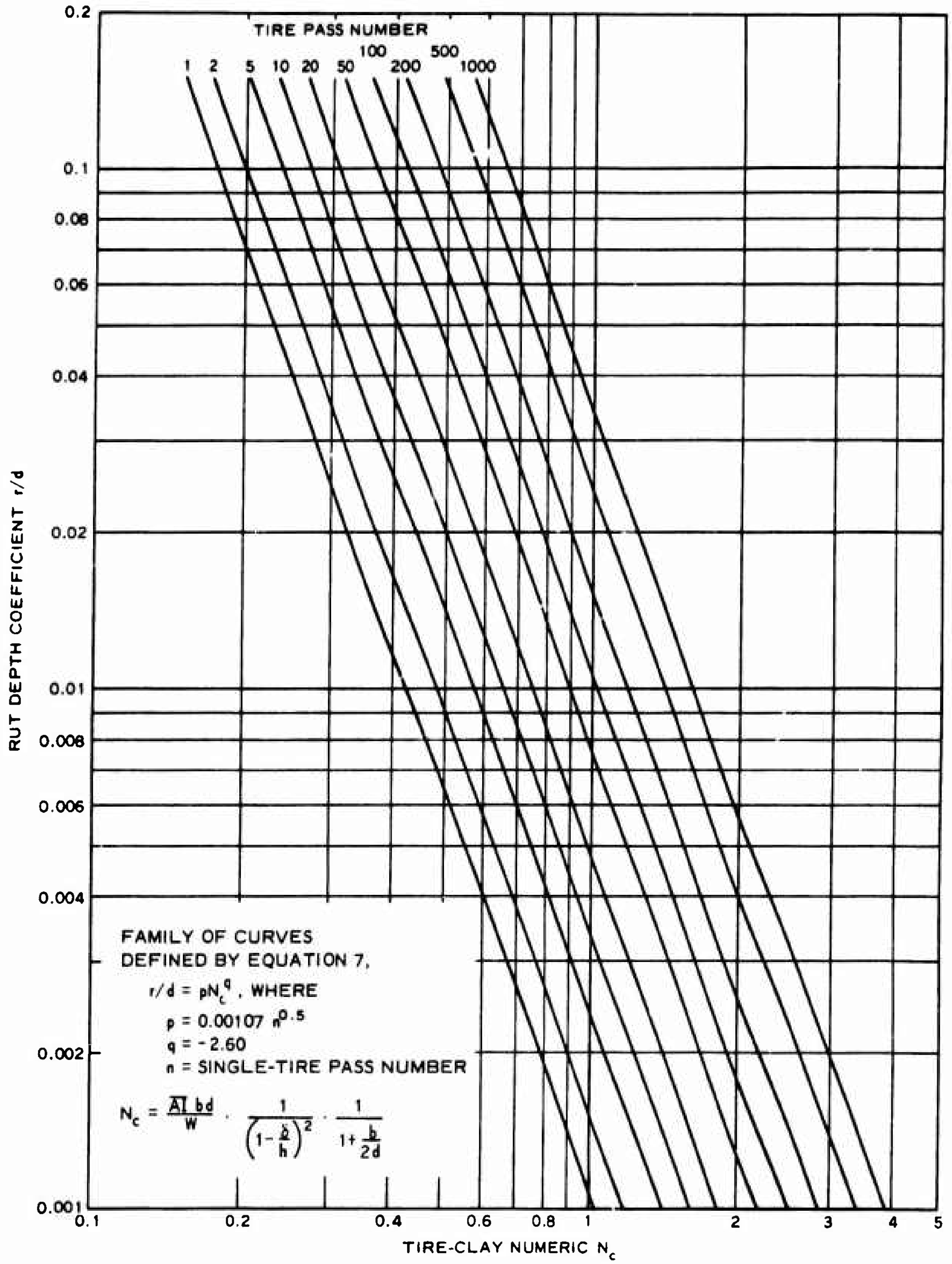

Figure 33. Relation of Rut Depth Coefficient to Tire-Clay Numeric N_c for Powered, Slow-Moving Tires

value, N_c 1.84 AI × bd/W.* When simplified in this fashion, the load-geometry portion of N_c can be described as a family of lines as in figure 30. With AI estimated from one of figures 27-29 and N_c/AI determined from figure 30, N_c is then simply the product.**

The procedure used to estimate aircraft tire N_c should not be limited to estimating AI from truck rut depths, and then either computing or estimating N_c. If a decision is made on the basis of the pre-landing forecast of aircraft tire ground performance to use a given airstrip, the estimate of N_c and number of aircraft passes can and should be checked and refined after the first landing. This is done by measuring actual aircraft tire rut depth, converting it to r/d, and using the relation shown in figure 31.

d. Using the Numeric System to Predict Aircraft Tire Performance

The primary objectives of this study are accomplished by use of the relations in figures 27-32. Two examples illustrate the procedures involved.

(1) Example 1

Problem. An earthen airstrip of unknown strength is being considered for use by a C130 aircraft loaded such that its landing gear wheels each carry 35,000 lb. The aircraft's tires are 20-20, 22-PR inflated to produce 32 percent deflection. A loaded M35A2 truck (outer wheels on second and third axles removed) develops a 0.50-in. rut after 10 passes. Can the C130 operate from this field? If so, how many passes can it make?

Solution. From figure 28b, the AI value that corresponds to r = 0.5 in. for 10 M35A2 truck passes (30 single-wheel passes) is 5.4. Values of b and d for the 20-20 tire are 19.6 in. and 56.4 in., respectively (b/d = 0.348). From figure 30, N_c/AI is 0.058 for W = 35,000 lb, bd = 1105 in.^{2}, and δ/h = 0.32. Then N_c = 0.313. Entering this value of

---

* Found on page 67.

** Further research is needed to define the load that should be used in aircraft tire-clay numeric N_c when multiple-wheel landing gear assemblies are considered. Equivalent single-wheel load (ESWL) would appear to warrant first attention, based on its definition, as follows: "The load on a single wheel, of the same contact area as one wheel of a multiple-wheel assembly, which produces maximum (soil) deflection equal to that produced beneath the multiple-wheel assembly." Values of ESWL for a large number of aircraft are tabulated in reference 10.

N_c in figures 31 and 32, the r/d and P_T/W values are 0.022 and 0.090, respectively, for pass 2. These values correspond to a rut depth of 1.2 in. which is well below the 3-in. failure criterion currently used (reference 1), and a towed force (free-rolling drag) of only 3150 lb. Thus, the C130 can land and take off one time from this airstrip.

To determine the maximum number of passes that an aircraft tire can safely make in the same rut, a maximum allowable cumulative rut depth of 3 in. is again used. For d = 56.4 in., this gives an r/d limit of 0.053. Based on an N_c value of 0.313, the C130 can make approximately six passes in the same rut (figure 31).

Suppose that aircraft tire rut depth after the first pass was measured at 0.6 in. (r/d ≈ 0.106). This would lead to a revised N_c estimate of 0.35, and indicate that the critical cumulative rut depth would not be reached until pass 10, all of which can be read directly from figure 31. P_T/W on the 10th pass at N_c = 0.35 is still only 0.092 (figure 32).

(2) Example 2

Problem. A C5A aircraft loaded such that its landing gear wheels each carry 25,000 lb needs to operate from an earthen airstrip. The aircraft's tires are 49-17, 26-PR inflated to 32 percent deflection. A loaded M35A2 truck (total weight = 23,100 lb, outer wheels on second and third axles removed) produces a rut of less than 0.3 in. after 10 passes. How many one-lane passes can the C5A make on this airstrip?

Solution. From figure 28b, the AI value corresponding to a rut depth of 0.3 in. after 10 passes (30 single-wheel passes) is 6.6. The airstrip AI value is accordingly estimated to be at least 6.6 and will be taken as equal to 6.6 in subsequent calculations. Values of b and d for the 49-17 tire are 16.95 in. and 47.5 in., respectively (b/d = 0.357). From figure 30, N_c/AI is 0.059 for W = 25,000 lb, bd = 805 in.^{2}, and δ/h = 0.32. Then N_c = 0.39. Entering this value in figures 31 and 32 for pass 2, the r/d and P_T/W values are 0.012 and 0.008, respectively. These values correspond to a rut depth of 0.6 in. (well below the 3-in. failure criterion currently used) and a towed force of only 200 lb. Thus, the C5A can land and take off safely at least once. Based on an N_c value of 0.39 and a maximum allowable rut depth of 3 in. (r/d = 0.063), the predicted maximum number of aircraft ground passes is about 20 (figure 31).

Suppose one pass was then made by the C5A and a rut of 0.30 in. was produced. With d = 47.5 in., this gives an r/d value of 0.0063. From figure 31 this indicates the N_c value of the aircraft is 0.44. Values of r/d and P_T/W are then read from figures 31 and 32 at N_c = 0.44 and the pass number of interest. Based on a maximum allowable rut of 3 in. (r/d = 0.063 for this problem), no more than about 40 passes can be made.

e. Closing Comments

It has been demonstrated for carefully prepared, remolded buckshot clay that the expedient technique of estimating soil strength (AI) from the rut produced by a truck can be accomplished. This AI value can then be incorporated in the aircraft tire-clay numeric N_c to predict aircraft tire ground performance (figures 31 and 32). For multiple passes of a truck's front tires or for a truck with single tires that nearly track, the estimate of soil strength is fairly precise when the truck rut is at least 0.3 in. deep. Figure 29b shows, however, that even for the loaded, 5-ton truck, 10 truck passes estimate an AI value of only 10.5 for a 0.3-in. rut. The unloaded 1-1/4-ton truck estimates AI = 1.9 for one truck pass and r = 0.3 in. Thus, truck rut depth provides a sensitive index of soil strength only for relatively small values of AI. Measured rut depths of less than 0.3 in. generally should be used only to indicate that the soil's AI value is at least as great as that corresponding to r = 0.3 in.

Note that while the truck rut-to-AI conversion is somewhat limited in the range of AI values that it can predict (for trucks up to the 5-ton class), it is not limited to the three trucks tested in this study (figures 27-29). Any given truck could be used if its values of W , b , d , and δ/h are known.* The procedure is to enter the observed value of truck tire r/d for the appropriate pass number in figure 33 (which presents graphically the family of curves described by equation 7), determine the corresponding N_c value, and then divide N_c by N_c/AI to obtain an estimate of AI . With a value of AI in hand, the user can then forecast aircraft tire performance from relations like those in figures 30-32, or from those illustrated in Appendix A.

* Use whole-truck rut depth with W = average tire load, and assure that the truck's tires very nearly track one another; or use the truck's front-tire ruts only with W = front axle load.

SECTION IV

SUMMARY, CONCLUSIONS, AND RECOMMENDATIONS

1. SUMMARY

Two aircraft tires were tested: the 20-20, 22-PR at 25,000- and 35,000-lb loads and 75- and 100-psi inflation pressures for each load, and the 49-17, 26-PR at 25,000-lb load and 90- and 110-psi inflation pressures. Tests were also conducted with three standard military trucks (the M715, 1-1/4-ton; M35A2, 2-1/2-ton, and M51, 5-ton) unloaded and loaded (loads of 6,290 and 9,305 lb; 13,160 and 23,095 lb; and 21,690 and 41,700 lb, respectively) with single wheels on each axle (i.e. with the outer wheels of the second and third axles of the M35A2 and M51 trucks removed), and all tires inflated to produce 15 percent deflection. The aircraft tires and trucks were each tested in large laboratory pits of buckshot (highly plastic) clay prepared to strength levels of approximately 120, 350, 475, and 600 CI.

A typical aircraft tire test consisted of 100 passes (50 forward and 50 backward) in the same rut, with measurements taken of rut depth, towed force (drag force acting on a nonpowered, free-rolling tire), and hub movement produced by passes 2, 10, 20, 50, and 100. A truck test was conducted by making 10 forward and backward passes in the same straight-line path, and measuring maximum rut depth produced by the truck's front tires only and by all the truck's tires after truck passes 2, 6, and 10. Tests of both the aircraft tires and the trucks were conducted at low speed (about 3 ft/sec), and a given test was terminated when a 6-in. rut was developed before 100 single-tire or 10 truck passes, respectively.

A dimensionless tire-clay numeric $N_c = \frac{\overline{AI}bd}{W} \cdot \frac{1}{(1 - \frac{\delta}{h})^2} \cdot \frac{1}{1 + \frac{b}{2d}}$ (where AI = airfield index, b = tire section width, d = tire carcass diameter, W = single-wheel load, δ = maximum hard-surface tire deflection, and h = tire carcass section height) was used to describe results of both the towed aircraft tire tests and the powered truck tests.* Equations 5 and 7

* The form of numeric N_c was developed from dimensional analysis and the results of tests of much smaller tires, wheel loads, soil strength values, and a much wider range of tire shapes and deflection conditions than were tested in this study (reference 7).

were developed for the towed- and powered-wheel conditions, respectively, to describe the relations among rut-depth coefficient r/d, numeric N_c, and single-tire pass number n. Equations 6 and 6a describe the relations among towed-force coefficient P_T/W, N_c, and n.

Families of curves were developed from equation 7 to relate rut depth to AI for one or multiple passes of each of the six truck test conditions (figures 27-29). An AI value from one of these curves is then multiplied by known or estimated aircraft tire N_c/AI to estimate the value of N_c for the aircraft tire. [For a conventionally shaped aircraft tire ($b/d \approx 0.35$), operating at 32 percent deflection (the usual tire design value), N_c/AI can be estimated as $N_c/AI = 1.84 \times \frac{bd}{W}$ (see figure 30). A more precise estimate of N_c/AI requires knowledge of the aircraft tire's exact b, d, W, and δ/h values.] Families of curves showing the relation of N_c to r/d and to P_T/W for multiple passes of an aircraft tire (figures 31 and 32, respectively) are then used to estimate rut depth and towed force for the aircraft tire pass number of interest. From reference 1, a rut depth of 3 in. is recommended as the maximum allowable for safe aircraft operation on an earthen airfield.

Estimates of AI can also be made from ruts produced by trucks other than those tested in this study. The truck tire r/d value is entered in the r/d versus N_c relation for self-powered wheels (figure 33) to estimate N_c. Then, N_c is divided by truck-tire $\frac{bd}{W} \cdot \frac{1}{\left(1 - \frac{\delta}{h}\right)^2} \cdot \frac{1}{1 + \frac{b}{2d}}$ to estimate AI. Also, a more direct estimate of the aircraft tire N_c value can be obtained by applying the r/d value produced by a given number of passes of the aircraft tire to the towed tire r/d versus N_c relation in figure 31.

Rut depths used to establish equations 4 and 7 were measured precisely by rod and level relative to the original soil surface. Straightedge-and-ruler measurements were also taken of the rut depths to simulate crude measurements that often must be taken in forward-area field situations. For rut depths of about 0.3 in. and larger, the straightedge-and-ruler method consistently gave values slightly larger than those by rod and level (figure 25); for smaller rut depths, the opposite was as likely to occur. Thus, straightedge-and-ruler measurements lead to conservative (slightly too low) estimates of soil strength for ruts of at least

0.3-in. depth. For ruts measured as less than 0.3 in. deep by straightedge and ruler, a conservative approach is to estimate soil strength as if a 0.3-in. rut were measured.

For the buckshot clay test soil, relations of CI and AI to CBR were determined (figure 15), and CI was related to AI by a ratio of 50:1. Measurements of rut depth relative to the rut shoulders were about 12/7 times larger than those measured relative to the original soil surface (figure 26). A fairly well-defined relation was found to exist between rut depth and wheel hub movement (figure 21).

2. CONCLUSIONS

Based on analysis of the results of this test program the following conclusions are made:

a. The tire-clay numeric $N_c = \frac{\overline{AI}bd}{W} \cdot \frac{1}{\left(1 - \frac{\delta}{h}\right)^2} \cdot \frac{1}{1 + \frac{b}{2d}}$ is effective in consolidating rut-depth and towed-force data to single N_c versus r/d and N_c versus P_t/W relations for a wide range of values of each variable included in N_c. Different N_c versus r/d relations are obtained for the free-rolling condition (aircraft tire tests) and for tires that are powered (the military truck tests), but the form of N_c is the same for both situations.

b. The effect of tire pass number n on the N_c versus r/d relation is to cause r/d to increase monotonically with pass number for a given value of N_c. For a given value of N_c, the value of P_T/W is very slightly larger on the first than on the second pass, and increases monotonically starting with pass number two.

c. AI can be estimated from AI versus rut-depth curves for single or multiple passes of the three military trucks tested loaded or unloaded at 15 percent tire deflection with single wheels on each truck axle (figures 27-29). AI can also be estimated from the rut produced by other trucks (figure 33). Better estimates of AI result if the rut depth value used is that produced by tires that follow exactly the same path (i.e., tires that track one another).

d. Curves showing the relations of N_c to rut-depth coefficient (r/d) and to towed force coefficient (P_T/W) for multiple passes of an aircraft tire can be used to forecast multipass aircraft tire rut depth and towed force (figures 31 and 32). The value of aircraft tire N_c can be computed as AI x N_c/AI , where AI is measured or is estimated from figure 33 or from one of figures 27-29, and N_c/AI is computed from known values of b , d , W , and δ/h for the aircraft's tires or is estimated from a relation like that in figure 30.

e. Aircraft tire N_c should be estimated from the N_c versus r/d relation (figure 31) when r/d is known for one or more aircraft tire passes. Forecasts of multipass aircraft-tire rut depth and towed force performance can be made using figures 31 and 32.

f. AI can be accurately estimated from truck tire rut depth only within a fairly limited range of AI values (on the order of 2 to 10 for a truck rut of at least 0.3 in.--see figures 27-29). Shallower ruts cannot be measured routinely with sufficient accuracy to make very precise estimates of AI.

g. Very careful measurements with straightedge and ruler usually produce rut depth values slightly larger than actual for a rut at least 0.3-in. deep. These values should be used without correction, since measuring rut depth slightly too large leads to conservative (slightly too small) estimates of AI. For rut depths smaller than 0.3 in., soil strength can be estimated conservatively as that which corresponds to a 0.3-in. rut.

h. For the remolded buckshot clay tested in the soil pits, CBR is related to AI and to CI on a curvilinear basis (figure 15). Measurements of AI and CI taken in this study tended to confirm that CI can be related to AI on a 50:1 basis for soils whose penetration resistance is nearly constant with depth of penetration.

i. Wheel hub movement can be estimated as 0.73 times rut depth for rut depths of at least 2 in. and the range of aircraft tire-load-soil conditions tested.

3. RECOMMENDATIONS

It is recommended that:

a. Tests be conducted in the field to determine the practical accuracy and reliability of using truck rut depth to estimate soil strength (figures 27-29 and 33) and, ultimately, aircraft tire performance (figures 31 and 32).

b. The range of application of the aircraft tire-clay numeric be extended to describe multiple-tire landing gear configurations and ground speeds of 100 mph and greater.

c. Study be made to determine whether maximum allowable rut depth for aircraft operation on earthen airstrips should be defined in terms relative to the size of the aircraft tires, e.g., in terms of rut-depth coefficient r/d .

APPENDIX

PREDICTION OF OPERATIONAL CAPABILITY OF AIRCRAFT ON UNSURFACED SOILS THROUGH USE OF GROUND VEHICLES

1. PURPOSE

This appendix provides a detailed example of the procedures by which criteria for prediction of operational capability for aircraft on unsurfaced airfields can be derived through use of results from an investigation of the type reported in the main text.

2. SCOPE

The procedures demonstrated can be used for any combination of soil, ground vehicle, and aircraft provided the following basic relationships have been developed:

a. Rut depth versus airfield index for specific soil and ground vehicle considered.

b. Airfield index (AI) versus California Bearing Ratio (CBR).

It is emphasized that these relationships must be for the specific soil and ground vehicle considered because these relationships vary with soil type and ground vehicle as shown in figures 34 through 37. The variation between AI and CBR for soils ranging from a well-graded sand (MCASS, Yuma) to a very plastic remolded clay (WES) are shown in figure 34. A comparison of the relationship between AI and rut depth as a function of type of ground vehicle, shown in figures 35, 36, and 37 indicates the wide variation possible for this relationship.

All predictions presented herein relative to operational capability of aircraft on unsurfaced airfields are for specific combinations of soil, ground vehicle, and aircraft as listed below:

a. Soil Type. Remolded buckshot clay.

b. Ground Vehicle. M715, 1-1/4-ton truck; M35A2, 2-1/2-ton truck; and M51, 5-ton truck.

c. Aircraft. C-130 and C-5A cargo planes.

3. VEHICLE CHARACTERISTICS

Pertinent characteristics of vehicles considered in this study are given in tables VI and VII.

Table VI

CHARACTERISTICS OF GROUND VEHICLES

Truck	Load Condition	Gross Weight kips	Tire Size	Tire Section Height* in.
M715	Unloaded	6.3	9.00-16, 8-PR	6.85
	Loaded	9.3		6.95
M35A2	Unloaded	13.16	9.00-20, 8-PR	7.45
	Loaded	23.1		7.54
M51	Unloaded	21.7	11.00-20, 12-PR	8.44
	Loaded	41.7		8.6

* Loaded section height is defined as the minimum distance from the lowest point of the lip flange to an unyielding surface on which the loaded tire is resting (see sketch in figure 35).

Table VII

AIRCRAFT CHARACTERISTICS

Type	Pass per Coverage Ratio	Tire Contact Area $in.^2$	Gross Weight kips	Single Wheel Load kips	Tire Inflation Pressure psi
C-130	2.0	400	85	21	53
			105	25	63
			146	35	88
C-5A	0.81	285	455	18	63
			578	23	81
			637	25	88

4. PROCEDURE

The procedures used to develop the criteria for predicting the operational capability of aircraft on unsurfaced soils from rut depth measurements resulting from operation of ground vehicles on these soils are demonstrated in the following paragraphs.

a. Determination of Equivalent Single-Wheel Loads (ESWL) for Aircraft

(1) C-130 aircraft.

(a) Calculate radius of a circle with an area equal to tire contact area.

$$\text{Contact Area} = 400 \text{ in.}^2$$

$$\text{Area} = \pi r^2 = 400 \text{ in.}^2$$

$$r = \sqrt{\frac{400}{\pi}} = 11.29 \text{ in.}$$

(b) Determine wheel spacing in radii. Wheel spacing for C-130 = 60 in. (figure 38). Wheel spacing in radii = $\frac{60}{11.29}$ or 5.3 in.

(c) Calculate ESWL. Read increase in single-wheel load for adjacent wheel from figure 39. For all practical considerations, the increase in single-wheel load for a wheel spacing of 5.3 radii is equal to zero; therefore, the ESWL for each of the gross aircraft weights considered is equal to the single-wheel load for each weight considered as shown below:

Gross Aircraft Weight kips	Single-Wheel Load kips	Increase %	ESWL kips
85	21	0	21
105	25	0	25
146	35	0	35

(2) C-5A aircraft.

(a) Calcualte radius of a circle with an area equal to tire contact area:

$$\text{Contact area} = 285 \text{ in.}^2$$

$$\text{Area} = \pi r^2 = 285 \text{ in.}^2$$

$$r = \sqrt{\frac{285}{\pi}} = 9.53 \text{ in.}$$

(b) Determine wheel spacing in radii. Minimum wheel spacing for C-5A = 34 in.* (figure 40). Wheel spacing in radii = $\frac{34}{9.53}$ or 3.57.

(c) Calculate ESWL. Read increase in single-wheel load for adjacent wheel from figure 39. For a wheel spacing of 3.57 radii, the single-wheel load is increased 33.5 percent; therefore, the ESWL for each of the gross aircraft weights considered is equal to the single-wheel load multiplied

* No increase in single-wheel load is required for other spacings since all other spacings are greater than 5.3 radii.

by 1.335 as shown below:

Gross Aircraft Weight kips	Single-Wheel Load kips	Increase %	ESWL kips
455	18	33.5	24
578	23	33.5	31
637	25	33.5	34

b. Determination of Operational Capability for Aircraft

In the following example, the operational capability of a C-130 aircraft with a gross weight of 85 kips will be determined for a 0.1-in. rut depth resulting from 5 passes of the M715 truck with a gross weight of 9.3 kips (loaded condition). Values shown in table VIII will be determined.

(1) Read AI values from figure 35 for a 0.1-in. rut depth and 5 passes (10 single-tire passes) of the loaded M715 truck. The AI value is 5.9 as shown in table VIII.

(2) Read CBR value equivalent to AI value of 5.9 from figure 41. The equivalent CBR value is 6.7, as shown in table VIII.

(3) Determine the operational capability of aircraft. The operational capability of aircraft on unsurfaced soils can be predicted through use of the nomogram shown in figure 42. The procedure for use of this nomogram is as follows:

(a) Data required: Type of aircraft - C-130

Gross aircraft load - 85 kips

Tire inflation pressure - 53 kips

ESWL - 21 kips

CBR - 6.7

(b) Procedure. Enter tire pressure scale of figure 42 at 53 psi; proceed vertically to 21-kip single-wheel-load curve (interpolate between 20- and 25-kip load curve); proceed to the right, horizontally, to right edge of tire pressure scale (300 psi); draw line from this point though 6.7 on CBR scale to 1000 coverages. Multiply coverages by operations per coverage ratio for specific aircraft considered to obtain operational capability in terms of passes: (1000 coverages) (2.0) = 2000 passes.

(4) Repeat all steps above for each rut depth, aircraft load, vehicle and number of ground vehicle passes considered to develop operational capability as required.

5. PREPARATION OF CRITERIA

Basic data used in preparation of the criteria presented herein is shown in tables VIII through XIII. These data were obtained in accordance with the procedures described in section 4. It is emphasized that these data were obtained by the writer by reading and interpreting various values from the six curves shown in figures 35, 36, 37, 39, 41, and 42 and that similar data so obtained by another individual would in all probability be somewhat different. This fact is of no consequence since the criteria so developed are considered to represent only an expedient method for obtaining approximate predictions for operational capability of aircraft on unsurfaced soils. Various procedures were investigated for determining the best way to develop the criteria shown in figures 43 through 54. In studying the basic data (tables VIII through XIII), it soon became apparent that the best plot of these data could be obtained on a log-log plot.

In general, a line through the plotted data tended to be a straight line on a log-log plot except for values relative to very shallow rut depths (0.1 and 0.2 in.). In these instances, a line through the data tended to form a concave (upward) curve. Since it is anticipated that it will be rather difficult to correctly measure very shallow rut depths in the field, it appears desirable to ignore the data in these instances and draw (visually) the best-fit line through the remaining data points. This procedure provides a built-in safety factor to compensate for difficulty in measuring shallow rut depths in the field. The procedure used in preparing the criteria shown in figures 43 through 54 is as follows:

a. Step 1. Plot data for the least gross aircraft weight considered and pertinent loaded ground vehicle (truck) on log-log paper.

b. Step 2. Draw (visually) the best-fit straight line through the plotted points, ignoring data points for very shallow rut depths (0.1 and 0.2 in.).

c. Step 3. Plot data for other gross aircraft weights and for both loaded and unloaded ground vehicle (truck).

d. Step 4. Draw (visually) the best-fit straight line through the plotted data parallel to line drawn in step 2 above. In some instances criteria are not presented for all gross aircraft weights shown in tables VIII through XIII. In those instances where a straight line through the plotted data indicated an operational acapability of 10 passes or less for a rut depth of 0.1 in., that line was not included as a part of the criteria.

6. APPLICATION OF CRITERIA

The criteria shown in figures 43 through 54 for prediction of operational capability of aircraft are applicable only to predictions of such capability for aircraft operation on remolded buckshot clay where rut depth measurements are made on ruts resulting from operation of one of the vehicles listed in table VI on remolded buckshot clay.

7. RESTRICTIONS ON USE OF CRITERIA

It is emphasized that no attempt should be made to use the criteria presented in figures 43 through 54 for prediction of operational capability of aircraft on soils other than remolded buckshot clay (even similar soils) except in a closely controlled, well-planned field investigation. In all instances (even on buckshot clay) where the predicted operational capability of an aircraft is less than about 25 passes, proceed with extreme caution.

Table VIII

CORRELATION OF VEHICLE RUT DEPTH RESULTING FROM FIVE PASSES OF AN M715,1-1/4-TON TRUCK* AND AIRCRAFT OPERATIONAL CAPABILITY OF C-130 AND C-5A

Rut Depth in.	Airfield Index	CBR	Coverages of Aircraft at Indicated Load Conditions** C-130† 85 kip/ 53 psi	C-130† 105 kip/ 63 psi	C-130† 146 kip/ 88 psi	C-5A†† 455 kip/ 63 psi	C-5A†† 578 kip/ 81 psi	C-5A†† 637 kip/ 88 psi
					Unloaded Truck			
0.1	4.0	4.3	70	16	1	18	2.3	1
0.2	3.1	3.2	11	2.8	-	2.8	-	-
0.3	2.6	2.6	3.5	-	-	-	-	-
0.4	2.3	2.3	-	-	-	-	-	-
0.5	2.1	2.1	-	-	-	-	-	-
0.8	1.8	1.8	-	-	-	-	-	-
					Loaded Truck			
0.1	5.9	6.7	1000	240	13	280	36	14
0.2	4.5	4.8	130	34	1.8	33	4.5	2
0.3	3.8	4.2	56	14	-	15	1.8	-
0.4	3.5	3.8	31	8	-	7.5	1	-
0.5	3.2	3.4	18	4	-	4	-	-
0.8	2.7	2.8	7.5	1.7	-	1.8	-	-

*

	Gross Weight kips	Section Height in.
Unloaded	6.3	6.85
Loaded	9.3	6.95

** Load conditions shown are gross weight/tire inflation pressure.

† Pass per coverage ratio for C-130 aircraft = 2.0.

†† Pass per coverage ratio for C-5A aircraft = 0.81.

Table IX

CORRELATION OF VEHICLE RUT DEPTH RESULTING FROM TEN PASSES OF AN M715, 1-1/4-TON TRUCK* AND AIRCRAFT OPERATIONAL CAPABILITY OF C-130 AND C-5A

Rut Depth in.	Airfield Index	CBR	Coverages of Aircraft at Indicated Load Conditions** C-130† 85 kip/53 psi	C-130† 105 kip/63 psi	C-130† 146 kip/88 psi	C-5A†† 455 kip/63 psi	C-5A†† 578 kip/81 psi	C-5A†† 637 kip/88 psi
				Unloaded Truck				
0.2	3.5	3.8	32	8	-	8.5	1	-
0.4	2.7	2.8	7	1.7	-	1.8	-	-
0.6	2.3	2.3	-	-	-	-	-	-
0.8	2.0	2.0	-	-	-	-	-	-
1.0	1.9	1.9	-	-	-	-	-	-
				Loaded Truck				
0.2	5.1	5.7	350	85	4.5	95	12	5
0.4	3.9	4.2	67	15.5	-	17	2.3	1
0.6	3.3	3.5	20	4.5	-	4.5	-	-
0.8	3.0	3.2	12	2.8	-	3	-	-
1.0	2.8	2.8	5.5	1.2	-	1.5	-	-
2.0	2.5	2.5	1.5	-	-	-	-	-

*

	Gross Weight kips	Section Height in.
Unloaded	6.5	6.85
Loaded	9.3	6.95

** Load conditions shown are gross weight/tire inflation pressure.

† Pass per coverage ratio for C-130 aircraft = 2.0.

†† Pass per coverage ratio for C-5A aircraft = 0.81.

Table X

CORRELATION OF VEHICLE RUT DEPTH RESULTING FROM TWO PASSES OF AN M35A2, 2-1/2-TON TRUCK* AND AIRCRAFT OPERATIONAL CAPABILITY OF C-130 AND C-5A

Rut Depth in.	Airfield Index	CBR	Coverages of Aircraft at Indicated Load Conditions** C-130† 85 kip/53 psi	C-130† 105 kip/63 psi	C-130† 146 kip/88 psi	C-5A†† 455 kip/63 psi	C-5A†† 578 kip/81 psi	C-5A†† 637 kip/88 psi
			Unloaded Truck					
0.1	4.3	4.8	136	32	1.7	35	4.6	1.9
0.2	3.3	3.5	20	4.5	-	5	-	-
0.3	2.8	2.9	6	1.5	-	1.7	-	-
0.4	2.5	2.5	2.5	-	-	-	-	-
0.5	2.3	2.3	1.5	-	-	-	-	-
0.8	1.95	1.95	-	-	-	-	-	-
			Loaded Truck					
0.2	5.6	6.4	760	185	9.5	210	25	11
0.4	4.3	4.8	136	32	1.7	35	4.6	1.9
0.6	3.7	4.0	43	10	-	10.5	1.5	-
0.8	3.3	3.5	20	4.5	-	4.5	-	-
1.0	3.0	3.2	12	2.8	-	3	-	-
1.5	2.6	2.6	3.5	-	-	-	-	-

* Outer tires removed from second and third axles.

	Gross Weight kips	Section Height in.
Unloaded	13.16	7.45
Loaded	23.1	7.54

** Load conditions shown are gross weight/tire inflation pressure.

† Pass per coverage ratio for C-130 aircraft = 2.0.

†† Pass per coverage ratio for C-5A aircraft = 0.81.

Table XI

CORRELATION OF VEHICLE RUT DEPTH RESULTING FROM FIVE PASSES OF AN M35A2, 2-1/2-TON TRUCK* AND AIRCRAFT OPERATIONAL CAPABILITY OF C-130 AND C-5A

			Coverages of Aircraft at Indicated Load Conditions**					
			C-130†			C-5A††		
Rut Depth in.	Airfield Index	CBR	85 kip/ 53 psi	105 kip/ 63 psi	146 kip/ 88 psi	455 kip/ 63 psi	578 kip/ 81 psi	637 kip/ 88 psi
				Unloaded Truck				
0.1	5.1	5.7	385	88	4.5	94	12	5
0.2	3.9	4.2	60	14	-	15	2	-
0.3	3.4	3.6	21	5	-	6	-	-
0.4	3.0	3.2	11	2.8	-	3	-	-
0.5	2.7	2.8	5	1	-	1.3	-	-
0.8	2.3	2.3	1.5	-	-	-	-	-
				Loaded Truck				
0.2	6.7	7.7	2300	550	30	580	75	32
0.4	5.1	5.7	385	88	4.5	94	12	5
0.6	4.4	4.7	120	32	1.5	31	4	1.7
0.8	3.9	4.2	60	14	-	15	2	-
1.0	3.6	3.7	28	6.5	-	7	-	-
1.5	3.1	3.3	13	3	-	3.5	-	-

* Outer tires removed from second and third axles.

	Gross Weight kips	Section Height in.
Unloaded	13.16	7.45
Loaded	23.1	7.54

** Load conditions shown are gross weight/tire inflation pressure.

† Pass per coverage ratio for C-130 aircraft = 2.0.

†† Pass per coverage ratio for C-5A aircraft = 0.81.

Table XII

CORRELATION OF VEHICLE RUT DEPTH RESULTING FROM ONE PASS OF AN M51, 5-TON TRUCK* AND AIRCRAFT OPERATIONAL CAPABILITY OF C-130 AND C-5A

Rut Depth in.	Airfield Index	CBR	Coverages of Aircraft at Indicated Load Conditions**					
			C-130†			C-5A††		
			85 kip/ 53 psi	105 kip/ 63 psi	146 kip/ 88 psi	455 kip/ 63 psi	578 kip/ 81 psi	637 kip/ 88 psi
			Unloaded Truck					
0.1	5.7	6.5	900	200	11	220	2.8	11
0.2	4.4	4.8	138	30	1.7	34	4.6	1.7
0.3	3.8	4.1	50	11	-	13	1.7	-
0.4	3.4	3.6	23	5	-	6	-	-
0.5	3.1	3.3	13	2.5	-	3.5	-	-
0.8	2.6	2.6	3.5	-	-	-	-	-
			Loaded Truck					
0.2	7.95	10	Unlimited	3000	150	3200	400	170
0.4	6.0	6.9	1260	290	15	300	40	17
0.6	5.2	5.8	480	110	6	115	15	6.5
0.8	4.6	5.0	180	40	2.2	44	6	2.5
1.0	4.1	4.5	90	21	1.2	23	3	1.3
1.5	3.6	3.7	28	6.5	-	3.5	-	-

* Outer tires removed from second and third axles.

	Gross Weight kips	Section Height in.
Unloaded	21.7	8.44
Loaded	41.7	8.6

** Load conditions shown are gross weight/tire inflation pressure.

† Pass per coverage ratio for C-130 aircraft = 2.0.

†† Pass per coverage ratio for C-5A aircraft = 0.81.

Table XIII

CORRELATION OF VEHICLE RUT DEPTH RESULTING FROM TWO PASSES OF AN M51,5-TON TRUCK* AND AIRCRAFT OPERATIONAL CAPABILITY OF C-130 AND C-5A

Rut Depth in.	Airfield Index	CBR	Coverages of Aircraft at Indicated Load Conditions** C-130† 85 kip/ 53 psi	C-130† 105 kip/ 63 psi	C-130† 146 kip/ 88 psi	C-5A†† 455 kip/ 63 psi	C-5A†† 578 kip/ 81 psi	C-5A†† 637 kip/ 88 psi
				Unloaded Truck				
0.1	6.6	7.7	2500	550	29	570	73	34
0.2	5.0	5.6	350	85	5	86	12	5.5
0.3	4.3	4.8	130	33	1.7	35	4.5	2
0.4	3.8	4.1	50	11.5	-	12	1.6	-
0.5	3.5	3.8	31	7.5	-	8.5	1	-
0.8	2.9	3.0	7	1.7	-	1.8	-	-
				Loaded Truck				
0.4	6.9	8.3	4000	900	50	1100	130	55
0.6	5.9	6.7	1025	240	12	260	33	15
0.8	5.3	5.8	480	107	6.5	112	15	6.8
1.0	4.8	5.3	250	60	3.3	67	8.5	3.5
1.5	4.1	45	91	22	1.2	23	3.1	1.3
2.0	3.7	4.0	42	10	-	11	1.3	-
3.0	3.2	3.4	17	3.8	-	4.2	-	-

* Outer tires removed from second and third axles.

	Gross Weight kips	Section Height in.
Unloaded	21.7	8.44
Loaded	41.7	8.6

** Load conditions shown are gross weight/tire inflation pressure.

† Pass per coverage ratio for C-130 aircraft = 2.0.

†† Pass per coverage ratio for C-5A aircraft = 0.81.

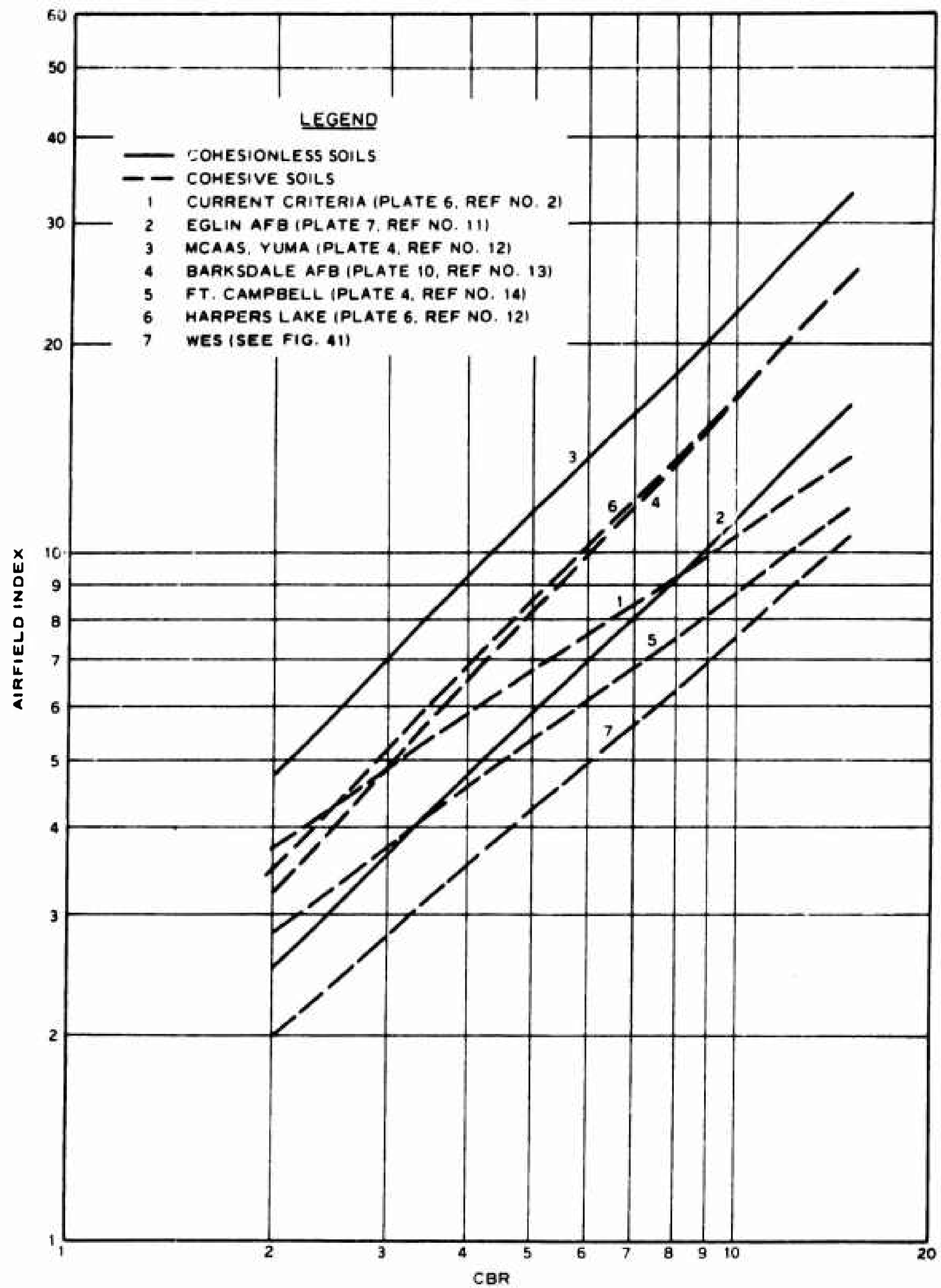

Fig. 34. Correlation Between Airfield Index and CBR

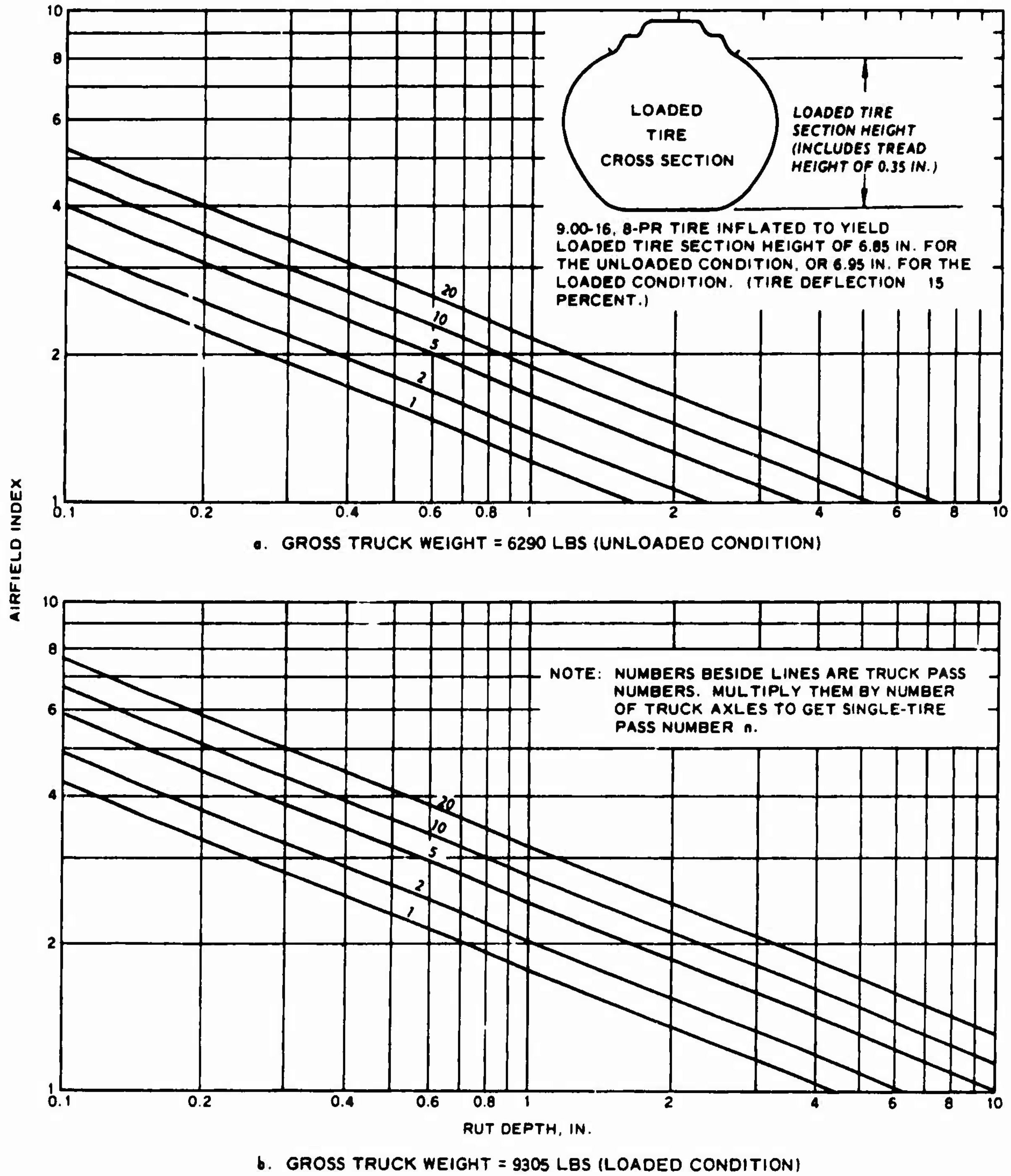

Fig. 35. Relation of Airfield Index to Rut Depth for Multiple Passes of the Unloaded and Loaded M715, 1-1/4-Ton Truck

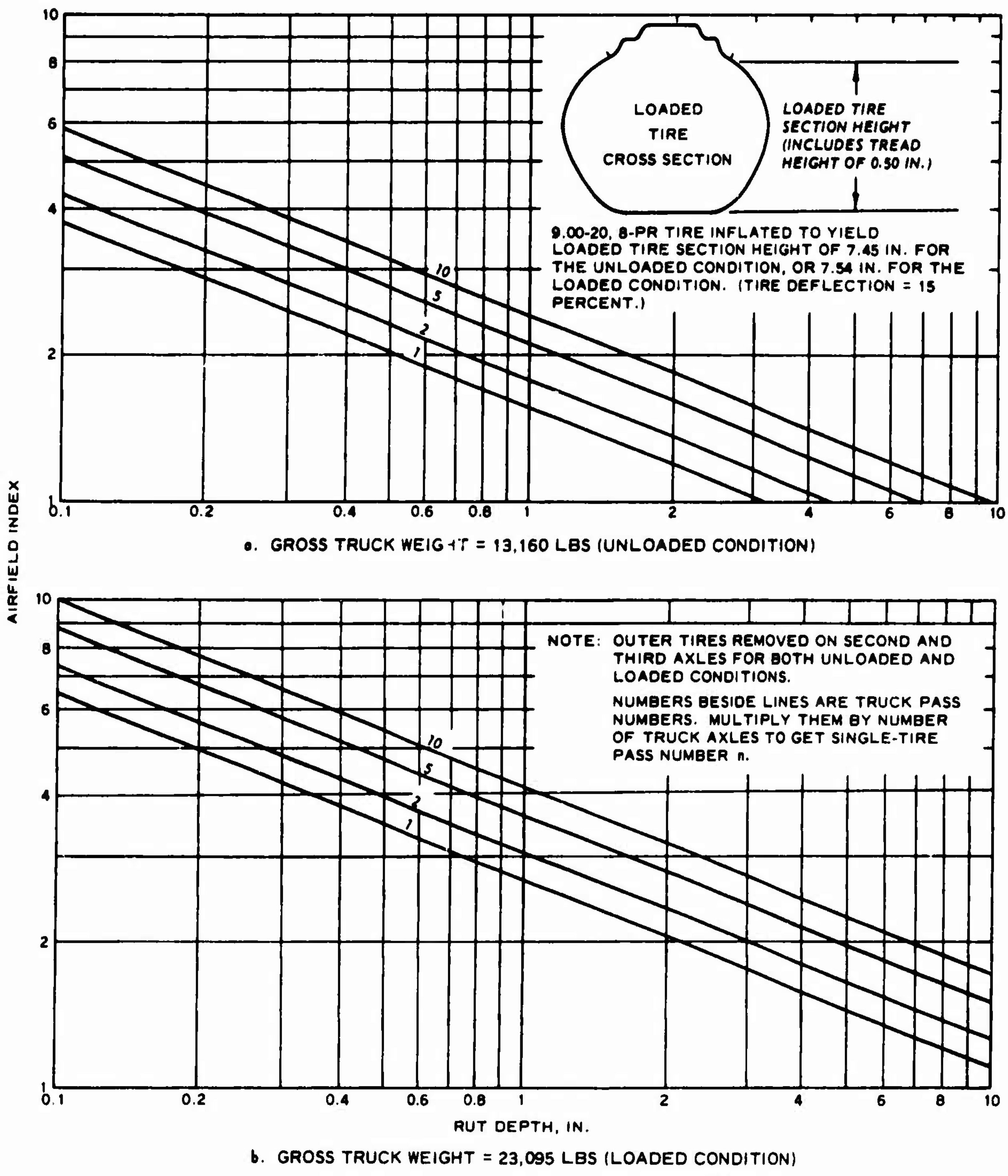

Fig. 36. Relation of Airfield Index to Rut Depth for Multiple Passes of the Unloaded and Loaded M35A2, 2-1/2-Ton Truck

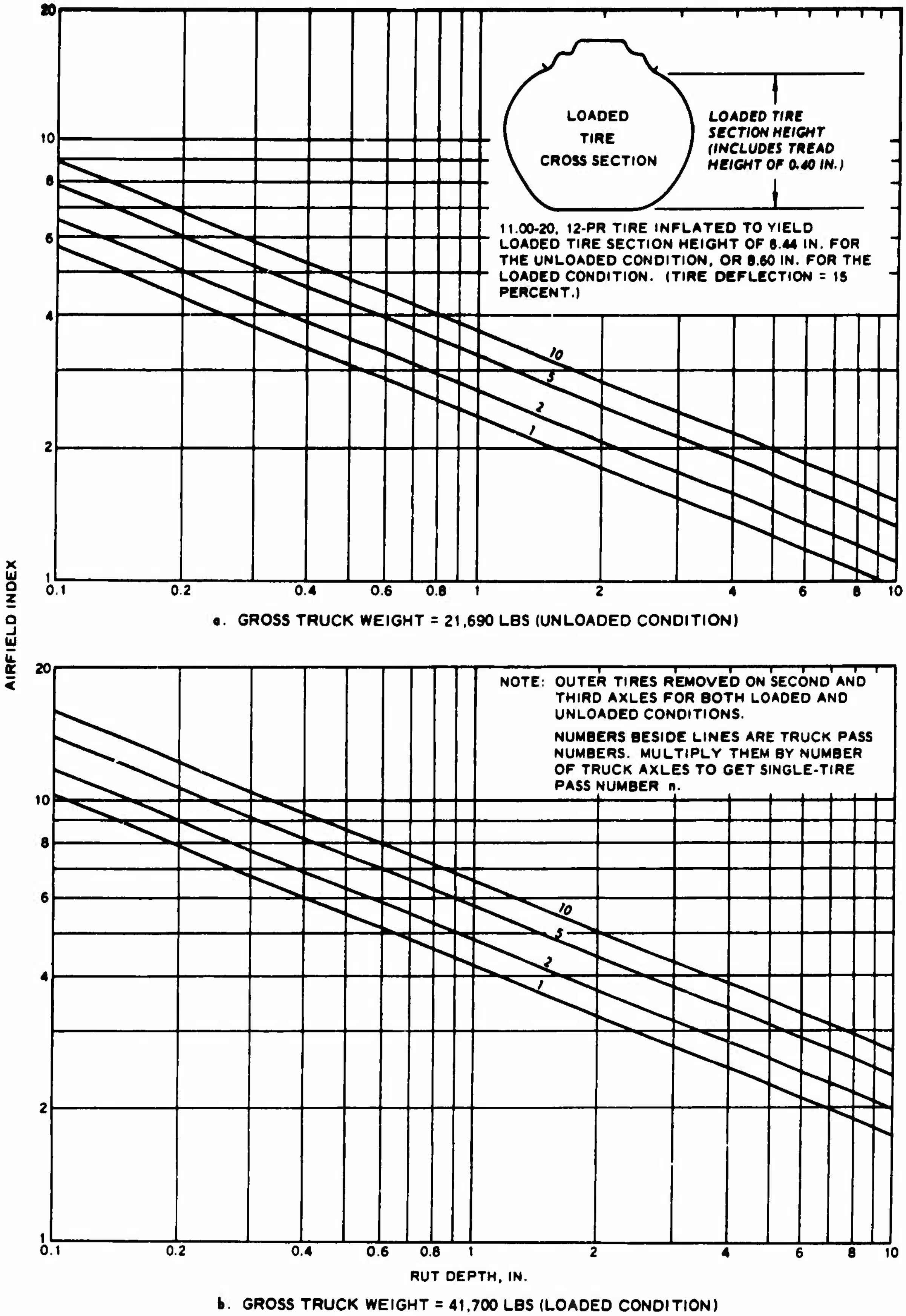

Fig. 37. Relation of Airfield Index to Rut Depth for Multiple Passes of the Unloaded and Loaded M51, 5-Ton Truck

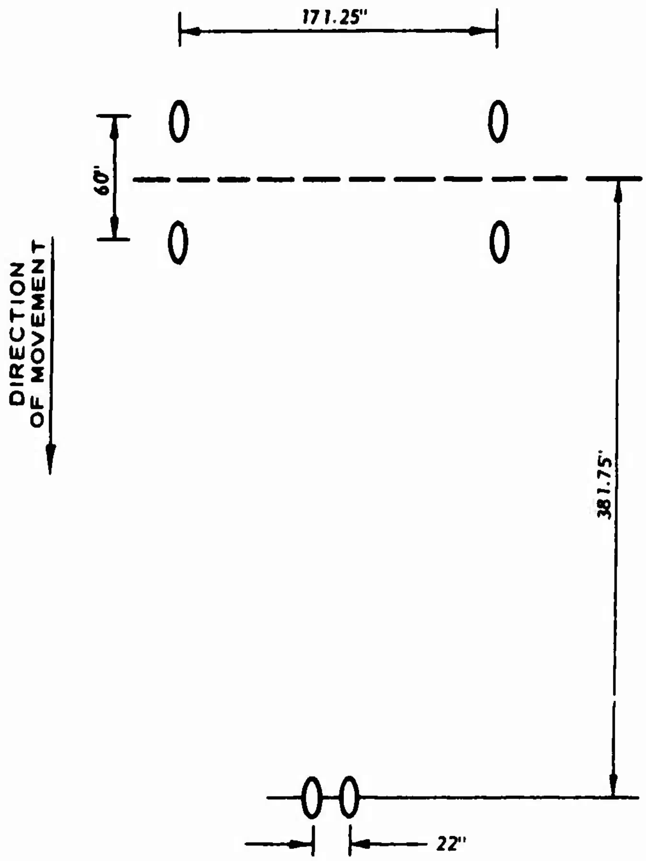

Fig. 38. C-130 Gear Configuration

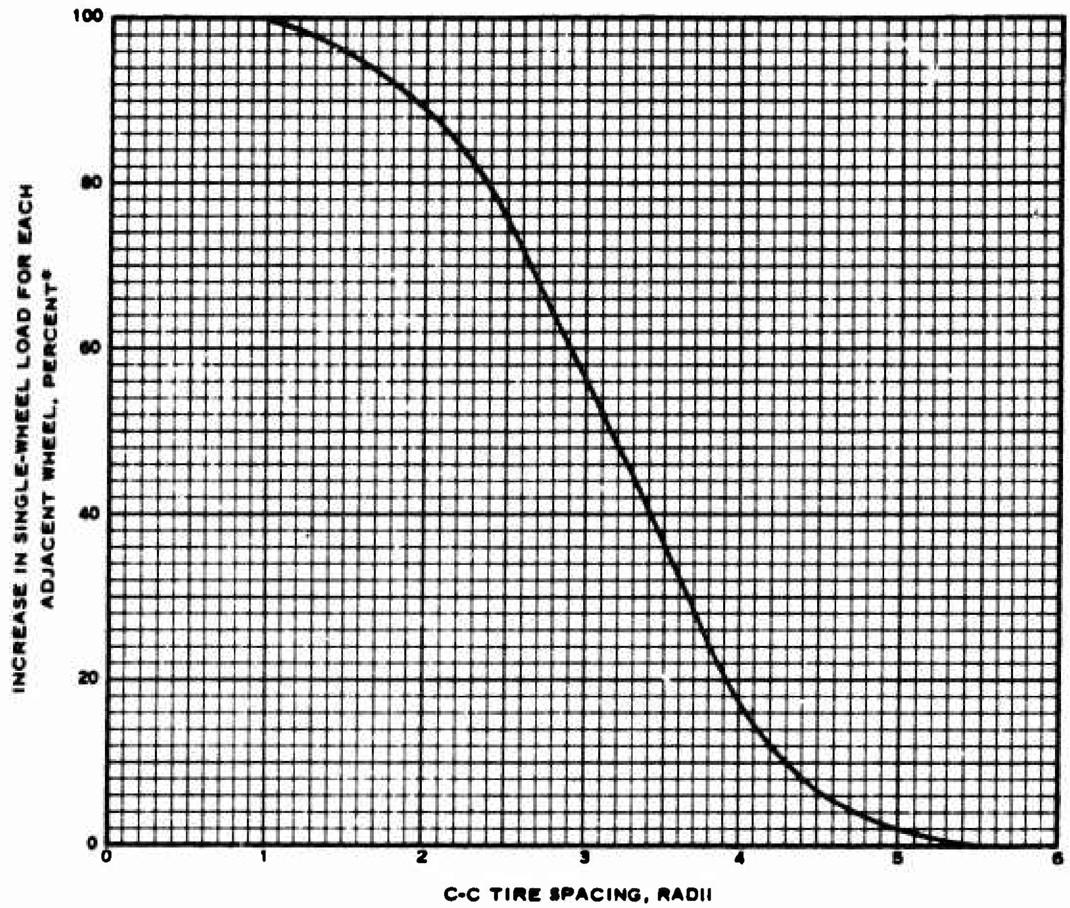

* INCREASE IN LOAD ON A SINGLE WHEEL OF A MULTIPLE-WHEEL GEAR TO ACCOUNT FOR EFFECTS OF ADJACENT WHEELS OF THE MULTIPLE-WHEEL GEAR IN ARRIVING AT AN EQUIVALENT SINGLE-WHEEL LOAD.

Fig. 39. Equivalent Single-Wheel Load-Adjustment Curve for Unsurfaced Soils

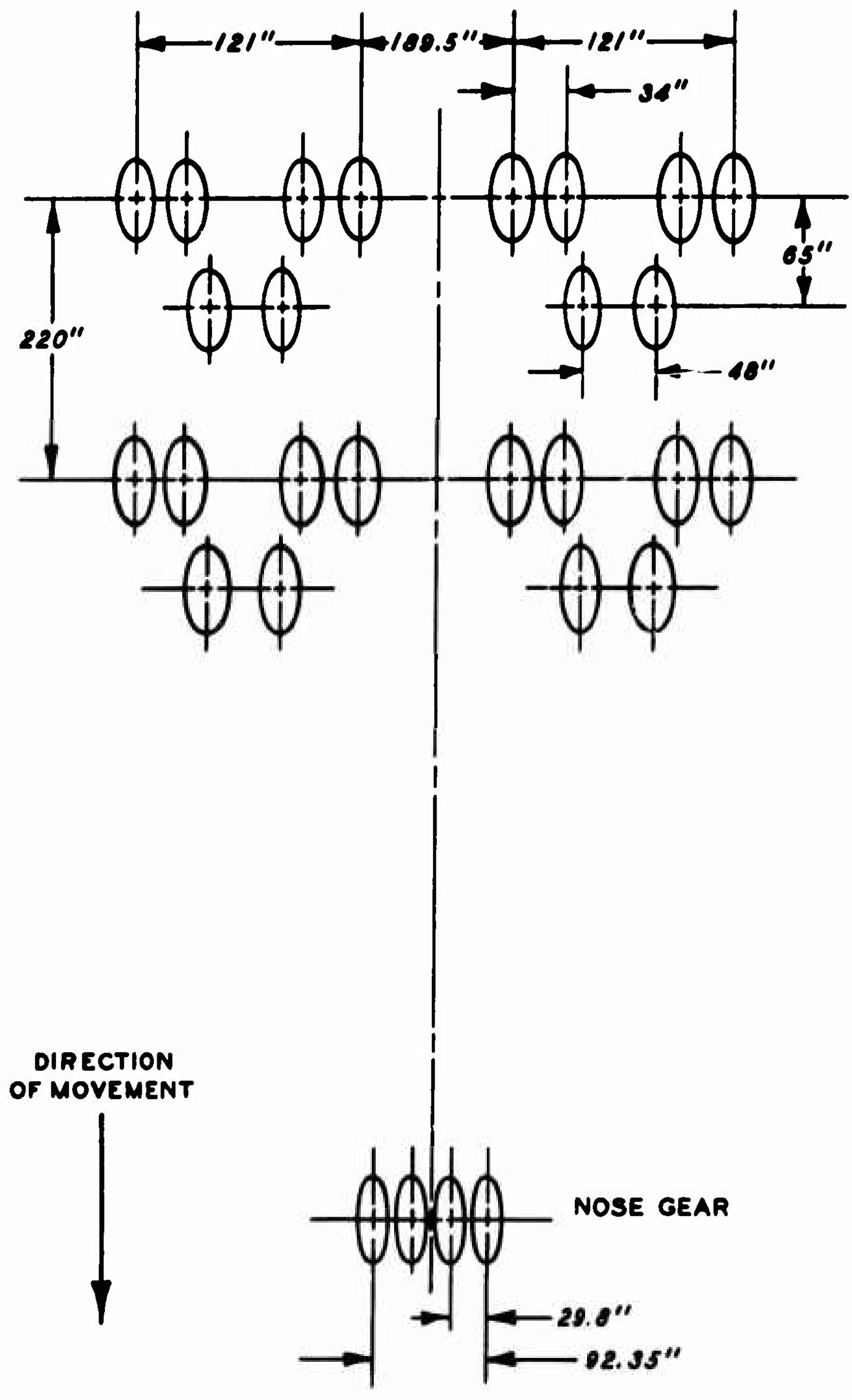

Fig. 40. C-5A Gear Configuration

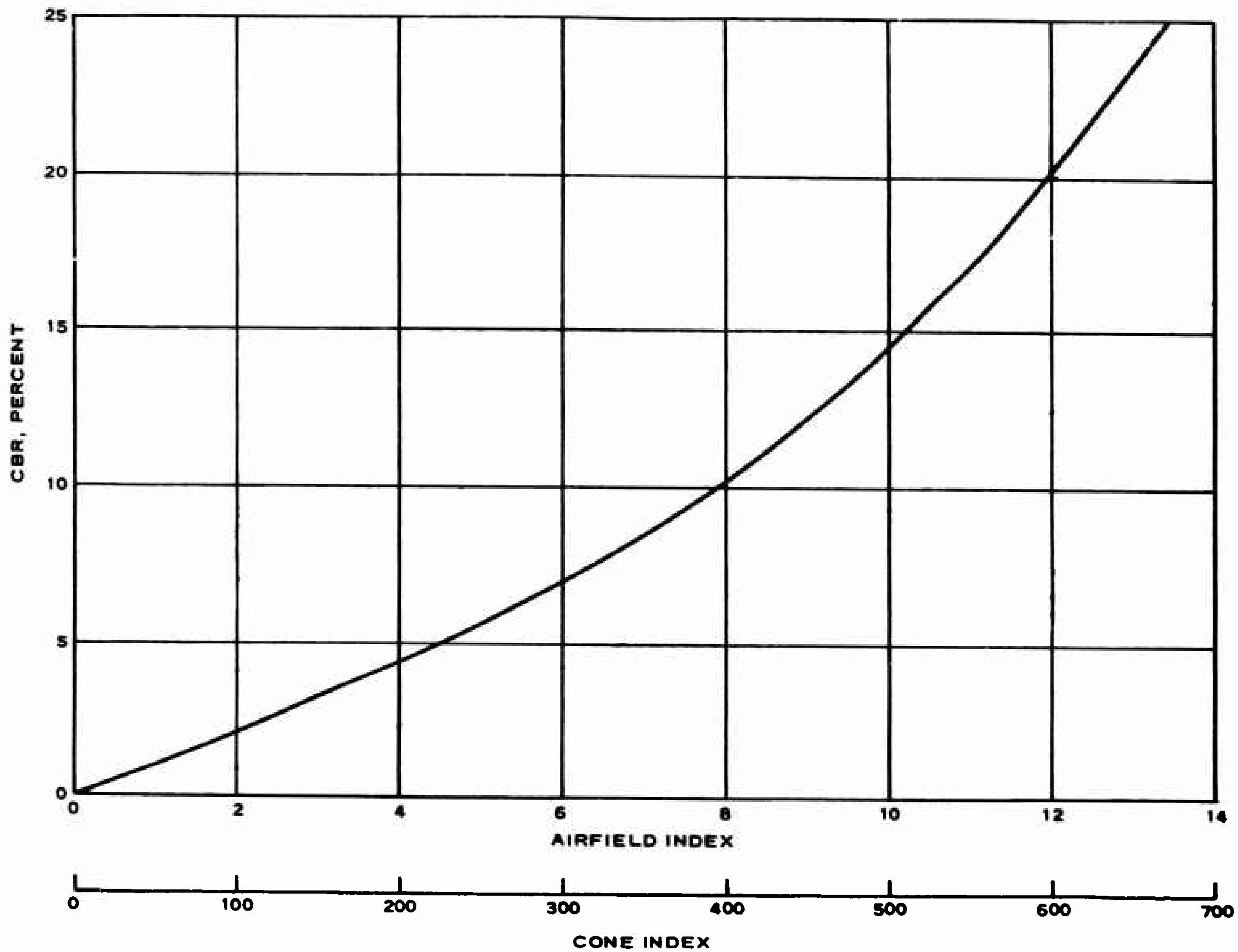

Fig. 41. Relation of CBR to Cone Index and to Airfield Index for Homogeneous Buckshot Clay

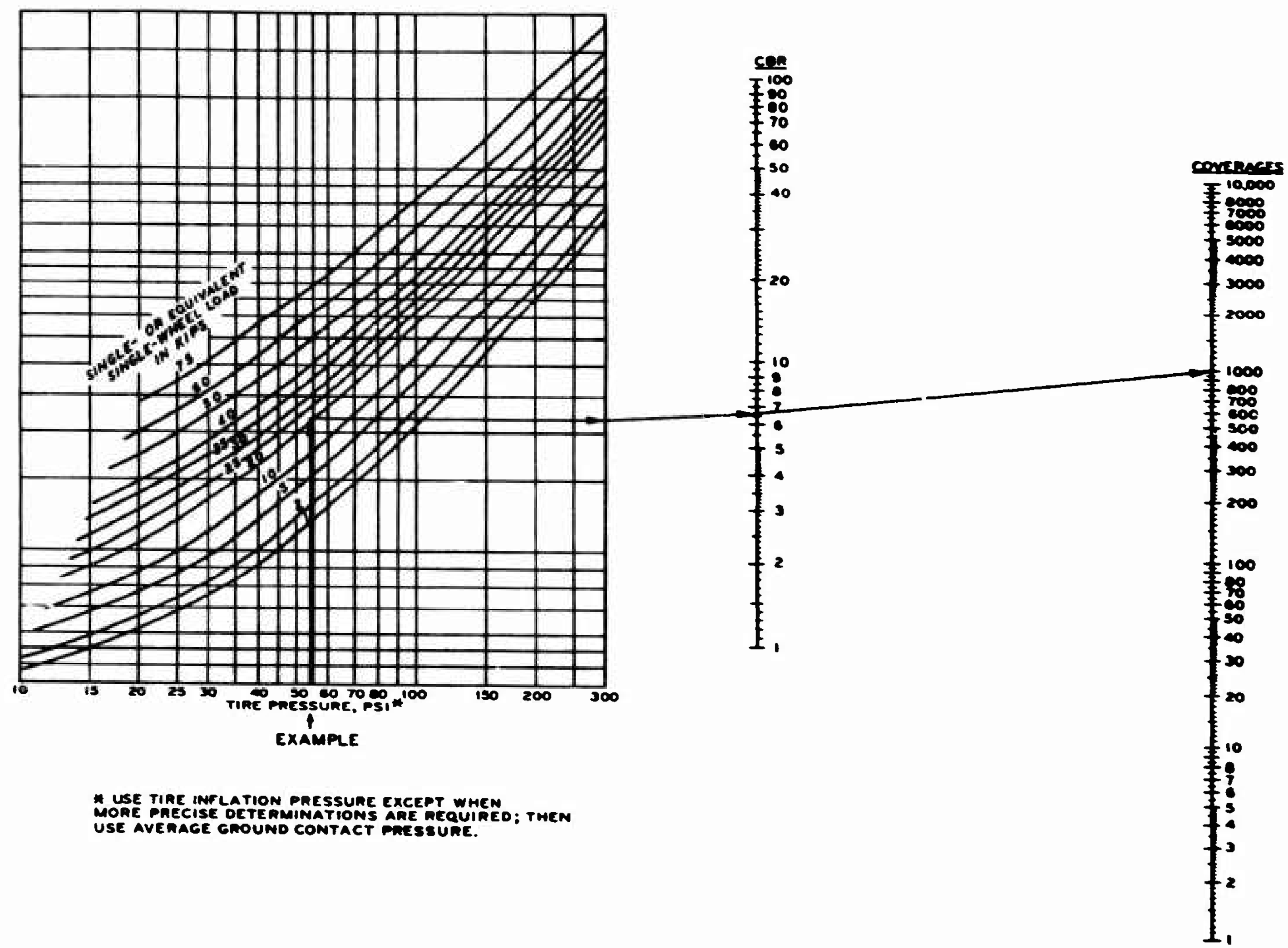

Fig. 42. CBR Required for Operation of Aircraft on Unsurfaced Soils

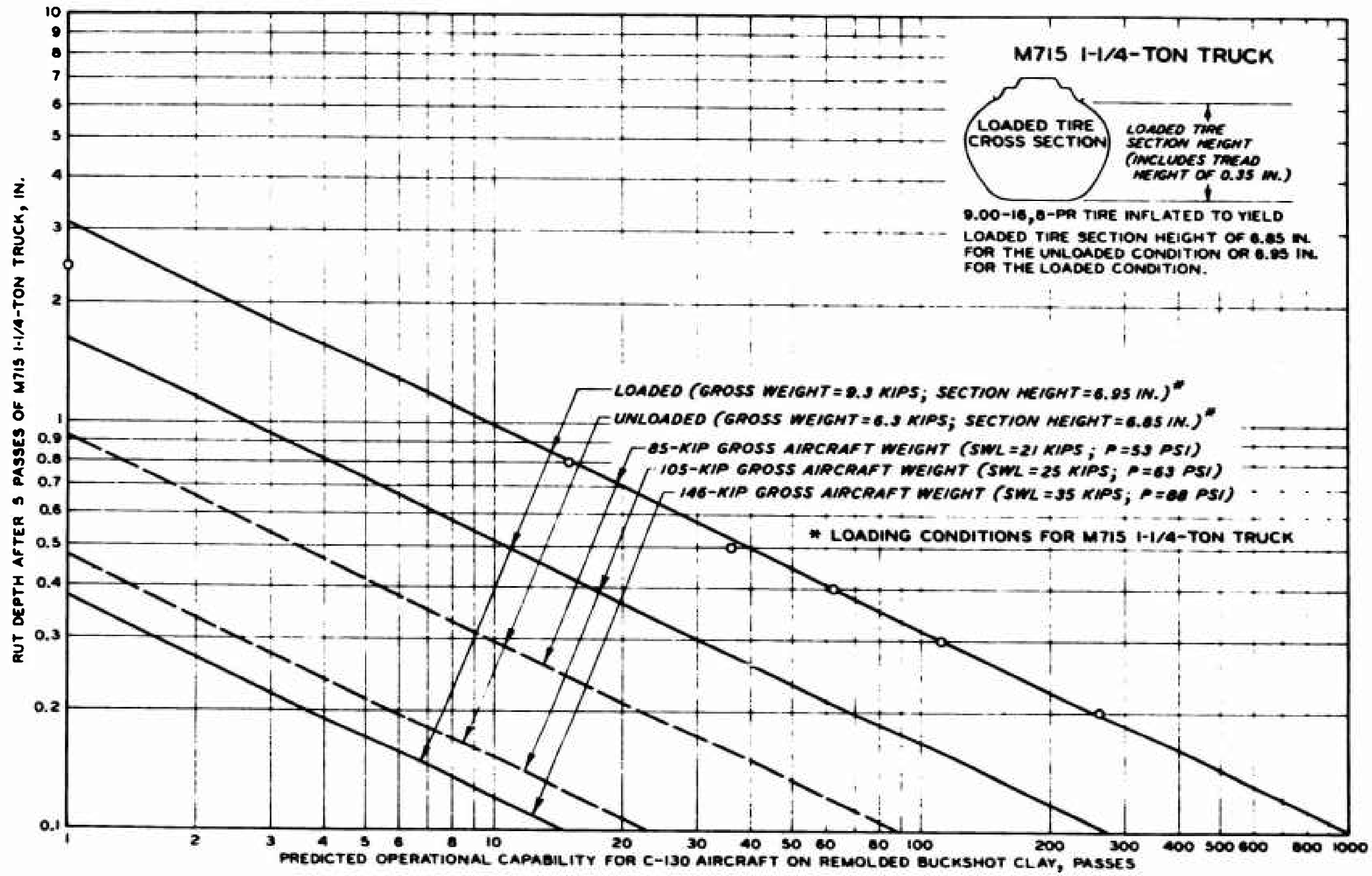

Fig. 43. Five-Pass Rut Depth for M715 Truck Versus C-130 Aircraft Operational Capability

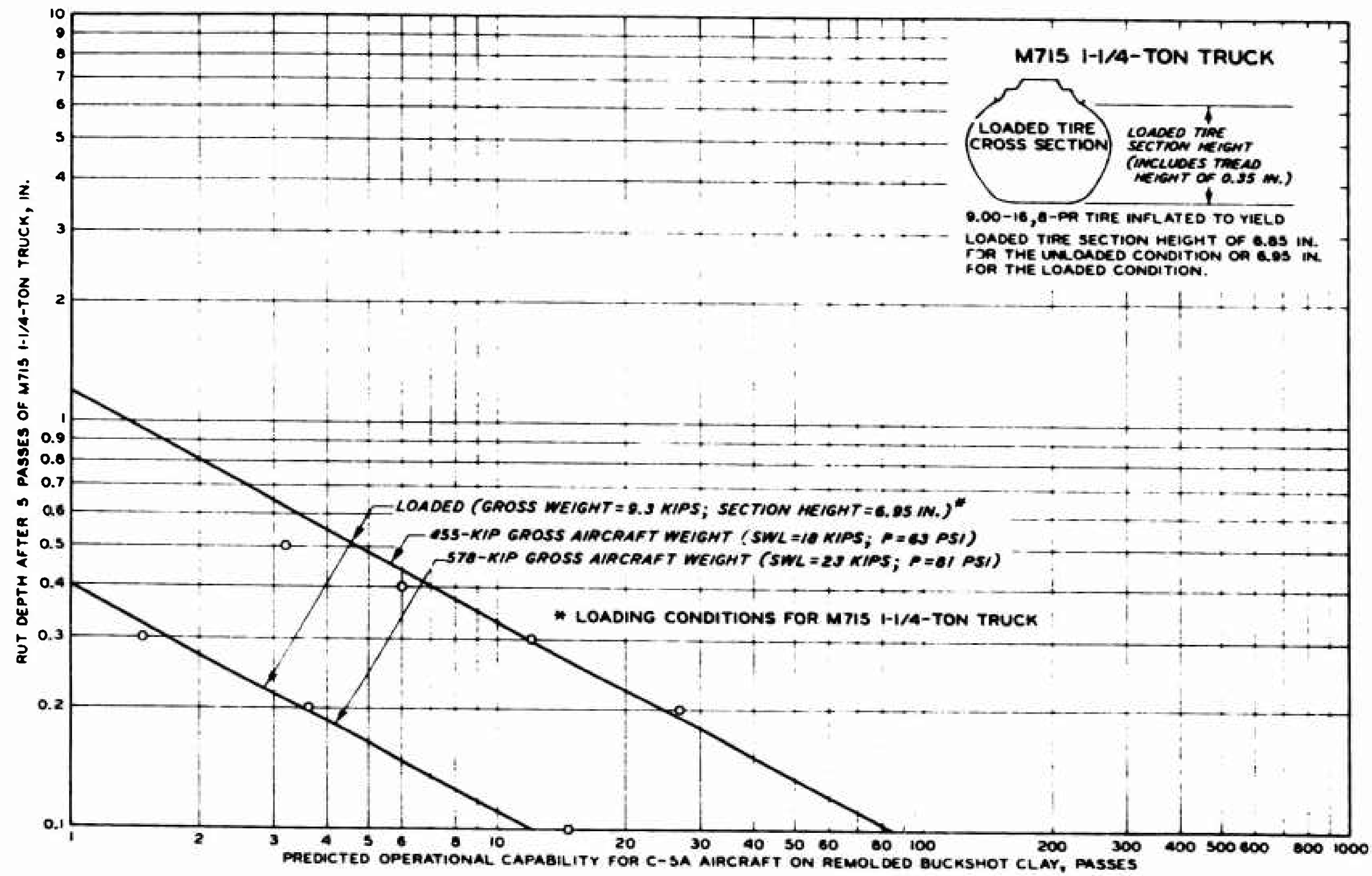

Fig. 44. Five-Pass Rut Depth for M715 Truck Versus C-5A Aircraft Operational Capability

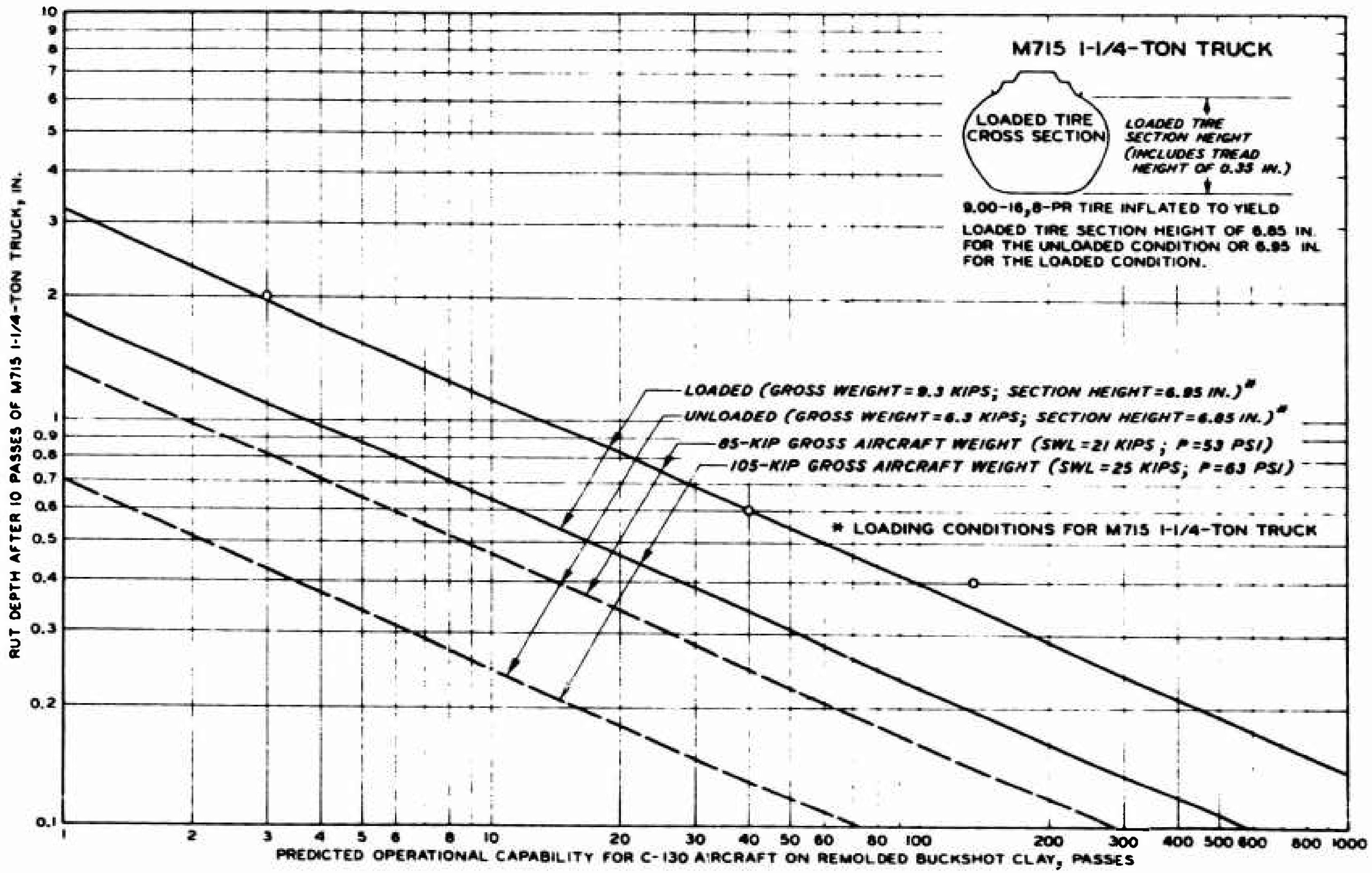

Fig. 45. Ten-Pass Rut Depth for M715 Truck Versus C-130 Aircraft Operational Capability

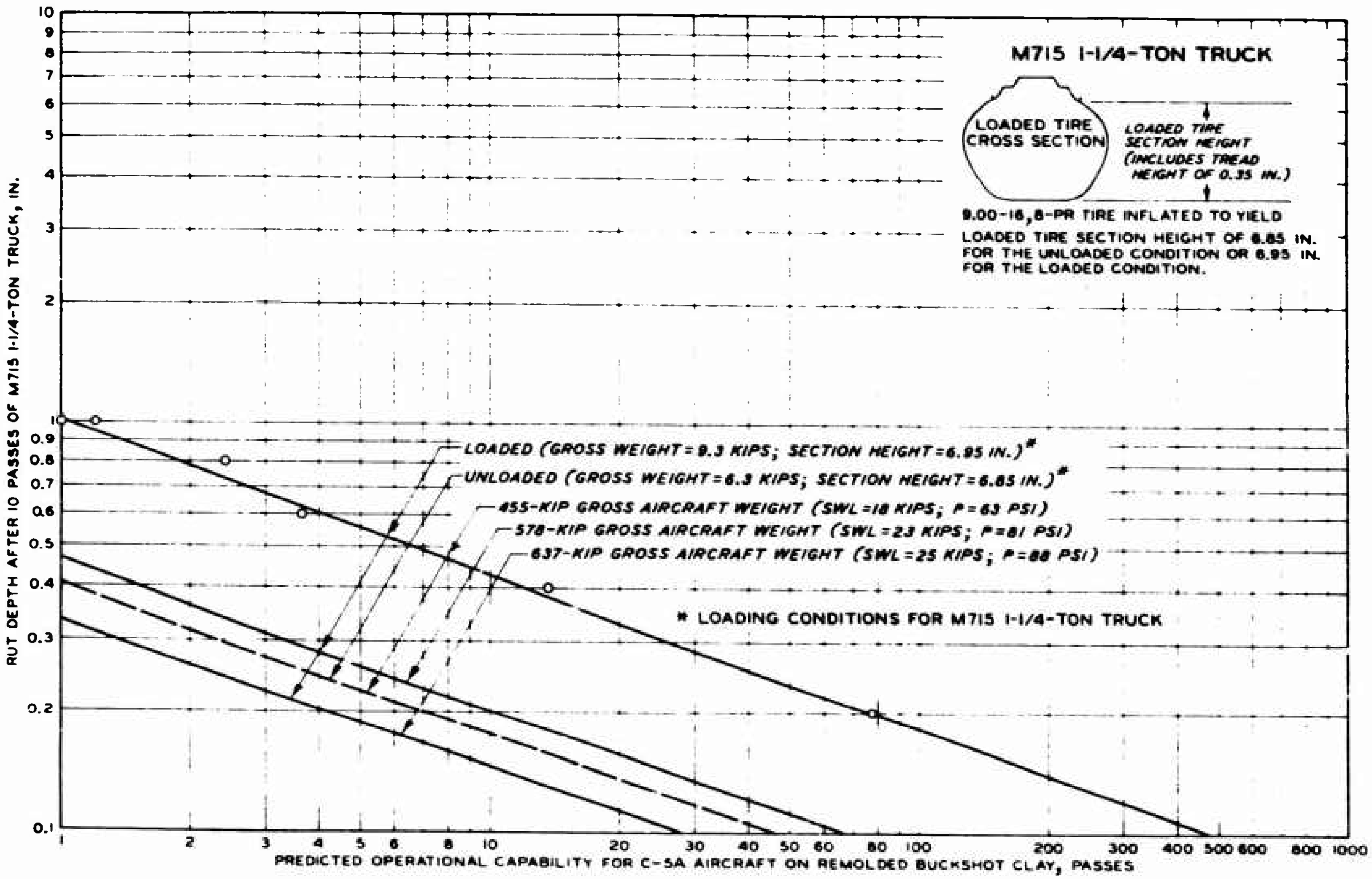

Fig. 46. Ten-Pass Rut Depth for M715 Truck Versus C-5A Aircraft Operational Capability

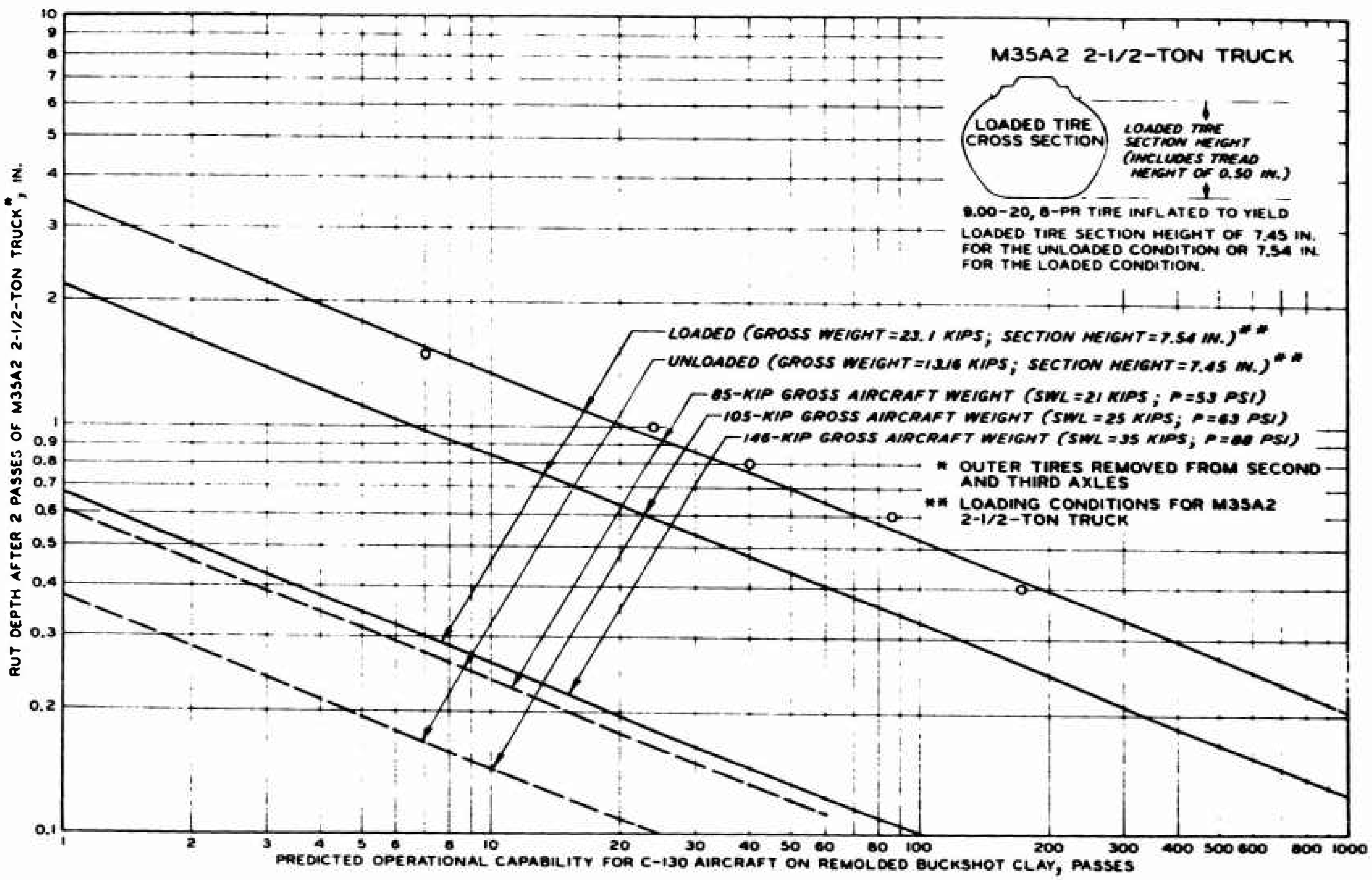

Fig. 47. Two-Pass Rut Depth for M35A2 Truck Versus C-130 Aircraft Operational Capability

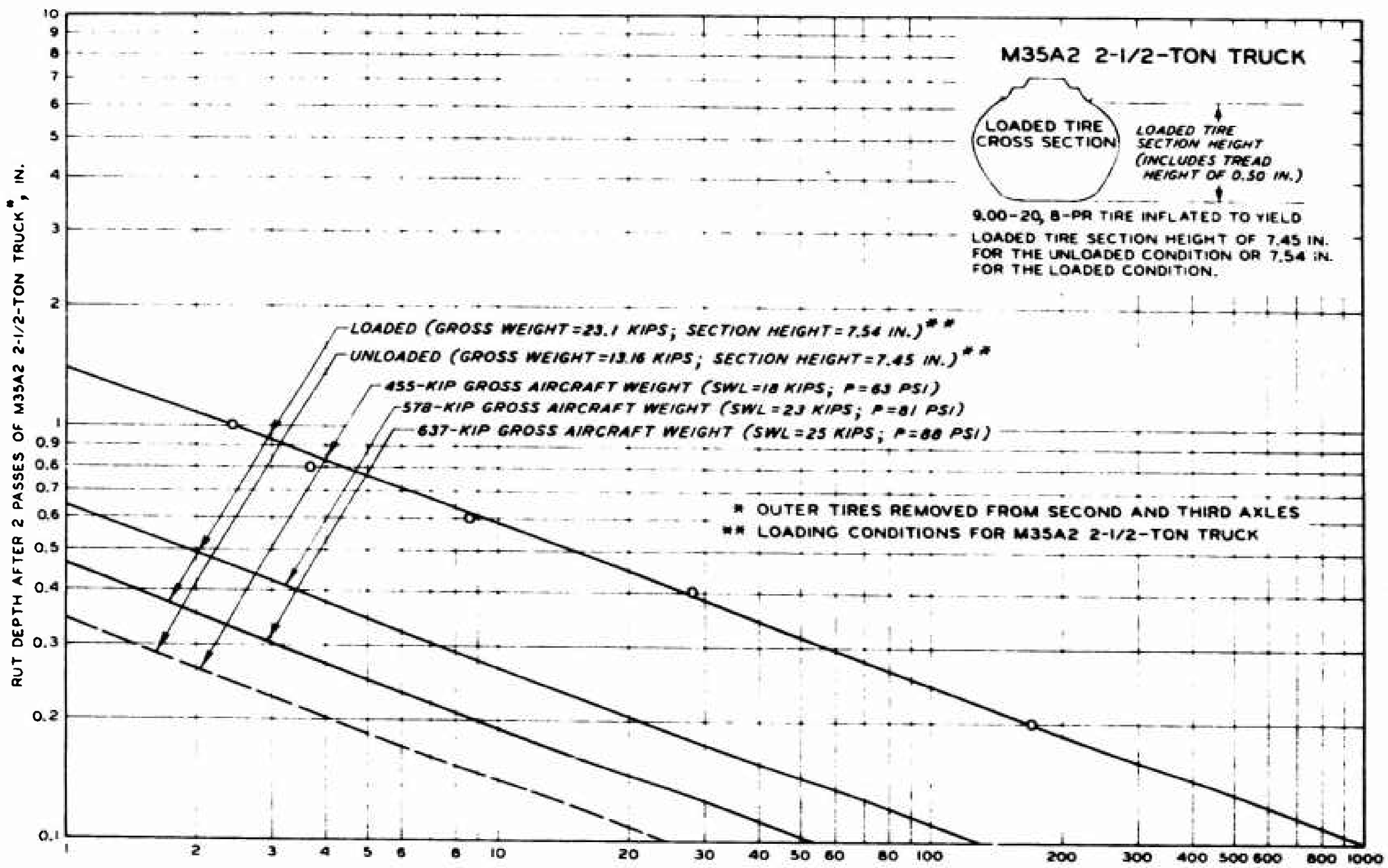

Fig. 48. Two-Pass Rut Depth for M35A2 Truck Versus C-5A Aircraft Operational Capability

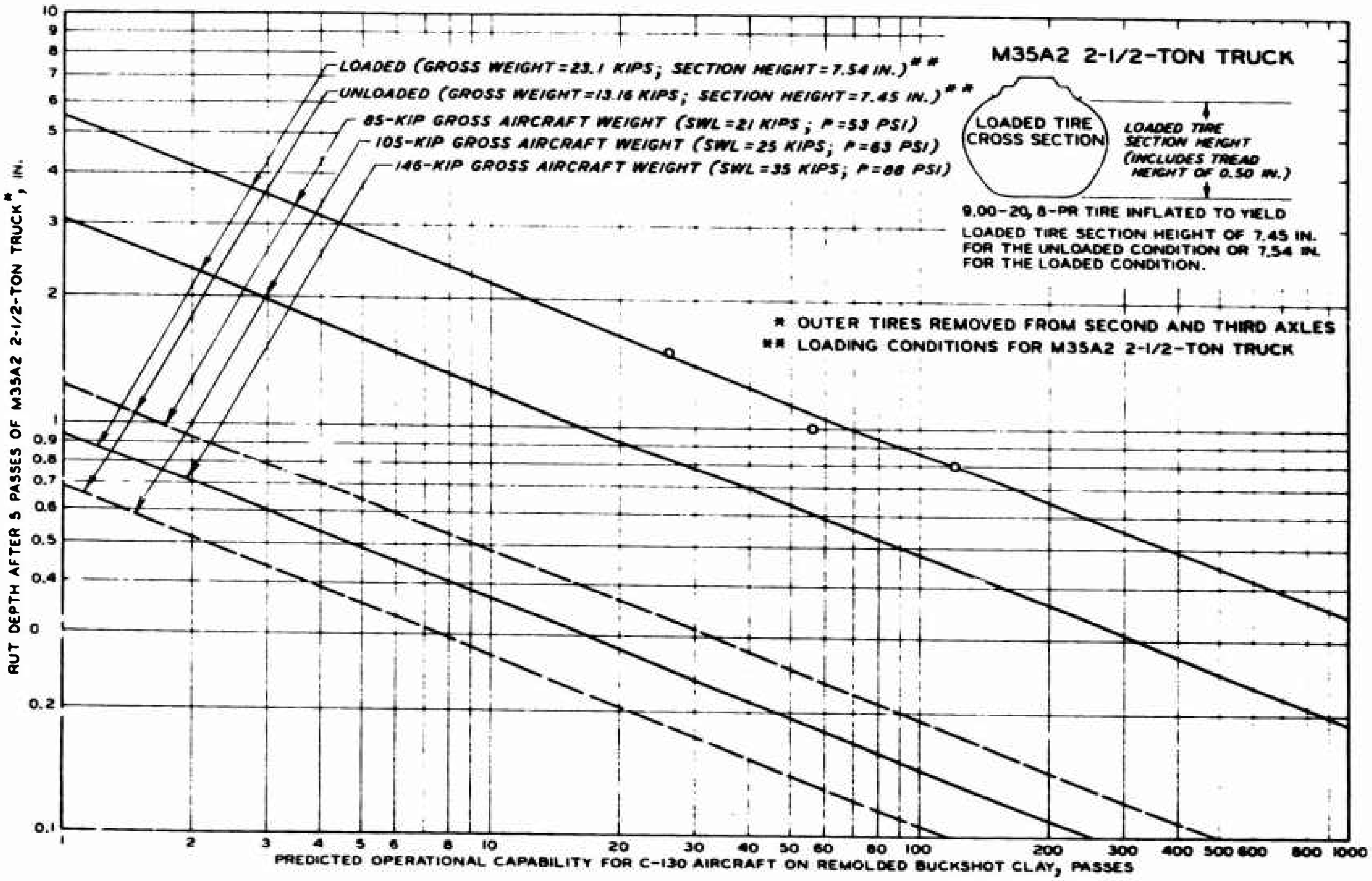

Fig. 49. Five-Pass Rut Depth for M35A2 Truck Versus C-130 Aircraft Operational Capability

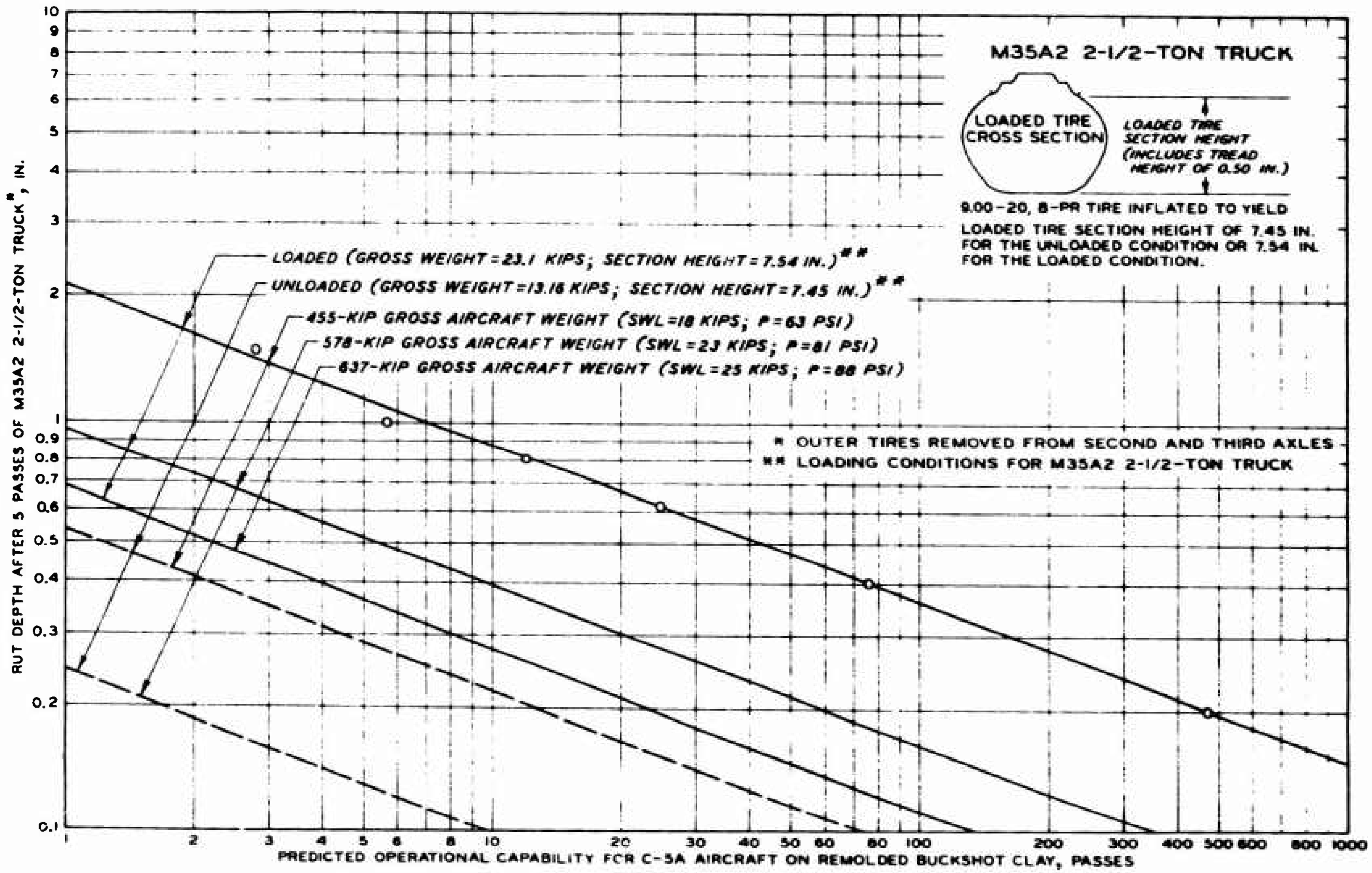

Fig. 50. Five-Pass Rut Depth for M35A2 Truck Versus C-5A Aircraft Operational Capability

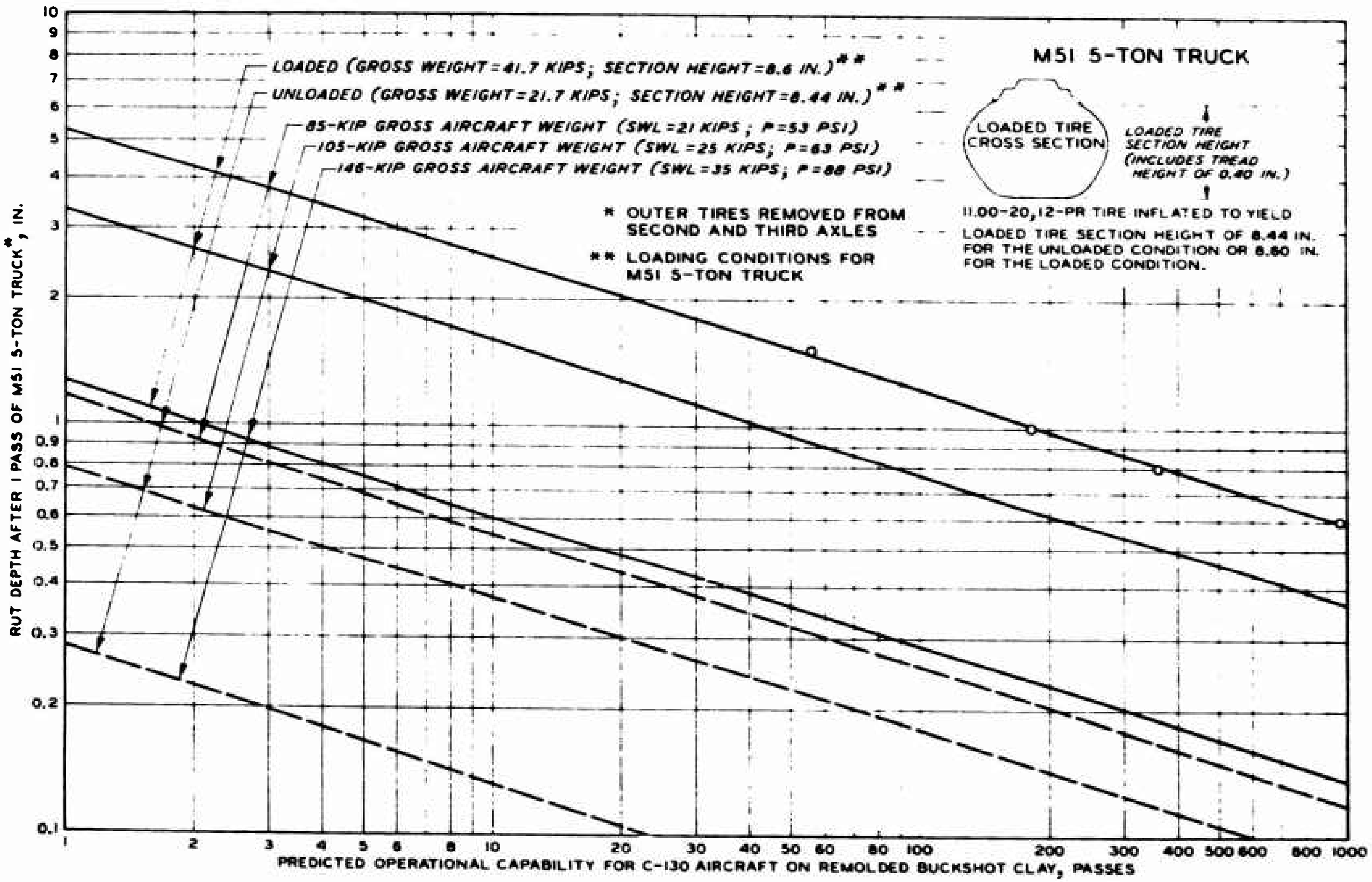

Fig. 51. One-Pass Rut Depth for M51 Truck Versus C-130 Aircraft Operational Capability

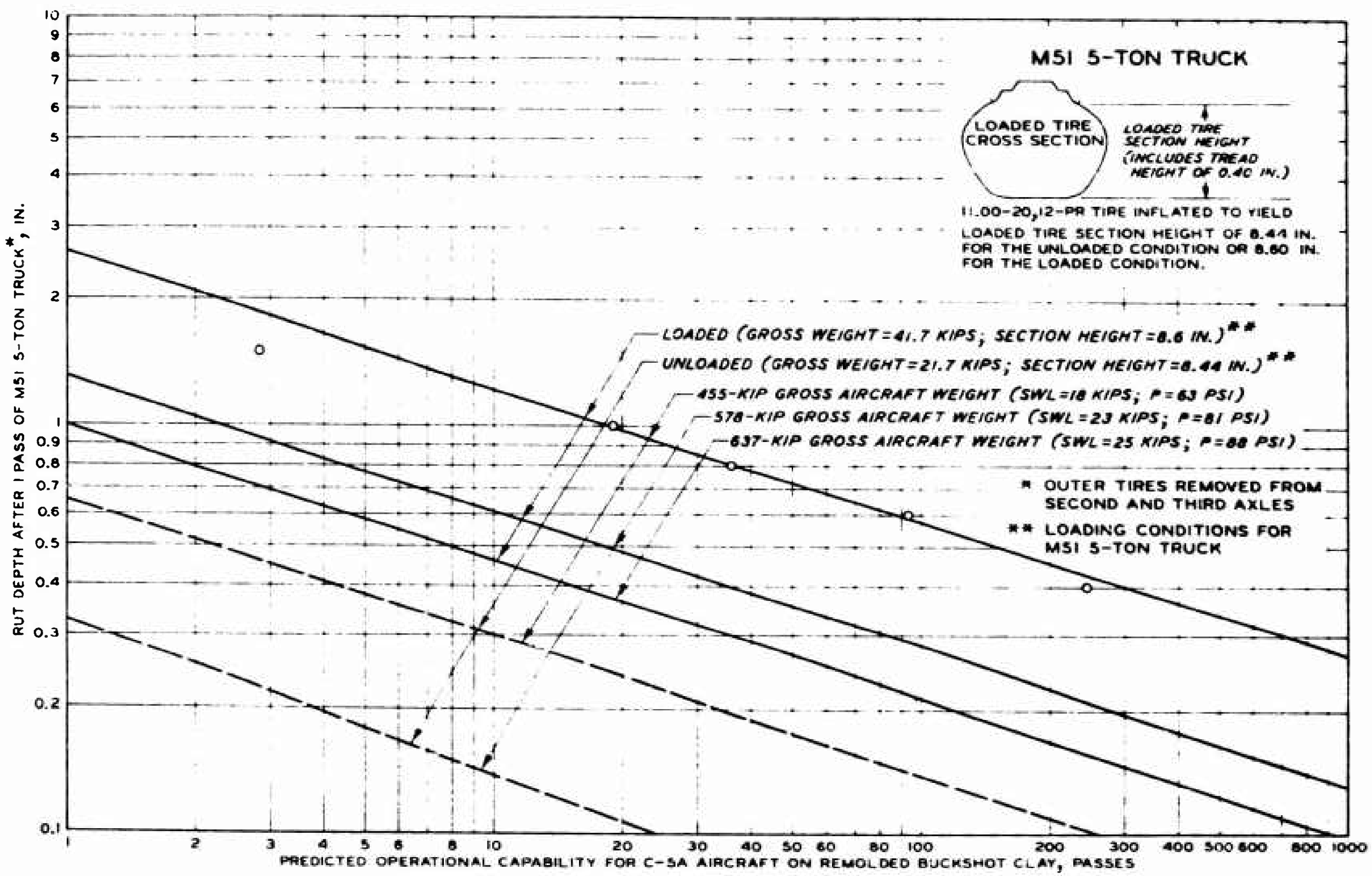

Fig. 52. One-Pass Rut Depth for M51 Truck Versus C-5A Aircraft Operational Capability

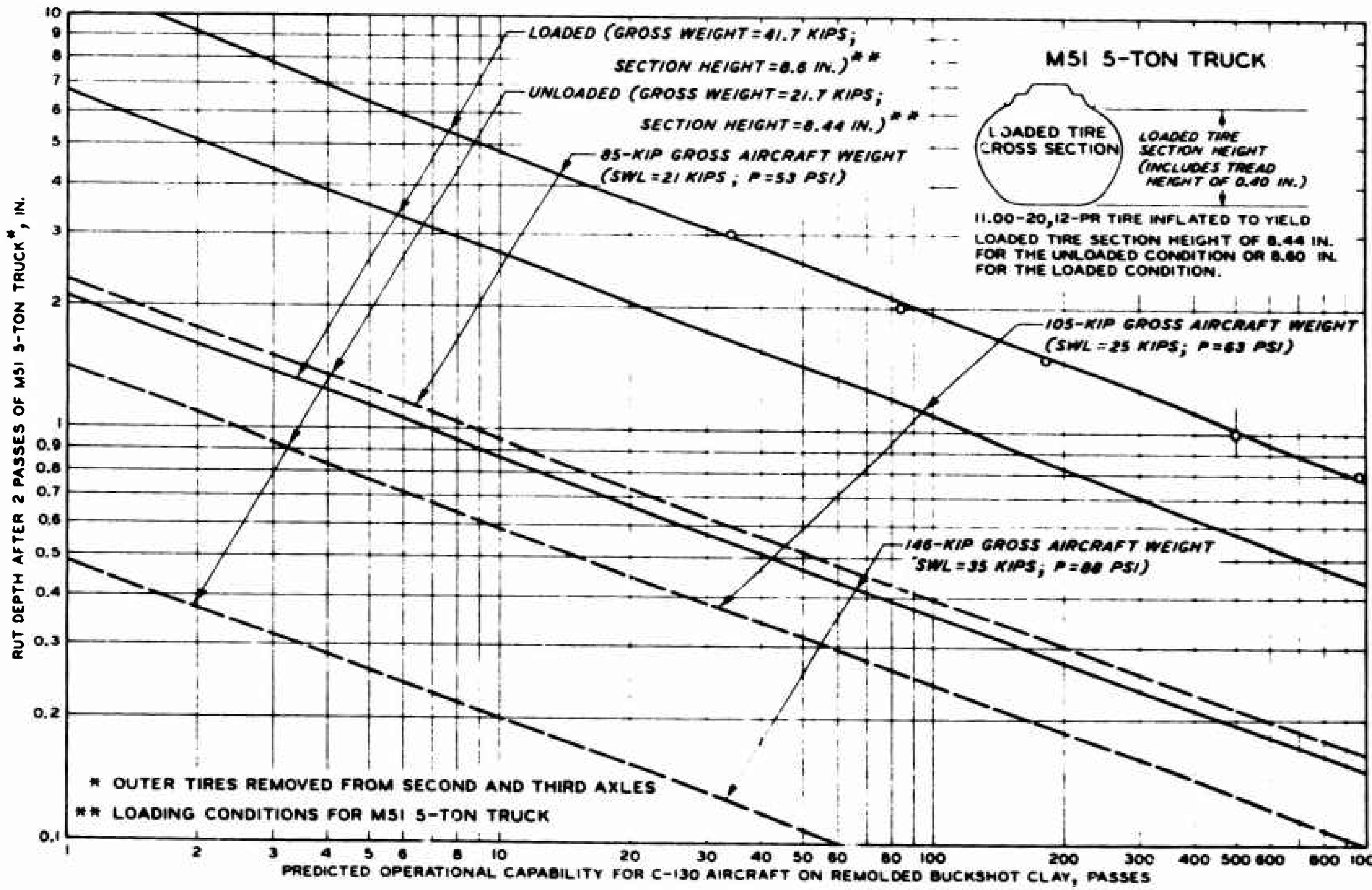

Fig. 53. Two-Pass Rut Depth for M51 Truck Versus C-130 Aircraft Operational Capability

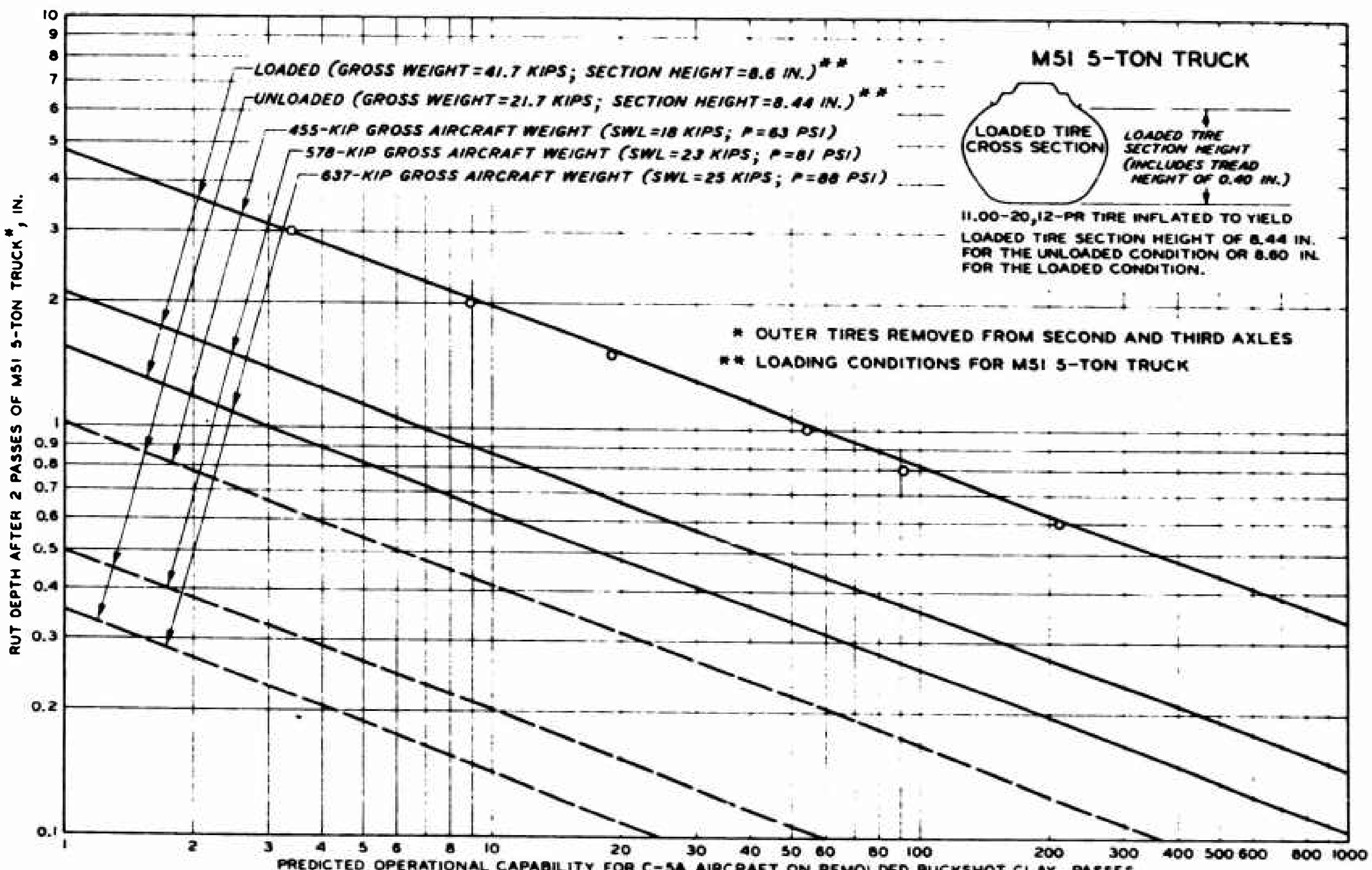

Fig. 54. Two-Pass Rut Depth for M51 Truck Versus C-5A Aircraft Operational Capability

REFERENCES

1. Ladd, D. M. and Ulery, H. H., Jr.,; Aircraft Ground-Flotation Investigation, Part I, Basic Report, Technical Report No. 3-737 (AFFDL-TDR-66-43), U. S. Army Engineer Waterways Experiment Station, CE, Vicksburg, Miss., August 1967.

2. Hammitt, G. M., II; Evaluation of Soil Strength of Unsurfaced Forward-Area Airfields by Use of Ground Vehicles, Miscellaneous Paper S-70-14, U. S. Army Engineer Waterways Experiment Station, CE, Vicskburg, Miss., May 1970.

3. Department of Defense; Military Standard; Test Method for Pavement Subgrade, Subbase, and Base-Course Materials, MIL-STD-621A, Government Printing Office, Washington, D. C., 22 December 1964.

4. Department of the Army, Corps of Engineers, Mississippi River Commission; Trafficability of Soils; Laboratory Tests to Determine Effects of Moisture Content and Density Variations, Technical Memorandum No. 3-240, First Supplement, U. S. Army Engineer Waterways Experiment Station, CE, Vicksburg, Miss., March 1948.

5. Meyer, M. P.; Comparison of Engineering Properties of Selected Temperate and Tropical Surface Soils, Technical Report No. 3-732, U. S. Army Engineer Waterways Experiment Station, CE, Vicksburg, Miss., June 1966.

6. Freitag, D. R.; A Dimensional Analysis of the Performance of Pneumatic Tires on Soft Soils, Technical Report No. 3-688, U. S. Army Engineer Waterways Experiment Station, CE, Vicksburg, Miss., August 1965.

7. Turnage, G. W.; Performance of Soils Under Tire Loads; Application of Test Results to Tire Selection for Off-Road Vehicles, Technical Report No. 3-666, Report 8, U. S. Army Engineer Waterways Experiment Station, CE, Vicksburg, Miss., September 1972.

8. Patin, T. R. and Swanson, G. D.; Small-Scale Mobility Tests in Fine-Grained Layered Soils, U. S. Army Engineer Waterways Experiment Station, CE (in preparation), Vicksburg, Miss.

9. Powell, C. J. and Green, A. J.; Performance of Soils Under Tire Loads; Analysis of Tests in Yuma Sand Through August 1962, Technical Report No. 3-666, Report 2, U. S. Army Engineer Waterways Experiment Station, CE, Vicksburg, Miss., August 1965.

10. Hay, D. R.; Aircraft Characteristics for Airfield Pavement Design and Evaluation, AFWL-TR-69-54, Air Force Weapons Laboratory, Albuquerque, N. M., October 1969.

11. Burns, C. D.; Validation of Soil-Strength Criteria for Aircraft Operating on Unprepared Landing Strips, Technical Report No. 3-554, U. S. Army Engineer Waterways Experiment Station, CE, Vicksburg, Miss., June 1960.

12. Burns, C. D.; Aircraft Operations on Unsurfaced Soil, Soil Measurements and Analyses, Project Rough Road Alpha, Technical Report No. 3-624, U. S. Army Engineer Wateraya Experiment Station, CE, Vicksburg, Miss., June 1963.

13. Womack, L. M.; Tests With A C-130 Aircraft on Unsurfaced Soils, Miscellaneous Paper No. 4-712, U. S. Army Engineer Waterways Experiment Station, CE, Vicksburg, Miss., February 1965.

14. Burns, C. D.; Evaluation of Forward Airstrip Criteria for Soil Strength, Miscellaneous Paper No. 4-104, U. S. Army Engineer Waterways Experiment Station, CE, Vicksburg, Miss., March 1955.